UiT THE ARCTIC UNIVERSITY OF NORWAY

Department of Electrical Engineering

Intelligent Load Frequency Control in an Isolated Wind-Solar PV-Micro Turbine-Diesel Based Micro-Grid using V2G Integration

—

Submitted by Wondwosen Eshetu Addisu

Master's thesis in Electrical Engineering, June 2017

Acknowledgement

First of all, I thank God for he has given me the chance to start and then the strength, courage and patience to finalize this study. Everything happened in his will.

I would like to express sincere gratitude to my academic supervisors, Associate Prof. Dr. Pawan Sharma and Dr. Charu Sharma. They have been wise, patient and trusted advisor throughout the entire process. This thesis would not have been possible without their support and encouragement. Their experience and input has been valuable during the thesis project.

Special thanks to Associate Prof. Dr. Trond Østrem, Dr. Bjarte Hoff, Prof. Lars Norum, Prof. Per-Ole Nyman and all the other lecturers for the guidance and lectures they provided in their respective courses. I would also like thanks to all my colleagues at UiT, The Arctic University of Norway, for these two years of studies, sharing their knowledge and participating in different projects and courses at the University.

I would like to thank my parents for being a constant source of encouragement and motivation throughout my pursuit of the master degree.

Last, but certainly not least, I want to thank my wife, Dirb Tilahun, and daughters, Yohanna and Kalkidan, for their love, faith and patience they were showing me during my whole work. I could not have accomplished this work without her support. Dirb is always my life!

Wondwosen Eshetu Addisu

Narvik, 06/06/2017

Abstract

Modern power systems need more intelligence and flexibility to maintain and control a generation load balance from subsequent serious disturbances due to the emerging of more renewable energy sources. This problem is becoming more significant today because of the increasing number of micro-grids (MGs). MGs usually use renewable energies in electrical production those fluctuate naturally. So, fluctuation and usual uncertainties in power systems cause the conventional controllers to be less efficient to provide a proper load frequency control (LFC) performance for a wide range of operating condition. Therefore, this thesis presents an intelligent control technique which is based on Adaptive Neuro-Fuzzy Inference System (ANFIS) architecture for an isolated wind-Solar PV-micro turbine-diesel based micro-grid (MG) system using Vehicle-to-Grid (V2G) integration. Accordingly, the V2G technology, the electric vehicle (EVs) may act as mobile energy storage units that could be a better solution for the inadequate LFC capacity and thereby to improve the frequency stability in an isolated MG. The performance of the proposed intelligent controller (ANFIs) is compared with conventional proportional-integral-derivative (PID) controller, Interval type-1 (IT1) Fuzzy controller and Interval type-2 (IT2) Fuzzy controller design methods. The results show that ANFIS based neuro-fuzzy LFC controller is having less settling time and improve dynamic responses for the considered MG system.

Keywords: Intelligent control technique; EV; V2G; LFC; Interval type-1 Fuzzy control; Interval type-2 Fuzzy control; Proportional-Integral-Derivative control; Adaptive Neuro-Fuzzy Inference System; Micro-Grid.

Contents

List of Tables

List of Figures

Chapter 1
Introduction

1.1 Research Motivation

In recent years, the impact of fossil fuel on the environment, especially the global warming and the harmful effects of carbon emissions have created a new demand for clean and sustainable energy sources [1]. Environmental issues are now playing an ever-increasing vital role on the political agenda. Power generation by conventional energy sources has always been a major source of air pollution, and much effort has been devoted to developing cleaner generation technologies. However, the relatively recent concerns about global warming and sustainability have started to change the way power systems operate and expand. It is estimated that power generation contributes about one-third of the global CO2 emissions so that many countries in the world have set a target for renewable energy generation (REG) to contribute 20% or more of their total energy production by about 2020 [2]. The renewable energy sources are used for power generation which could be integrated to the distribution voltage level. A micro-grid (MG) concept is needed to integrate the renewable energy sources (RES) in the electric grid.

MGs are small power grids: - it can be part of an electric distribution system or can be a small independent power grid of an isolated or remote area, i.e., where there is no access of primary grid power. If a MG is grid connected, the loads can be supplied by the connected primary grid power system. Otherwise, the system is working in an isolated mode. In islanded mode, the unavailability of grid requires specific management of micro-sources (MSs) and load, because they cannot simply generate and consume by their willing. MG disconnection from main grid demand that total power produced by MSs should equal to the power consumed by the loads plus the line losses within micro-grid.

1.2 Micro Grid as a Viable Alternative

Micro-grids (MG) are becoming viable alternative to centralized generation and bulk transmission of power by offering a localized power production, regulation, and consumption. According to the 24^{th} edition of the World Energy Resources report, most countries have achieved more diversified energy integrating with growth in community ownerships and an evolution of micro-grids [53]. A typical MG consists of distribution sources, for example, micro-turbines, diesel generators, renewable sources and loads. Rapid improvements in performance and cost of energy storage technologies during the last few years are making MGs an economically viable option for the power system in the near future [3], [47], [48].

1.3 Technical challenges facing for Micro-grids implementation

Nowadays, smart grids-micro grids are facing various challenges due to renewable energy source penetration, load fluctuation, and electric vehicles EVs integration. MG frequency, voltage, and protection are the most critical challenges facing for MGs implementation.

Due to the intermittent nature of renewable energy sources, large frequency fluctuation occurs when the load frequency control capacity is not enough to compensate for the imbalance of generation and demand. This problem may become intensified when the system is working in isolated operation mode [30]. In an isolated power system, the operation is often very challenging because of their small system inertia. Although, the inertia energy in a power system can partly overcome the disturbances which caused whether by the load or by the intermittent nature of renewable energy sources, it is still difficult to keep the frequency deviation within the acceptable limits [3].

1.4 The Problem; Load Frequency Control in a Micro Grid using V2G

Due to renewable sources fluctuation and electric vehicles integration, the isolated MG system state parameters and operating conditions change rapidly. Moreover, there are some constraints in the LFC units including generation rate constraints and capacity constraints, which conventional controllers cannot overcome. Thus, for isolated MG LFC with V2G, a controller with robust performance over a wide range of system operation conditions is highly desirable [3].

1.5 Proposed Solution; Intelligent Load Frequency Control Technique

This thesis has presented an intelligent control technique of the isolated micro-grid system with EVs, distributed generations to obtain a satisfied performance on the load frequency control by using Adaptive Neuro-Fuzzy Inference System (ANFIS). Accordingly, the vehicle to grid (V2G) technology, the electric vehicle (EVs) may act as mobile energy storage units that could be a better solution for the inadequate LFC capacity thereby improving the frequency stability in an isolated micro grid. This intelligent control, in turn, will improve the frequency stability with complex operation conditions like the random renewable energy sources and the load disturbances. Neuro-Fuzzy system can combine the parallel and learning abilities of neural networks (NNs) with human-like knowledge representation and explanation abilities of fuzzy system. The performances of ANFIS based controller, Interval Type-1 and Type-2 Fuzzy Logic Control (FLC) and the conventional PID control are compared to highlight the supremacy of hybrid controller over conventional controller.

1.6 Thesis Organization

The organization of the thesis is as follows:

Chapter 1 gives a general introduction to Micro-Grid LFC. The viability of MG as an alternative, technical challenges facing for MG implementation, the problem on LFC in MG using V2G, the proposed solution presented the main motivation and at the last thesis contributions are briefly reviewed.

Chapter 2 presents literature study. The past achievement in the Vehicle to Grid (V2G) technology, the role of V2G technology in a power system, LFC, LFC in MGs, LFC in MGs with V2G, Intelligent techniques for LFC in MGs and Intelligent techniques for LFC in MG with V2G literature is reviewed.

Chapter 3 presents modelling of the isolated MG using V2G integration. The MG modelling, model of MT, EVs, DG, wind turbine and solar PV and general scheme of the MG with LFC controller designed state space equation based on the model are presented in briefly.

Chapter 4 propose different controllers for MG LFC. (1) Conventional Controller, Proportional Integral Derivative (PID). (2) Artificial intelligent controller: - (2.1) Interval type-1 Fuzzy Logic controller (IT1 FLC) and (2.2) Interval type-2 Fuzzy Logic controller (IT2 FLC) (2.3) Adaptive Neuro-Fuzzy Controller (ANFIS) and its procedural steps to design the ANFIS.

In Chapter 5 the robustness and effectiveness of the proposed ANFIS over the conventional PID, IT1 and IT2 fuzzy controller is presented numerical time-domain simulated results.

Conclusion and future scopes are stated in Chapter 6.

1.7 Thesis Contributions

The main contribution of this thesis are as follows:

I. A literature study of the V2G technology in a power system.

II. State space modelling of the considered isolated MG using V2G Integration.

III. Present an intelligent coordination control techniques for LFC between micro-turbine, diesel generator, and EVs to achieve a satisfied performance on load frequency.

IV. Demonstrate the performance of ANFIS with system stability performances, the considered isolated micro-grid with MT, DG, EVs, solar PV, and wind farm is modelled in MATLAB/SIMULINK environment.

Chapter 2
Literature Study

2.1 Vehicle to Grid (V2G) Technology

Amory Lovins determined V2G in 1995 and was developed by William Kempton. The primary concept of V2G is that EVs can provide energy to the electric power systems when it is parked, the battery of EVs can charge during low demand times and discharge when power is needed. Statistically speaking, private cars remain idle for almost 95% of the day [3], [4].

V2G describes a system in which the EVs communicates with the power grid to provide grid support by either delivering power to the grid or by throttling their charging rate.V2G technology utilizes the stored energy in the electric vehicles' batteries and supplies this energy to the grid, whenever requested by the grid operators. A fleet of such electric vehicles would provide a considerable amount of energy storage. Thus, like distributed energy resources, the V2G technique can reduce the stress on the overloaded distribution systems by meeting demand locally, especially during peak hours [5].

2.2 Role of V2G technology in a power system

V2G technology can provide many services to achieve various benefit. The implementation of V2G can provide frequency regulation, harmonics filtering and even failure recovery to power system during blackout. The advantage of V2G is not only the privilege for power utility in micro-grids but also EV owners [6], [7], [8].

V2G can help improve the reliability and stability of the grid, alleviate power shortages, reduce air pollution, improve ancillary services, frequency regulation to grid operation, and improve overall system efficiency. For instant, V2Gs can play a significant role in helping to balance supply and demand by valley filling and peak shaving. The electric vehicle battery pack charged at night during low demand, and then the stored power can be fed power back into the grid during high demand periods, thus helping to stabilize the grid's voltage and frequency, and providing a spinning reserve to meet sudden power demand changes. The most important role for V2G may also be used to support renewable energy sources. The two largest renewable sources likely photovoltaic PV and wind turbines both are intermittent, for example, they store excess energy produced during windy periods, and feeding it back into grid during high loads, thus effectively stabilizing the intermittency of wind power [8], [9], [10].

According to [11] peak-shaving and valley-filling control using V2G system proposed and the simulation results demonstrate that the V2G peak-saving and valley-filling control strategy and its constraints are reasonable and efficient.

2.3 Load Frequency control

Load frequency control (LFC) is a critical issue in power system operation and control of supplying for sufficient and reliable electric power with high quality. LFC is one of the important control problems in electrical power system operation and design; Nowadays is becoming more significant. Because of the increasing changing structure, size, emerging new distributed renewable energy sources with uncertainties, environmental constraints, and as well as the Micro Grid and Battery storage technologies has made frequency control a challenging task. Many studies have focused on damping frequency control and voltage stability and related issues, but there has been much less work on the power system frequency control, in the last two decades [12], [13].

Significant frequency fluctuation occurs when the load frequency control capacity less efficient to provide the imbalance of power generation and demand. This problem may become enlarged when the system is working in an isolated operation mode. LFC Control Strategies

In general, in research papers LFC controllers techniques are proposed based on:

1. Classical control techniques

A) LQR based controlling techniques

B) Proportional, derivative, integral controlling techniques

2. Soft computing artificial intelligence techniques

A) Fuzzy logic-based techniques

B) Neural Network-based techniques

C) Genetic algorithm based techniques

D) Particle swarm based techniques

E) Hybrid and other based techniques

The descriptions of load frequency control techniques are described by different researchers [27].

Load frequency control problem for single area thermal power system is presented [14], the LFC scheme of one area thermal system with single time delay is introduced in [15]. For single area hydropower system LFC problem is presented, the transient speed response of a single, isolate-governed hydro-generator operating at near full load discussed in briefly in [16]. In [17], the LFC of an isolated small hydropower system presented.

The LFC problem becomes even more complex by integration of renewable energy sources such as wind farms because of fluctuating output power due to intermittent nature of wind speed. Thus the LFC needs to be addressed differently [12]. The authors of [18] discuss in detail modification of unit commitment, economic dispatch, regulation and frequency regulation control when the level of wind generation capacity is significant.

LFC control methods have been applied in traditional thermal power generation system and hydro power generation power system. In [19] Fosha and Elgerd used a state variable model and regulated problem of optimal control theory to develop new feedback control law for two-area interconnected non-reheat type thermal power system. In [20], a linear regulator design method proposed for frequency control based on optimal linear regulator theory.

2.4 LFC in micro-grids

Recently, economical harvesting electrical energy on a vast scale considering the environment issues is undoubtedly one of the big challenges, micro-grid might consider as a best solution. The MGs promise to facilitate the widely penetration of renewable energy and energy storage devices into the power system. Due to high diversity in generation and loads, the MGs exhibit large nonlinearities, changing dynamics, and uncertainties that may require advanced robust/intelligent control strategies to solve [13].

In [20], to intensify the frequency control performance and robustness in the presence of uncertainties, the mixed $H2$ / $H\infty$ and PSO-based mixed $H2$ / $H\infty$ are proposed for tuning proportional-integral-derivative parameters. The authors of [21] proposed a fuzzy-based proportional-integral (PI) control strategy, the stability of hybrid MG system.

2.5 LFC in micro-grid with V2G

The battery storage of the electric vehicle is one of the emerging technologies; it can act as a load reacting to the change in power supply. Literature shows that very little work has been done on control aspect of EVs and the grid. In [22] [23], to utilize an EVs for frequency control has been discussed by developing an optimal aggregator and a similar work is found in [24]. There where an integration of V2G in a Danish farm has been reviewed in detail; on the other hand, more importance has been given to energy storage rather than the V2G concept. The authors of [25] [26] analyses the impact of EVs on distribution grid using load flow techniques, these works, nevertheless, haven't used any controlled techniques for charging or discharging of EVs energy to the grid.

2.6 Intelligent Techniques for LFC in micro grids

Modern power systems require increased intelligence techniques and flexibility in the control and optimization to ensure the performance of maintaining a generation-load balance, following serious disturbances, this issue is becoming more significant today because of the increasing number of MGs. The LFC classical controllers are not visible in practical system because of nonlinear characteristics generation rate constraint and saturation [28]. Therefore, there is a need to controller techniques which can overcome the problem. The soft computing / Artificial Intelligence (AI) techniques like Fuzzy, Neural Network, Genetic Algorithm, hybrid and other techniques approach is more suitable for such a case.

The concept of fuzzy logic developed by Lotfi Zadeh in 1969 address uncertainty and imprecision which widely exist in engineering problems. The FLC concept departs significantly from traditional control theory, i.e., mainly based on mathematical models of the controlled process. The mathematical modeling of Fuzzy: - is the method of describing characteristics of a system by using fuzzy inference rules. The method has a differentiating feature in that it can denote linguistically complex nonlinear systems. It is, however, very hard to identify the rules and tune the membership functions of the fuzzy reasoning. Fuzzy controllers commonly built with the use of fuzzy rules. These fuzzy rules are obtained either from domain experts or by inspecting the people who are professional on currently using this control. Membership functions of the fuzzy sets will be determined from the information accessible from the domain experts. The structure of such rules and membership functions require tuning. That is, performance of the controller must be measured and membership function and rules adjusted based upon the performance.

The Modern era of artificial neural networks (ANN) began with the pioneering work of McCulloch and Pitts in 1943 with the/known McCulloch-Pitts model. ANNs usually referred to neural networks; have been driven by the recognition that the human brain does certain tasks much more efficiently in an entirely different way than the conventional digital computers. They are non-linear by nature, which excellent features like fault-tolerance and capability for self-learning, which gives them robust and quite suited for parallel processing. ANN performs the function of non-linear mapping. If an input set of data corresponds to a definite signal pattern, network can be trained to give correspondingly desired pattern at the output. ANN techniques are relatively easy to implement and do not require any prior knowledge of the system model [29].

To enable a system to deal with cognitive uncertainties in a manner more like humans, one combines the concept of fuzzy logic into the neural networks. The resulting hybrid system is called neural fuzzy, fuzzy neural, fuzzy-neuro or neuro-fuzzy network.

The LFC problem in micro-grids has tackled in the literature by different intelligent techniques [1], [21], [28], [37].

2.7 Intelligent techniques for LFC in micro-grid with V2G

The complexity and uncertainty of the power system raised by the entrance of distributed generation sources and micro-grids. The fluctuation in the generated power might cause some problems in the function of conventional controllers. As a result, modern power system requires an increased intelligent techniques and flexibility in the control and optimization to ensure the capability of a generated load balance, following serious disturbances. The authors of [31], proposed a new combination of the General Type II Fuzzy Logic Sets (GT2FLS) and the Modified Harmony Search Algorithm (MHSA) technique was applied for adaptive tuning of Proportional-Integral (PI) controller.

Chapter 3
Modelling of the Isolated Micro-Grid using V2G Integration

3.1 Micro-grid modelling

A Micro-Grid shown in Figure 1 is a low Voltage (LV) network composed of single bus-bar, a wind turbine, Solar PV array, micro turbine, diesel generation, EVs, and loads. With the same model, the micro-grid can be operated in two alternative modes, i.e., isolated mode and grid connected model. By controlling the circuit "breaker" in Figure 1, the MG can switch from one mode to other modes. If the MG is in grid-connected mode, much of loads can be supplied by the connected main grid. If not, in the isolated mode, the loads will be supplied by coordinated control of Micro Turbine, Diesel generator and EVs.

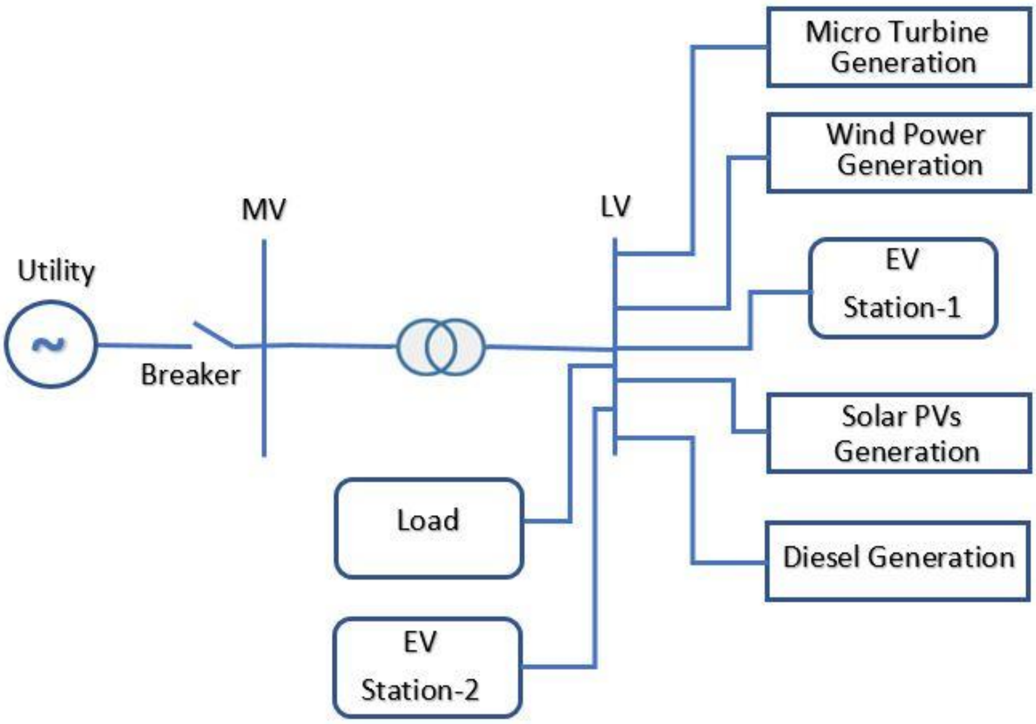

Figure 1 - Layout of isolated micro-grid

3.2 Model of MT

A micro turbine is a small-scale power generation equipment. It has an advantage of fast starring speed, durability, and high efficiency, compared with traditional generators. MT can follow load demand variations by using a power control mechanisms within short intervals of time. The MT varies its output via the fuel regulation when power demand fluctuates. The continuous time transfer function model of the MT for LFC shown in figure 2. In this figure, the relationship between LFC signal and output power of MT is represented, which simulate the dynamic process of the MT output power following the LFC signal. The figure consists of a governor, fuel system and gas turbine of the MT. The equivalent models of the fuel system and turbine are denoted by first-order inertia plants.

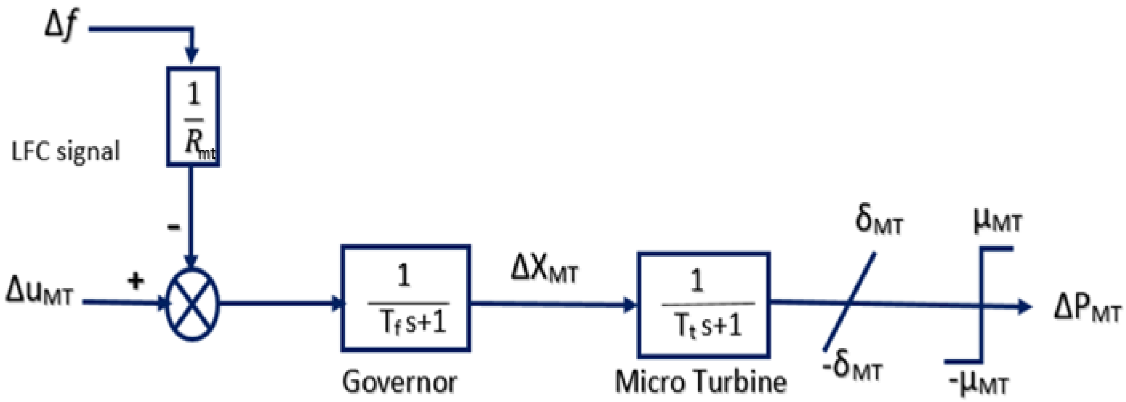

Figure 2 - The transfer function model of the Micro Turbine for LFC

In the above figure, Δf is the frequency deviation, Δu_{MT} is the LFC signal dispatched to MT, ΔX_{MT} is the value position increment of the governor, T_f is the time constant of the governor, T_t is the time constant of the MT, R_{MT} is the speed regulation coefficient of the MT, $\pm\delta_{MT}$ are the power ramping rate limits, and $\pm\mu_{MT}$ are the power increment limits. ΔP_{MT} is the output power increment. If $\Delta P_{MT} = 0$, the output power of MT is a threshold value that balances the load without grid disturbance. In such circumstances, frequency deviation is equal to zero, i.e. $\Delta f = 0$. In general, this certain output power threshold is determined by the power balance of the grid. $\Delta P_{MT} > 0$ indicates that the output power of MT is greater than the threshold value, whereas $\Delta P_{MT} < 0$ indicates that the output power of MT is less than the threshold value.

3.3 Model of Electric Vehicle

In this section, I propose the equivalent EV model that parameterize each EV with different inverter capacities, because there are different number of EVs in each electric vehicle stations. Figure 3 and figure 4 from [23] illustrates the equivalent EV model used for LFC and the total energy model respectively. The total charged or discharged power of the EVs in the controllable state are calculated by using this model.

In figure 3, Te is the time constant of EV, Δu_E is the LFC signal dispatched to EV, $\pm\mu_e$ are the inverter capacity limits, and $\pm\delta_e$ are the power ramp rate limits. s is the complex frequency and $s = \delta + jw$. E is the current energy of the EV battery. E_{max} and E_{min} are the maximum and minimum controllable energy of the EV battery, respectively. K_1 and K_2 are difference between limited energy and current energy of the EV battery, respectively. They can be calculated as $K_1 = E\text{-}E_{max}$ and $K_2 = E\text{-}E_{min}$. Finally, ΔP_E is the charging/discharging power. $\Delta P_E = 0$ means EV is in the idle state, $\Delta P_E > 0$ means EV is in the discharging state and $\Delta P_E < 0$ means EV is in the charging state. The EV can be charged and discharged only within the range of $\pm\mu_e$. However, if the energy of the EV exceeds the upper limit (i.e., E_{max}), the EV can only be discharged within the range of $(-\mu_e)$. Also, if the energy of the EV is under the lower limit (i.e., E_{min}), the EV can only be charged within the range of $(-\mu_e \sim 0)$.

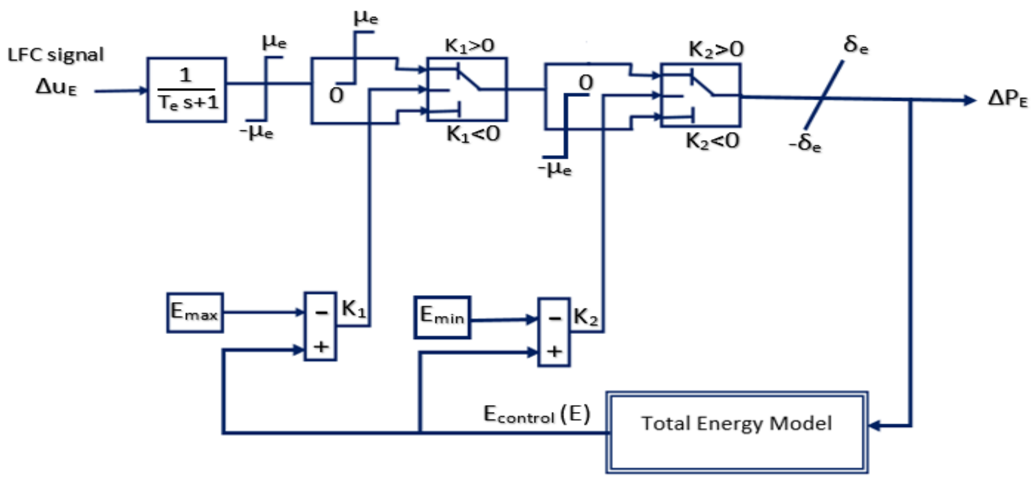

Figure 3 - The transfer function model of EV model for LFC

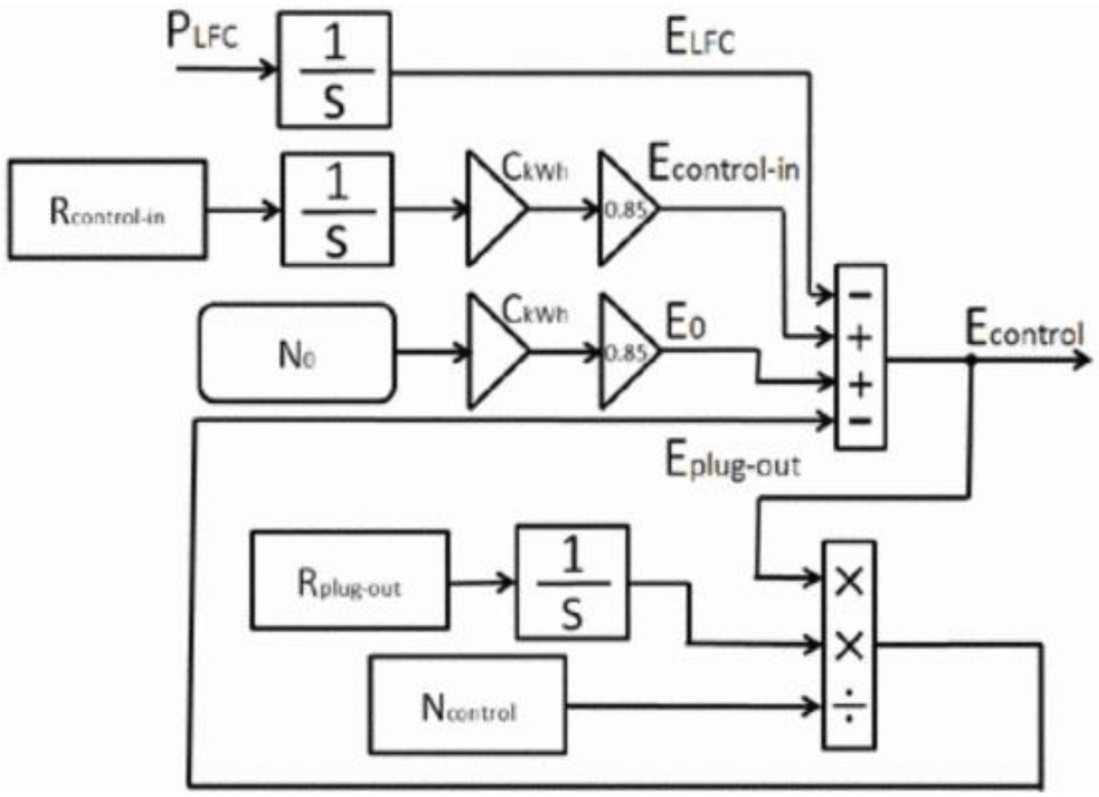

Figure 4 - Total energy model [23].

In the above figure, it is assumed that the initial state of charge (SOC) of the all controllable EVs is 85%. The response to the LFC signal can be limited by the number of controllable E Vs and by the EV customers' convenience indicated by the specified SOC. ELFC is the energy corresponding to the LFC signal, Econtrol-in is the energy increase due to EVs which change the state from the charging one to the controllable one. The number here is calculated from the integral of the control-in rate (Rcontrol-in), Eo is the initial energy, Eplug-out is the energy decrease due to the plug-out EVs, Ncontrol-in is the number of controllable EVs and N0 is the initial controllable EVs. Details of the equivalent EV model including battery and charger based on the charging and discharging characteristics can be found in literature [23].

3.4 Model of DG

To simulate the complete dynamics of a diesel generator, a complex and high model will be required. But, from framework and speed dynamics point of view, it is adequate to utilize a much lower order model. DG is a small-scale unit that have some desirable features such as being fast starting with durable and highly efficient.

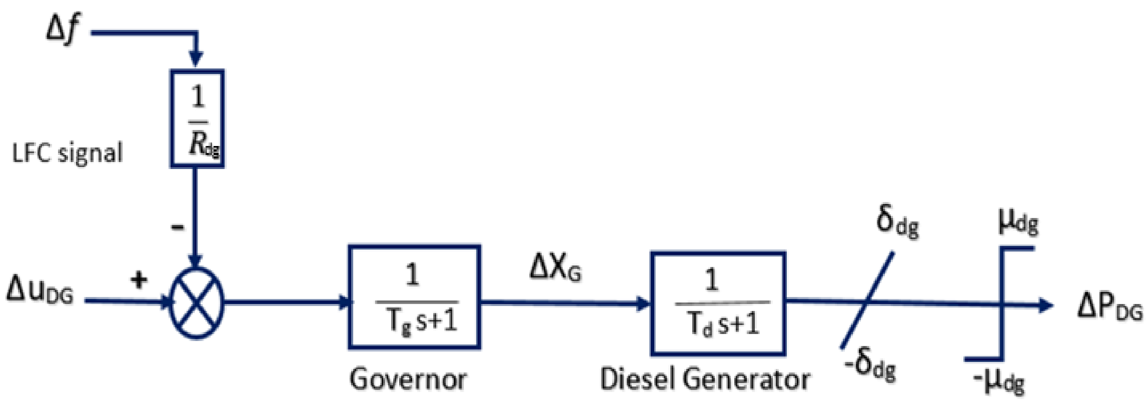

Figure 5 - The transfer function model of Diesel Generator for LFC

DG can detect load variations instantly by using power control mechanisms [34]. The governor regulates the fuel input to an engine via a valve mechanism. When the DG faces power demand fluctuation, it regulates its fuel consumption and thereby adjust its output power. The relationship between load frequency control signal and the output power of DG is described in figure 5. In this figure, the governor and the diesel generator is modelled by using a first-order function [35].

In Figure 5, Δf is the frequency deviation, Δu_{DG} is the LFC signal dispatched to DG, ΔX_G is the value position increment of the governor. Furthermore, T_g is the time constant of the governor, T_d is the time constant of the DG, R is the speed regulation coefficient of the DG, $\pm\delta_{dg}$ are the power ramping rate limits, and $\pm\mu_{dg}$ are the power increment limits. ΔP_{DG} is the output power increment. If $\Delta P_{DG} = 0$, the output power of DG is a threshold value that balances the load without grid disturbance. In such circumstances, frequency deviation is equal to zero, i.e. $\Delta f = 0$. In general, this certain output power threshold is determined by the power balance of the grid. $\Delta P_{DG} > 0$ indicates that the output power of DG is greater than threshold value, whereas $\Delta P_{DG} < 0$ indicates that the output power of MT is less than the threshold value.

3.5 Wind turbine and solar PV model

Owing to time-variant wind speed and wind direction, the output power of wind turbine is fluctuant as a natural source [3].

PV cells produce power from semiconductors upon illumination. Power is produced as long as the light is incident on the solar cell. When the performance of controllers for MT, DG, and EV is considered the inner characteristics of wind turbine and solar PV have little effect on LFC of the micro-grid. Hence the fluctuation of wind power and solar PV power output is relatively large; they can be all equalized to the disturbance source in the LFC model [36].

3.6 General scheme of the MG with LFC controller

The structure of the proposed LFC controller in isolated micro-grid which consists of MT, DG, two equivalent EVs (EV1 and EV2) and the power disturbance ΔP_D are constructed as shown in figure 6. In this thesis, ΔP_D consists three parts (i.e., the load disturbance ΔP_L, the fluctuation of wind power generation ΔP_w and the fluctuation of solar PV generation ΔP_{pv}.). Additionally, in this figure, $2H_t$ denotes the equivalent inertia constant of the all directly connected generators and motor loads plus the inertia response provided by the micro-source controllers expressed the system base [3] [32].

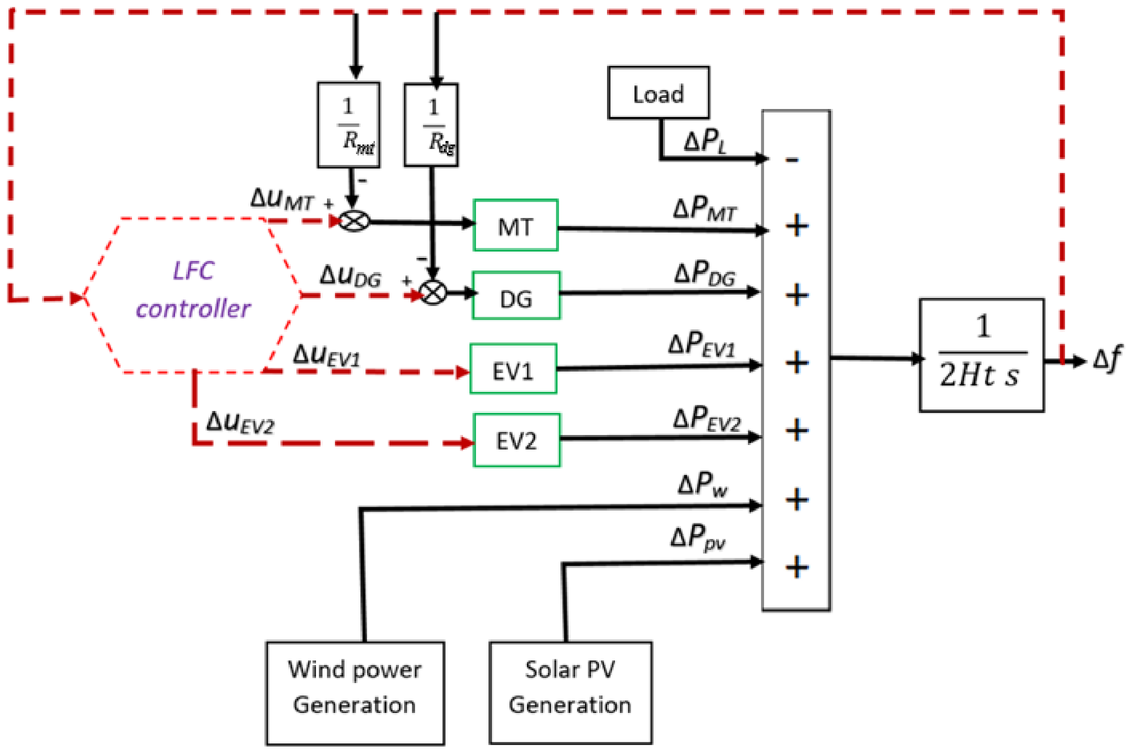

Figure 6 - The control model of the Micro-Grid including LFC.

Based on this model, the state space can be denoted as follows:

$$x(t) = [\Delta f(t)\ \ \Delta P_{MT}(t)\ \ \Delta X_{MT}(t)\ \ \Delta P_{DG}(t)\ \ \Delta P_{EV1}(t)\ \ \Delta P_{EV2}(t)]^T \tag{1}$$

and the LFC problem is expressed as a differential equation:

$$\begin{cases} \dot{x}(t) = Ax(t) + Bu(t) + Fw(t) \\ \Delta f(t) = Cx(t) \end{cases} \tag{2}$$

Where:

$$u = [\Delta u_{MT} \quad \Delta u_{DG} \quad \Delta u_{EV1} \quad \Delta u_{EV2}]^T \tag{3}$$

$$w = [\Delta P_D]^T \tag{4}$$

$$A = \begin{bmatrix} 0 & \frac{1}{2H_t} & \frac{1}{2H_t} & 0 & 0 & \frac{1}{2H_t} & \frac{1}{2H_t} \\ 0 & -\frac{1}{T_t} & \frac{1}{T_t} & 0 & 0 & 0 & 0 \\ -\frac{1}{R_{mt}T_f} & 0 & -\frac{1}{T_f} & 0 & 0 & 0 & 0 \\ 0 & 0 & 0 & -\frac{1}{T_d} & \frac{1}{T_d} & 0 & 0 \\ -\frac{1}{R_{dg}T_g} & 0 & 0 & 0 & -\frac{1}{T_g} & 0 & 0 \\ 0 & 0 & 0 & 0 & 0 & -\frac{1}{T_{e1}} & 0 \\ 0 & 0 & 0 & 0 & 0 & 0 & -\frac{1}{T_{e2}} \end{bmatrix}$$

$$B = \begin{bmatrix} 0 & 0 & 0 & 0 \\ 0 & 0 & 0 & 0 \\ \frac{1}{T_f} & 0 & 0 & 0 \\ 0 & 0 & 0 & 0 \\ 0 & \frac{1}{T_g} & 0 & 0 \\ 0 & 0 & \frac{1}{T_{e1}} & 0 \\ 0 & 0 & 0 & \frac{1}{T_{e2}} \end{bmatrix} \quad F = \begin{bmatrix} -\frac{1}{2H_t} \\ 0 \\ 0 \\ 0 \\ 0 \\ 0 \\ 0 \end{bmatrix} \quad C = \begin{bmatrix} 1 \\ 0 \\ 0 \\ 0 \\ 0 \\ 0 \\ 0 \end{bmatrix}$$

The matrixes A, B, F and C are the system state matrix, the input matrix, the disturbance matrix and the output matrix, respectively. Also,x, u, w are the state variables, the controlled input and the uncontrolled input (power disturbance), respectively. The MG model parameters are shown in Table 1. Some of the values are chosen referring to [3], [30], [34].

Table 1 - Parameters of the micro-grid model.

Grid component	Parameters		Values	unit
MT	T_f		0.1	s
	T_t		10	s
	R_{MT}		2.5	Hz/pu.MW
	δ_{MT}		0.01	pu.MW/s
	μ_{MT}		0.04	pu.MW
DG	T_g		0.1	s
	T_d		8	s
	R_{DG}		2.5	Hz/pu.MW
	δ_{DG}		0.01	pu.MW/s
	μ_{DG}		0.04	pu.MW
EV1	T_{e1}		1	s
	δ_{e1}		0.05	Pu.MW/s
	μ_{e1}		0.025	pu.MW
	$E_{max.}$		0.95	pu.MWh
	$E_{min.}$		0.80	pu.MWh
EV2	T_{e2}		1	s
	δ_{e2}		0.05	Pu.MW/s
	μ_{e2}		0.015	pu.MW
	$E_{max.}$		0.90	pu.MWh
	$E_{min.}$		0.80	pu.MWh
Grid Inertia	H_t	Isolated Mode	7.11	s
		Grid-connected Mode	21.08	s

Chapter 4
The Proposed Controllers

4.1 Conventional Controller

In conventional control scheme, Proportional integral derivative (PID) controller is considered as the standard control design, and it is also taken as a generic control loop feedback mechanism which is broadly accepted by industrial applications. The performance specification of the system depends on the values of proportional gain K_p, integral gain K_i, and derivative gains K_d. By varying the gain, parameters required performance of the system can be achieved. The controller output u(t) in terms of error e(t) is given as [1]:

$$u(t) = K_p e(t) + K_i \int e(t)dt + K_d \frac{de(t)}{dt} \tag{5}$$

This equation can be written as;

$$u(t) = K_p \left(e(t) + \frac{1}{T_i} \int e(t)dt + T_d \frac{de(t)}{dt}\right) \tag{6}$$

Where T_i, and T_d are integral and derivative time constants. The variable error, i.e., e(t), is equal to the real system frequency deviation (Δf). The proposed PID controller, figure 6, is implemented as per equation (5).

4.2 Artificial Intelligent Controller

To regulate a quality of generation of electricity in any power system must control the system output so that the voltage and frequency maintained. Accordingly, the control system is necessary for power systems, particularly at isolated hybrid system [37].

In this study, I used three different intelligent controllers, i.e., Interval Type-1 Fuzzy (IT1 Fuzzy), Interval Type-2 Fuzzy (IT2 Fuzzy) logic controller and Adaptive Neuro-Fuzzy Controller to control the LFC of the MG power system.

4.2.1 Interval Type-1 Fuzzy Logic Controller

Fuzzy logic is a thinking process or problem-solving control methodology incorporated in control system engineering, to control systems while inputs are either imprecise or the mathematical model are not present at all [38]. The structure of interval type-1 fuzzy logic controller is shown in figure 10 and the block diagram is shown in figure 7. The system frequency deviation Δf and its derivative are the two input signals, and the provided control signal used by the LFC participants' units. To obtain normalized inputs and output for fuzzy logic controller, the constant gain blocks are used as scaling factors K_e, K_{ec}, and K_u, respectively as shown in figure 7.

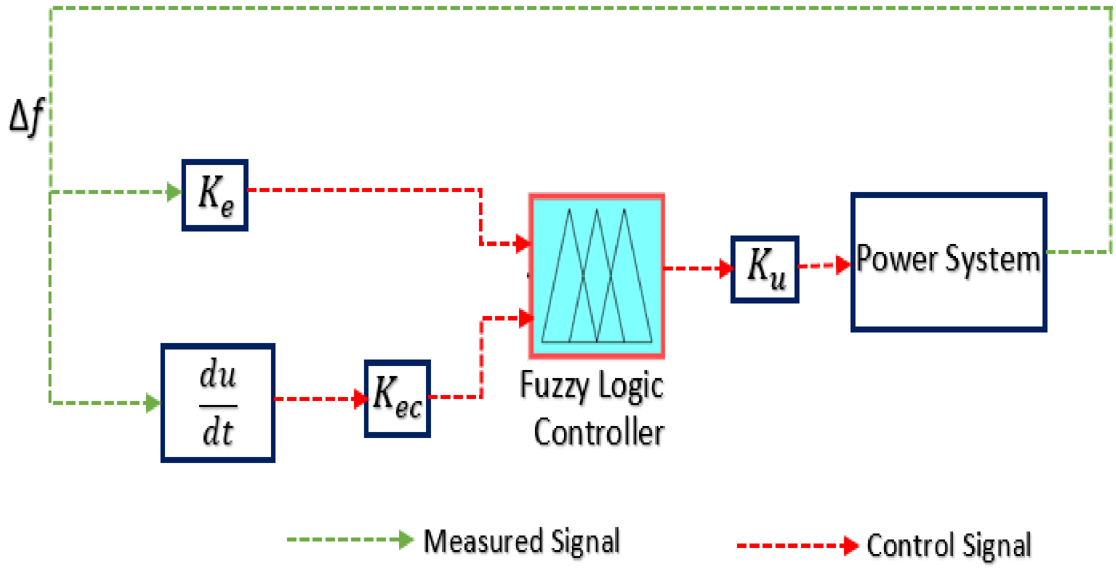

Figure 7 - Block diagram of Fuzzy logic controller (for both IT1 and IT2).

The two well-known fuzzy rule-based inference systems are Mamdani fuzzy method and Tagaki-Sugeno (T-S) fuzzy method. Mamdani fuzzy inference system has advantages of the following: (I) It's intuitive, (II) It has widespread acceptance and (III) It's well-suited to human cognition. The Mamdani fuzzy inference system shows its advantage in output expression and used in this thesis [39], [40], [41]. In figure 8 shows, the Mamdani Interval Type-1 Fuzzy logic designer with two inputs, Δf and dΔf/dt, and one controllable output.

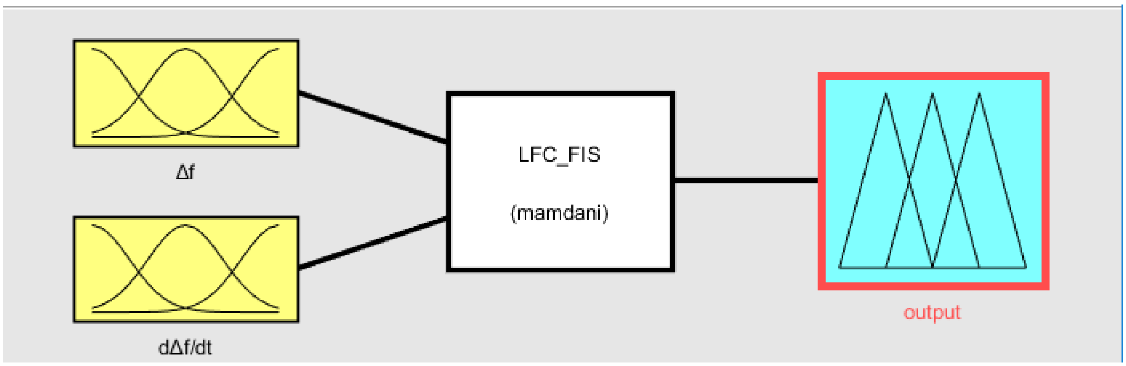

Figure 8 - FIS editor of Mamdani Interval type-1 Fuzzy logic toolbox.

(I)

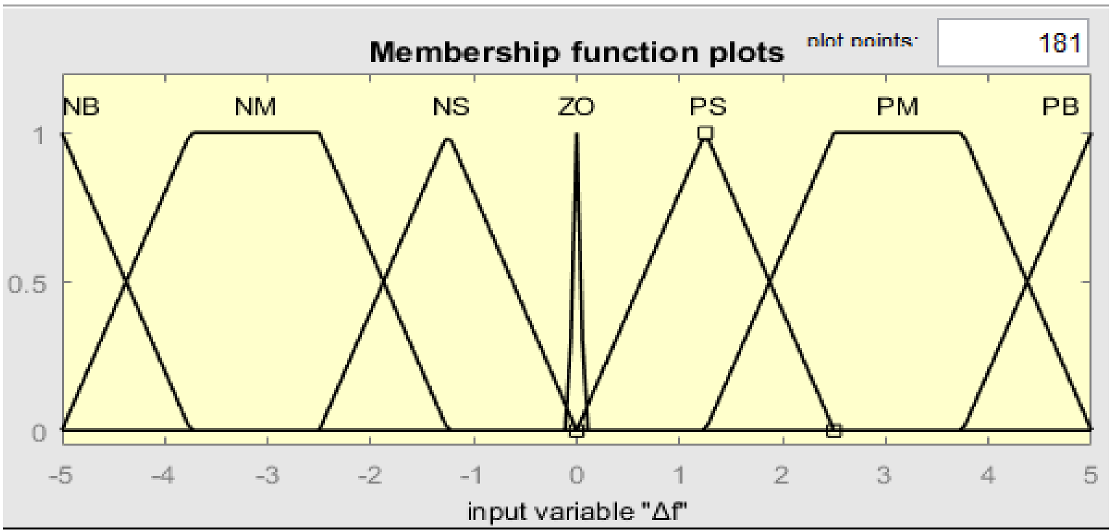

II)

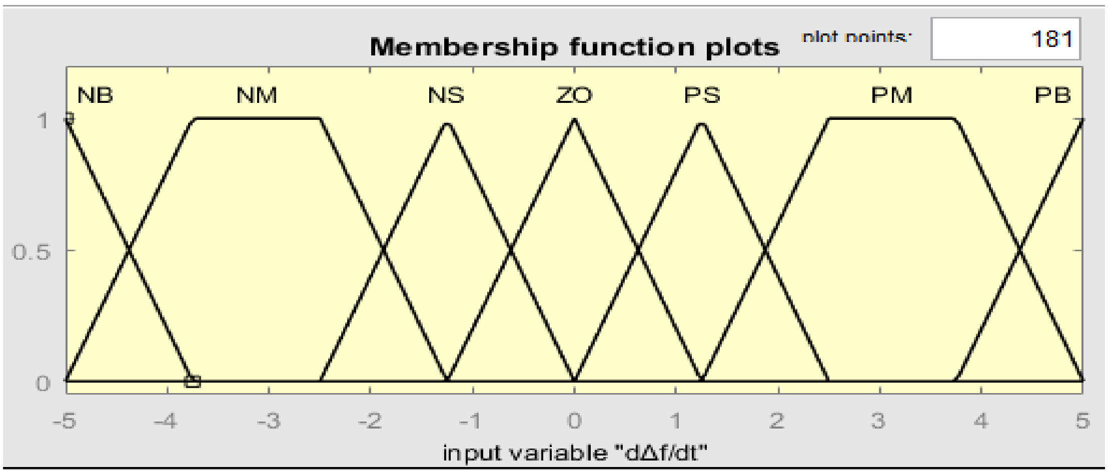

III)

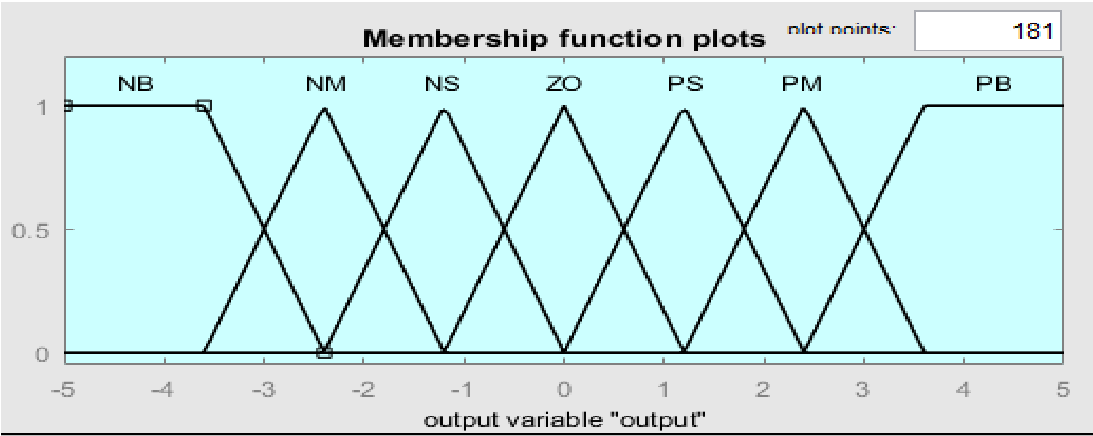

Figure 9 - Membership functions of IT1 fuzzy control used in this thesis; (I) and (II) are input patterns (III) is output pattern.

The membership for the input and output variables are sown in figure 9. As can be observed from this figure, trapezoidal and triangular membership functions are both applied. The input and output variables in the proposed controller are represented as set of seven-linguistic variables and defined namely as the following,

NB - Negative Big
NM - Negative Medium
NS - Negative Small
ZO - Zero
PS - Positive Small
PM - Positive Medium, and
PB - Positive Big.

Each the above fuzzy variable has a member of the subsets with a degree of membership varying between [-5, 5].

There are totally 49 fuzzy rules that are considered in this design, which is shown in Table 2. This rule base works on the vector composed of the two input signals. The "T-norms" are based on interpreting the "and" by taking the minimum of the two membership values. First crisp inputs are mapped to linguistic values and then combined based on all the rules by using "sum" method. Finally, the "centroid" method is used for defuzzification, for converting the output to a crisp value [42].

Table 2 - Rule base fuzzy logic controller.

Inputs		Δf						
		NB	NM	NS	ZO	PS	PM	PB
dΔf/dt	NB	NB	NB	NB	NB	NM	NS	ZO
	NM	NB	NB	NB	NM	NS	ZO	PS
	NS	NB	NB	NM	NS	ZO	PS	PM
	ZO	NB	NM	NS	ZO	PS	PM	PB
	PS	NM	NS	ZO	PS	PM	PB	PB
	PM	NS	ZO	PS	PM	PB	PB	PB
	PB	ZO	PS	PM	PB	PB	PB	PB

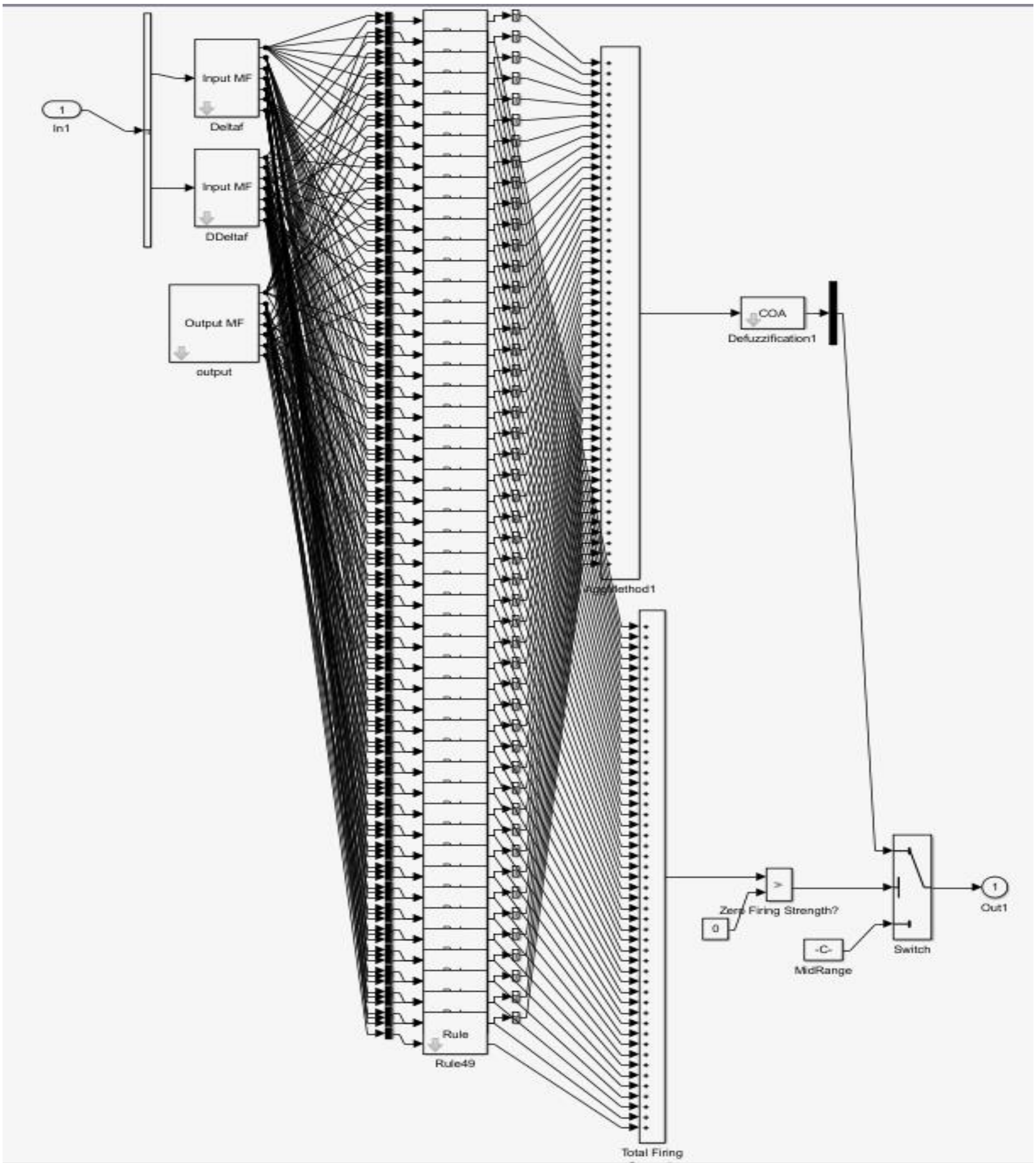

Figure 10 - Structure of IT1 fuzzy logic controller.

4.2.2 Interval Type-2 Fuzzy Logic Controller

The Interval Type-2 Fuzzy Logic Controller uses interval type-2 fuzzy sets to represent the inputs and outputs of the controller. In contrast with IT1 FLC, the IT2 FLC consists of five elements, as we seen from figure 11, i.e. the fuzzifier, the fuzzy rule base, the inference engine, the type reducer, and de-fuzzifier [50].

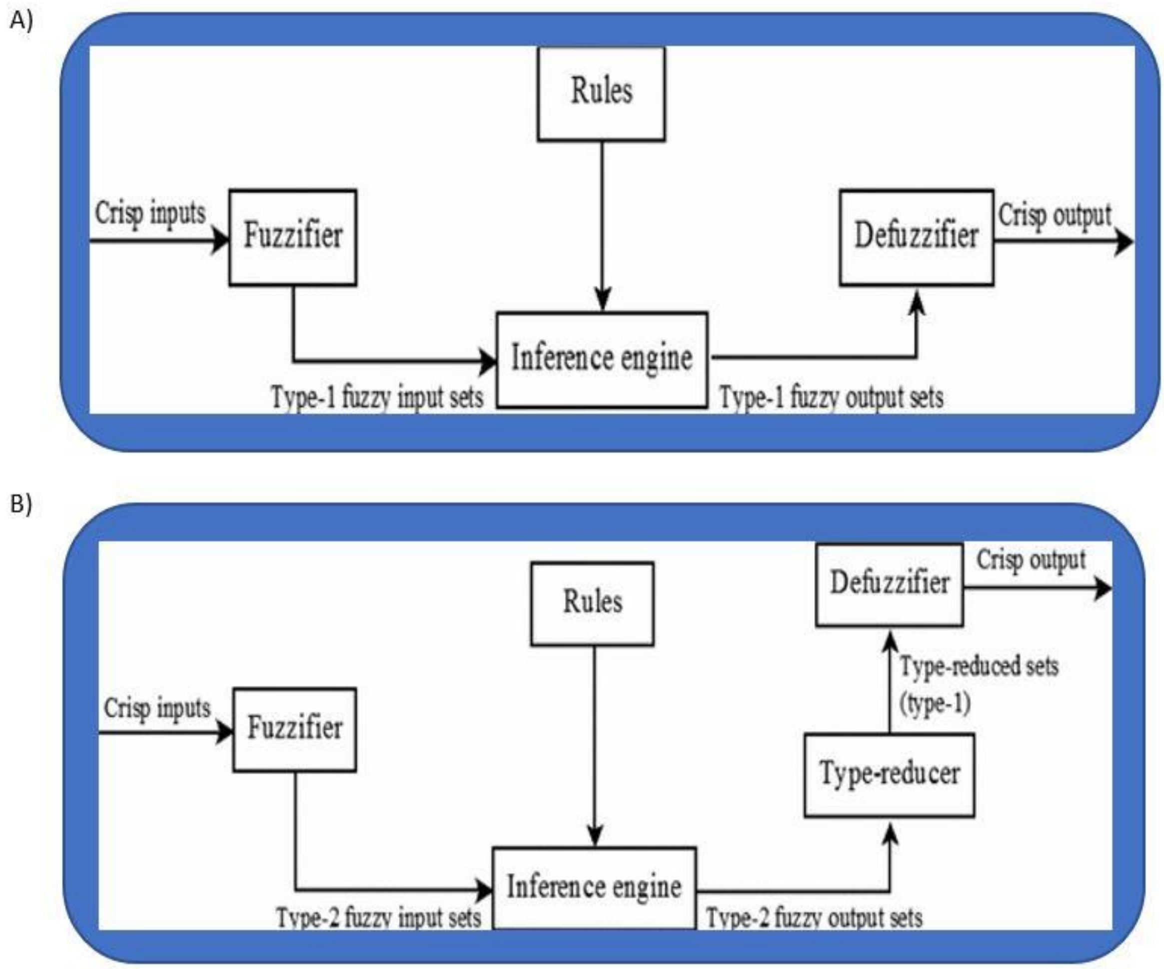

Figure 11 - The Structure of FLC, (A) is interval type-1 and (B) is interval type-2.

The structure of IT2 FLC is similar to its type-1 counterpart as shown in figure 11, the key difference being that at least one of the fuzzy sets in the rule base is type-2. So, the output of the inference engine is type-2 sets and a type-reducer is needed to change them into type-1 sets before de-fuzzification can be carried out.

The output of the inference engine is a type-2 fuzzy set, it must be a type-reducer before the defuzzifier can be used to generate a crisp output, this is the main structural difference between type-1 and type-2 FLCs. The most commonly applied type-reduction method is the center-of-sets type-reducer, in this study also used. A more detailed description of interval type-2 FLCs could be found in [50], [51].

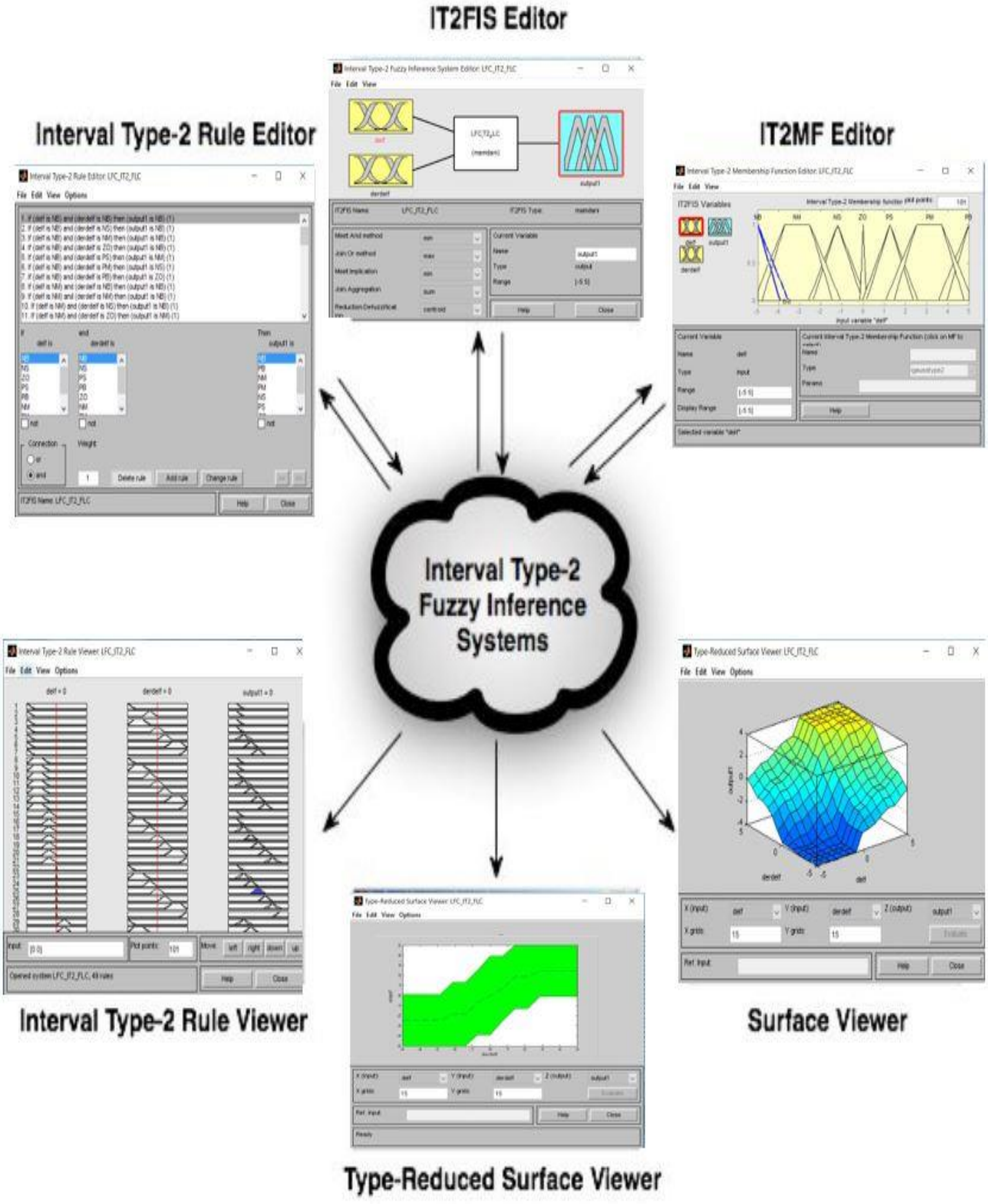

Figure 12 - Implementation of Type -2 Fuzzy inference system in MATLAB

(I)

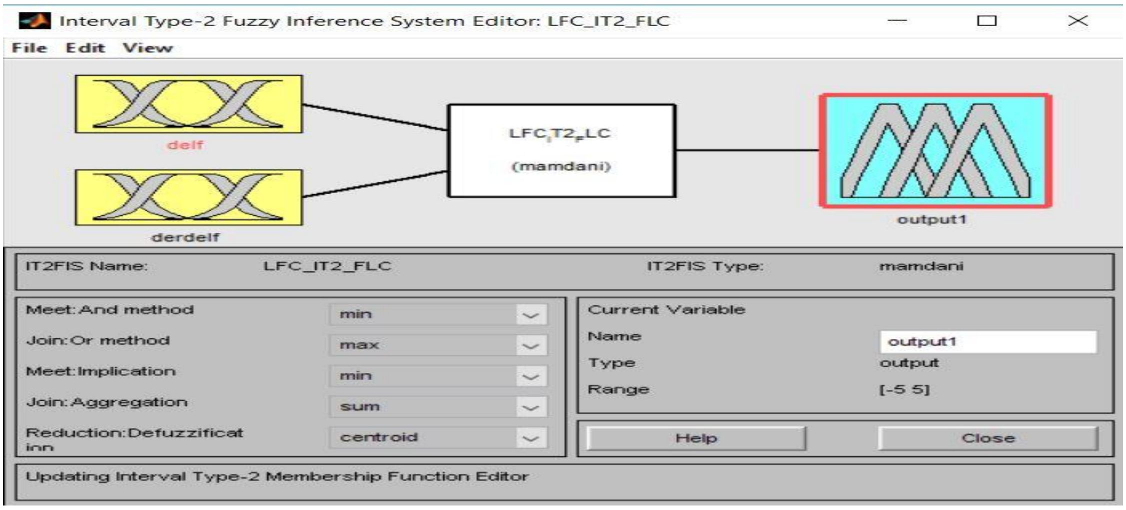
Interval Type-2 Fuzzy Inference System Editor: LFC_IT2_FLC
File Edit View
delf
derdelf
LFC_IT2_FLC
(mamdani)
output1
IT2FIS Name: LFC_IT2_FLC
IT2FIS Type: mamdani
Meet:And method min
Join:Or method max
Meet:Implication min
Join:Aggregation sum
Reduction:Defuzzification centroid
Current Variable
Name output1
Type output
Range [-5 5]
Help
Close
Updating Interval Type-2 Membership Function Editor

II)

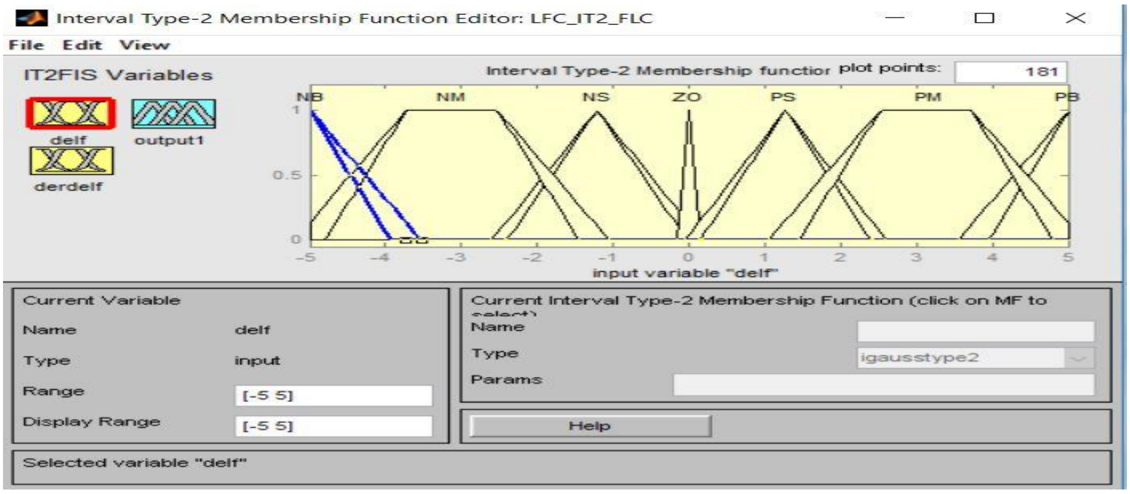
Interval Type-2 Membership Function Editor: LFC_IT2_FLC
File Edit View
IT2FIS Variables
delf
output1
derdelf
Interval Type-2 Membership function plot points: 181
NB NM NS ZO PS PM PB
input variable "delf"
Current Variable
Name delf
Type input
Range [-5 5]
Display Range [-5 5]
Current Interval Type-2 Membership Function (click on MF to select)
Name
Type igausstype2
Params
Help
Selected variable "delf"

III)

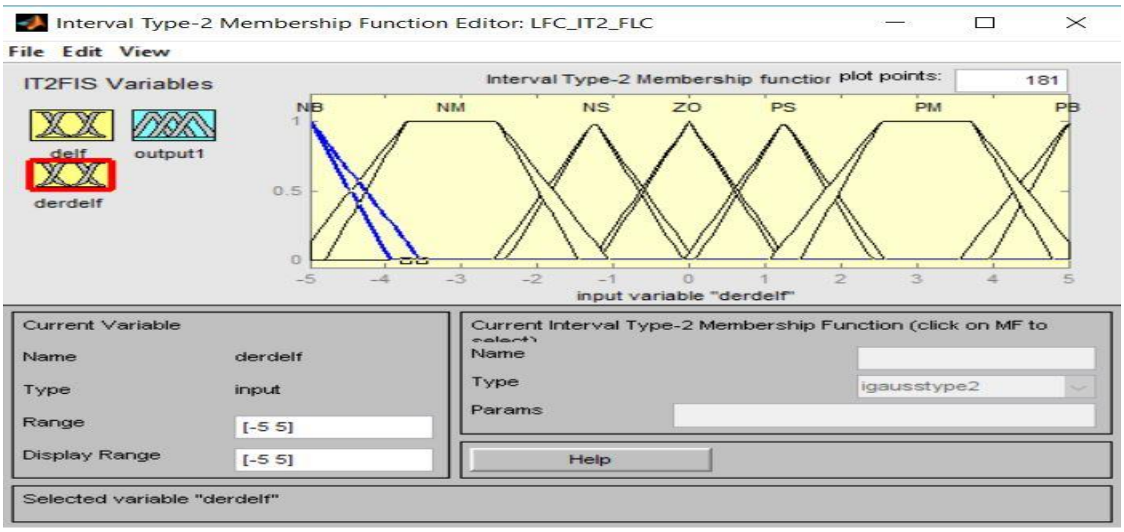
Interval Type-2 Membership Function Editor: LFC_IT2_FLC
File Edit View
IT2FIS Variables
delf
output1
derdelf
Interval Type-2 Membership function plot points: 181
NB NM NS ZO PS PM PB
input variable "derdelf"
Current Variable
Name derdelf
Type input
Range [-5 5]
Display Range [-5 5]
Current Interval Type-2 Membership Function (click on MF to select)
Name
Type igausstype2
Params
Help
Selected variable "derdelf"

IV)

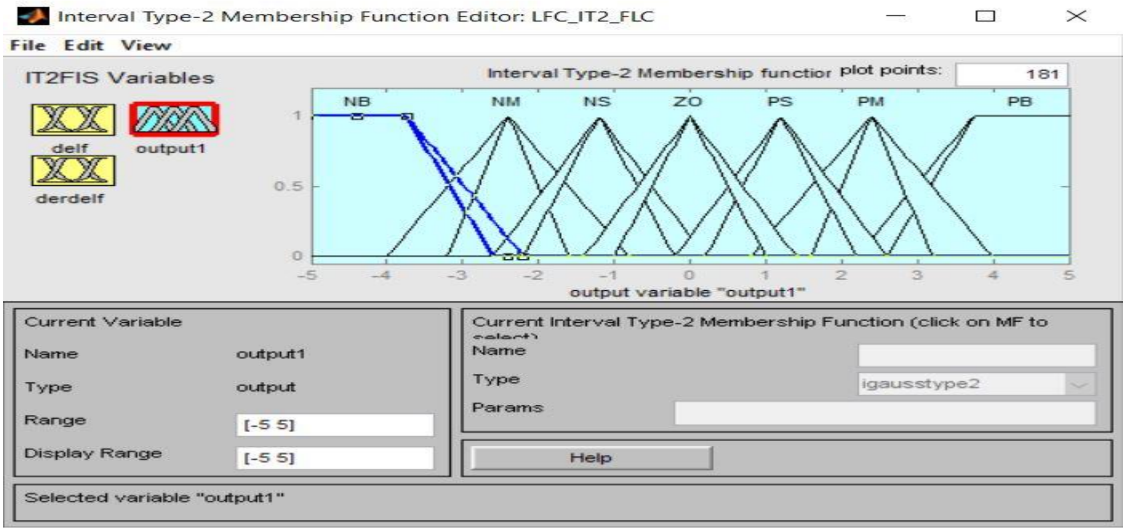

Figure 13 - The FIS editor of Mamdani Interval type-2 Fuzzy logic toolbox (I) and Membership functions of IT2 fuzzy control used in this thesis; (II) and (III) are input patterns (IV) is output pattern.

The interval type-2 fuzzy rules are the same to as IT1 Fuzzy rules as shown in Table 2, In the IT2 FLC delf means Δf, and similarly, derdelf means $d\Delta f/dt$. The rules of IT2 FLC are edited using Mamdani method as given in figure 13.

4.2.3 Adaptive Neuro Fuzzy controller (ANFIS)

I) ANFIS structure and control

Adaptive Neuro-Fuzzy Inference System (ANFIS) is an intelligent neuro-Fuzzy technique, which was originally proposed by Jang in 1993 [43]. Neuro-fuzzy techniques are developed from the fusion of Artificial Neural Network (ANN) and Fuzzy Inference Systems (FIS). ANFIS have an advantage of both fuzzy and ANN [43], [44]. It combines the learning power of neural network with knowledge representation of fuzzy logic to implement a different mode of functions and consequently to tune the parameters of fuzzy inference system. The proposed block diagram of the neuro-fuzzy controller for this study is given in figure 14 [44]. In this figure, the control signal (the control input U) represents all controllable variables, i.e., (Δu_{MT}, Δu_{DG}, Δu_{EV1}, and Δu_{EV2}).

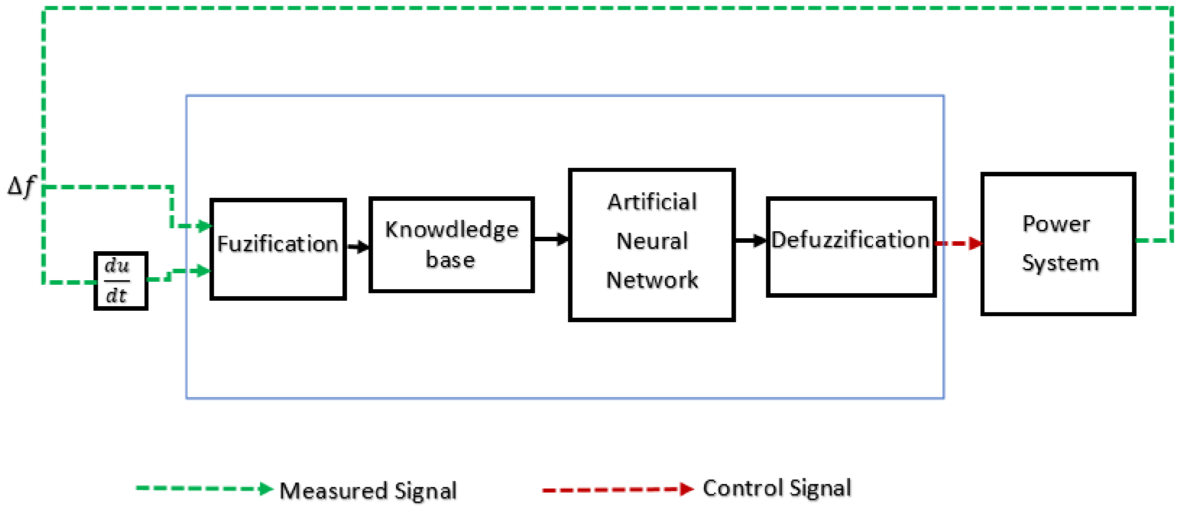

Figure 14 - Block diagram of Neuro-Fuzzy controller.

The ANFIS is a multi-layer adaptive neural network-based fuzzy inference system. The architecture of the ANFIS system is shown in the Figure 15 [43], [44]. In this study, the fuzzy inference system has two sets of inputs Δf and $\Delta\dot{f}$ and one output$U$. Suppose that the rule base contains two fuzzy if-then rules of Takagi and Sugeno's type. For example,

Rule 1: If Δf is X1 and $\Delta\dot{f}$ is Y1 , then $u_1 \;= p_1\Delta f + q_1\Delta f + r_1$
Rule 2: If Δf is X2 and $\Delta\dot{f}$ is Y1 , then $u_2 \;= p_2\Delta f + q_2\Delta f + r_2$

Layer 1: This layer is an adaptive node and also known as fuzzification layer. The values of parameters of this layer are changes according to the error signal and generate the proper value of each membership function, each node denoted as i, and adaptive with a node function, as shown;

$$o_i^1 = \mu_{X_i}(\Delta f) \quad \text{for } i = 1,2 \quad \ldots\ldots(7)$$
$$o_i^1 = \mu_{Y_{i-2}}(\Delta\dot{f}) \quad \text{for } i = 3,4 \quad \ldots\ldots(8)$$

where, Δf (or $\Delta\dot{f}$) is input at node i, while X_i (or Y_i) is a linguistic label (fuzzy sets: Big, Small, …) μ_{X_i} and μ_{Y_i} represents the member ship functions of each nodes. The parameters in this layer the basic parameters or named as precondition parameters.

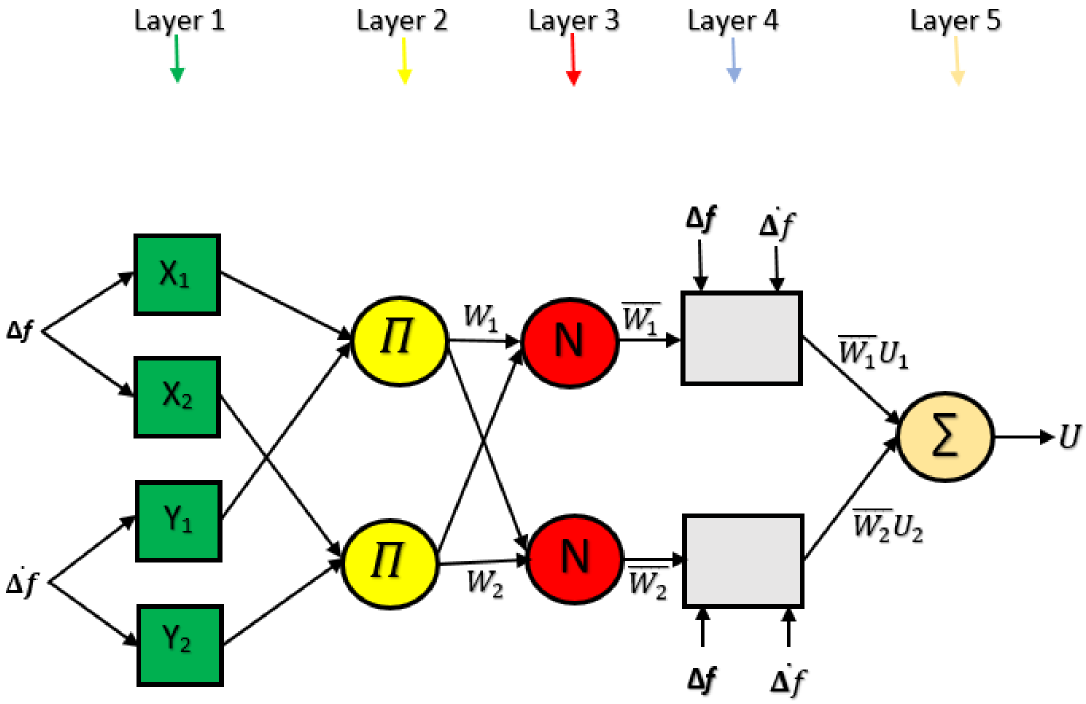

Figure 15 - Architecture of ANFIS

Layer 2: In this layer, the outputs of the first layer are multiplies with each other and forwards it to the next layer. The node in this layer is a fixed node and labelled Π (AND or Multiplication), which is used to calculate the degree of activation or (firing strength) w_i of a rule. The output obtained from each node of this layer is given by;

$$o_i^2 = w_i = \mu_{X_i}(\Delta f)\times\mu_{Y_i}(\Delta\dot{f}) \text{ for } i = 1,2 \ldots\ldots\ldots\ldots\ldots\ldots (9)$$

Layer 3: This layer calculates the normalized firing strength of each rule and labelled as N (Normalization). Each node in this layer is also a fixed [44].The output of this layer is the normalized firing strength of each node which is calculated as the ratio of the i^{th} rule's firing strength to the sum of firing strengths of all the rules, the output from the i^{th} node is the normalized firing strength ($\overline{w_i}$) and is given by ;

$$o_i^3 = \overline{w_i} = \frac{w_i}{w_1+w_2} \text{ for } i = 1,2 \ldots\ldots\ldots\ldots\ldots\ldots (10)$$

Layer 4: Each node in this layer is an adaptive node and the output obtained from this layer is given as follows;

$$o_i^4 = \overline{w_i}\, u_i = \overline{w_i}(p_i\Delta f + q_i\Delta\dot{f} + r_i) \text{ for } i = 1,2 \ldots\ldots\ldots\ldots\ldots\ldots (11)$$

where, $\overline{w_i}$ is the output of the third layer and $\{p_i, q_i, r_i\}$ is the parameter set of this node. The parameter in this layer are referred to as consequent parameter.

Layer 5: This layer is the last layer of ANFIS architecture which result the output U and labelled as $\sum$, which computes the overall output as a summation of all incoming signals to the node which is given by;

$$o_i^5 = U = \sum \overline{w_i} u_i = \frac{\sum w_i u_i}{\sum w_i} \quad \text{...(12)}$$

The ANFIS methods of implementing a hybrid-learning algorithm that consists of a combination of, the least squares methods are used to set the parameters of linear consequently, as well as gradient-descent, which is used to identify the parameters of the premise.

Since ANFIS designer starts with the pre-structured system, the input and output membership functions variables contain more information that Neural Network has to drive from sampled data sets. Knowledge regarding the system under design can be used right from the start, the rules are in the linguistic forms and so intermediate results can be analysed and interpreted easily. Modification of rules is possible during the training and optimization can be analysed and interpreted easily [45].

II) Procedural steps to design the ANFIS

The first step for making an adaptive neuro-fuzzy is to draw a load frequency control using fuzzy logic controller i.e. figure 7, [44]. The data of two inputs and output of fuzzy controller gives the training data. The data arranged as column vectors. Input 1, frequency deviation and input 2, the derivative of frequency deviation and the third column data is fuzzy output. ANFSEDIT toolbox is used to generate ANFIS.fis file in MATLAB software. The data loaded in ANFISEDIT. The ANFIS tanning process sown in figure 16 [12], [44]. We generate the initial FIS model before starting FIS training by defining the number and type of membership functions for input. The two partitioning techniques are used by ANFIS to generate the initial FIS model, i.e., Grid partition and Subtractive clustering. Grid partition generates a single-output Sugeno-type FIS by using grid partition on the data whereas Subtractive clustering generate an initial model for ANFIS training by first applying subtractive clustering on the data.

In this thesis, I have chosen the grid partition method to define the fuzzy partition of input data. The ANFIS provide 8 types of membership function (MF) including, Triangular membership function, Gbell MF type, Gaussian MF, etc. The Gbell membership function was suitable for the present study.

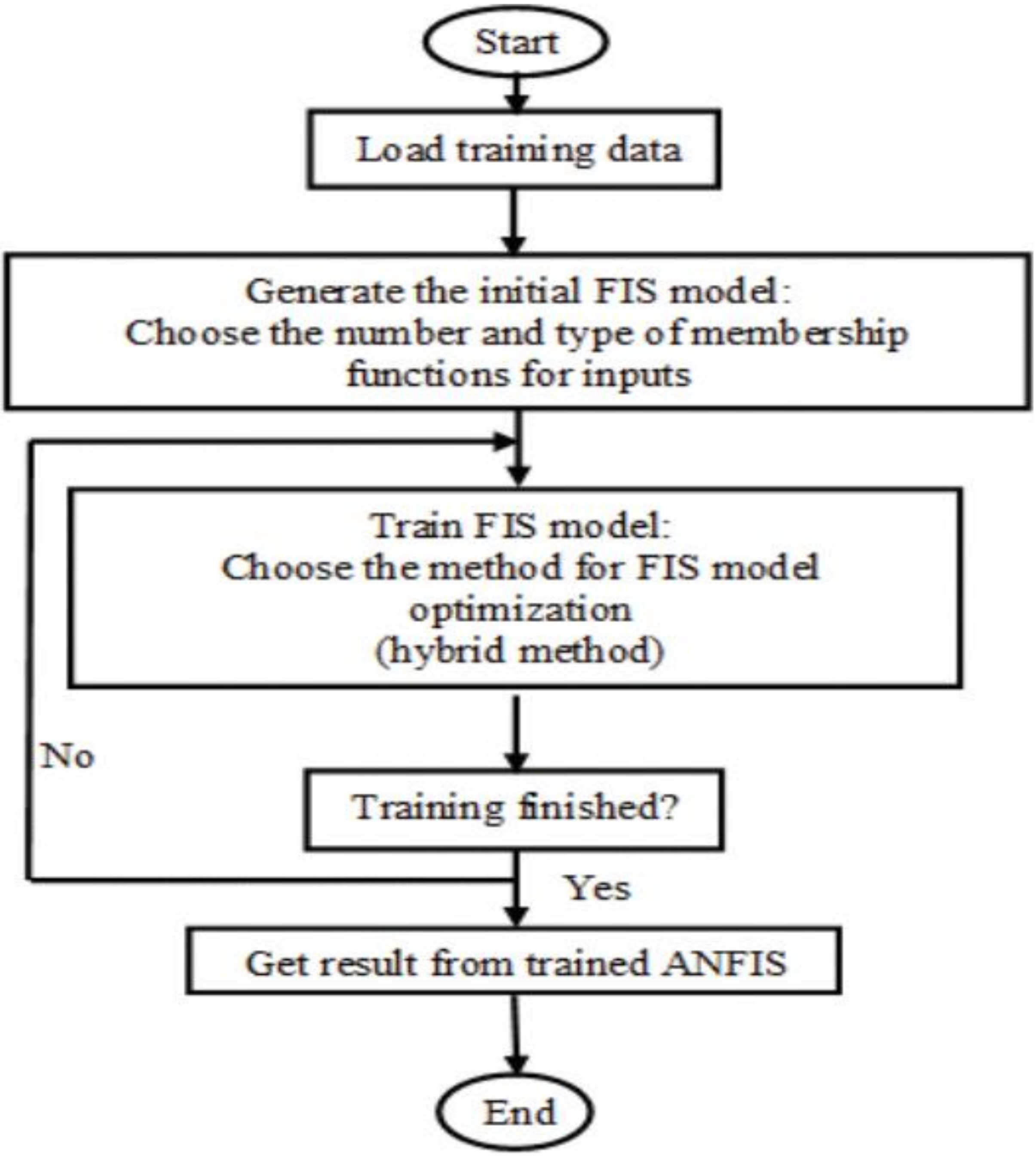

Figure 16 - ANFIS training process

After loading and generating the training data and the initial FIS structure, respectively, then we can start training the FIS. There are two learning algorithms in MATLAB ANFIS, back propagation, and hybrid algorithm. For this study, the input/output data trained through hybrid algorithm by selecting the appropriate number of epochs with zero error tolerances. The great advantage of ANFIS design method comparing with fuzzy design method consists in the small number of input and output membership functions (usually 2…4), which implies the same maximum number of rules. Hence, the rule base and the occupied memory became very small [49].

The frequency deviation and derivative of frequency deviation has been taken with four numbers of membership functions in the first case, the dynamic response to load disturbance. After the application of fuzzy inference system 16 rule base have been developed with 16 output membership function, then after application of DE fuzzification has been extracted one output. The MATLAB model of rule base is give in figure 17 and Figure 18, shows the overall structure of adaptive neuro-fuzzy model FIS Wizard [44], [45], [46].

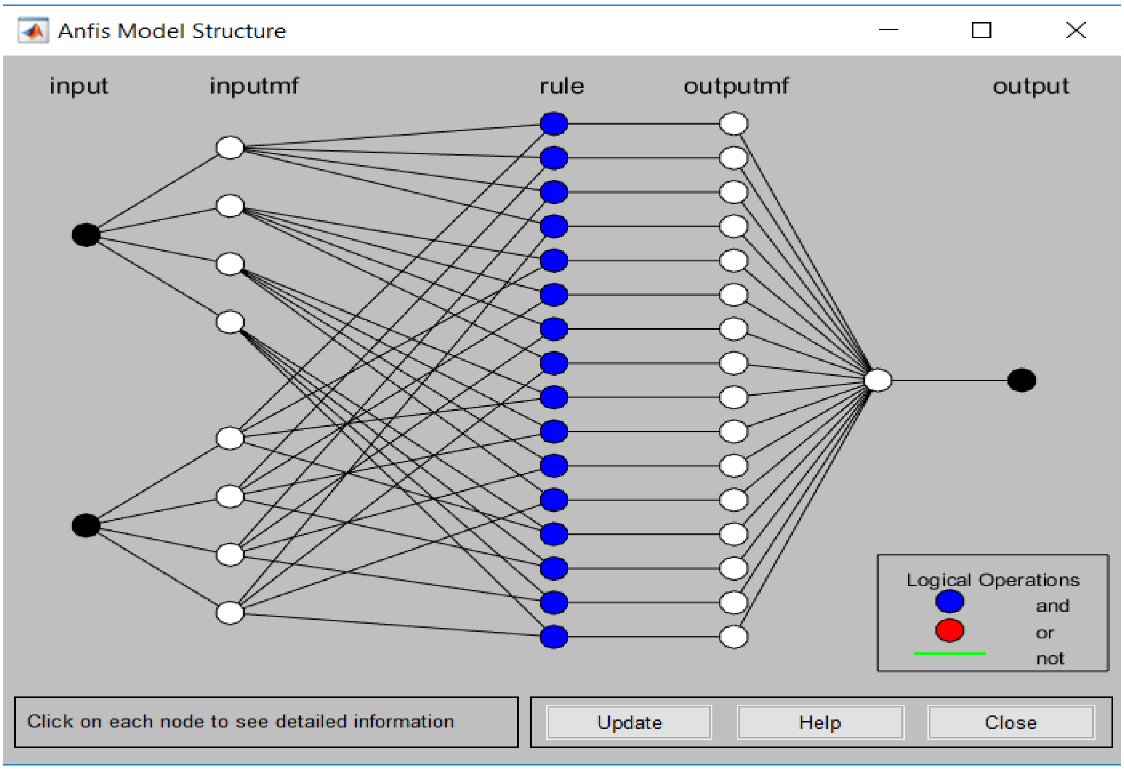

Figure 17 - MATLAB ANFIS model of rule base for the first case.

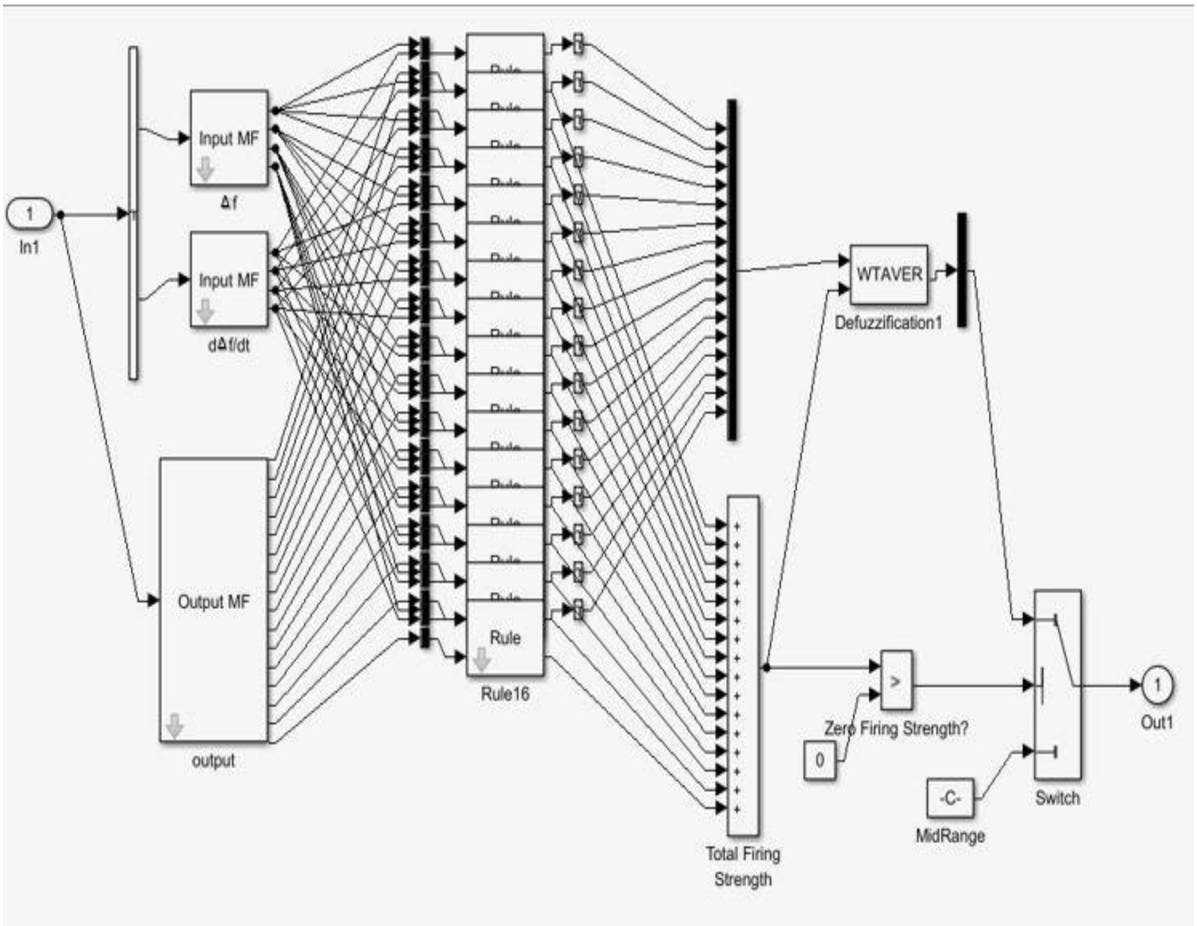

Figure 18 - Structure of adaptive neuro-fuzzy model FIS Wizard for the first case.

Table 3 - Parameters of the PID and Fuzzy controllers.

Controllers	Parameters	Description	Value
PID	K_P	Proportional gain	4
	K_i	Integral gain	1.18
	K_D	Derivative gain	0.5
FUZZY LOGIC	K_e	Scaling factors 1	5000.3
	K_{ec}	Scaling factors 2	156.99976
	K_u	Scaling factor 3	0.0211572

Chapter 5
Simulation Results

In this chapter, to demonstrate the performance of the proposed LFC based on ANFIS controller; several simulations are presented. The simulations are carried out based on the model as mentioned earlier of Micro-grid, i.e. figure 5 with the system parameters given in table 1 and table 3.

A. The comparison of the PID controller, interval type-1 fuzzy controller (Mamdani model), interval type-2 fuzzy controllers (Mamdani model) and ANFIS based Neuro-Fuzzy controller to damp the modelled MG system frequency oscillation are presented without the consideration of the constraints of MT, DG, and EVs in each first sub cases has presented, i.e. Case1(A), Case2(A), Case3(A), Case4(A), Case5(A) and Case6(A).

B. The comparison of the PID controller, interval type-1 fuzzy controller (Mamdani model) and ANFIS based Neuro-Fuzzy controller to damp the modelled MG system frequency oscillation are presented with the consideration of the constraints of MT, DG, and EVs in each second sub cases has presented. i.e. Case1(B), Case2(B), Case3(B), Case4(B), Case5(B) and Case6(B).

It is stablished in the MATLAB/SIMULINK environment. The simulations of cases studies are achieved by using MATLAB version R2016b and for Interval type-2 fuzzy MATLAB version 7.8.0 (R2009a).

5.1 Case 1: Load Disturbance

In this case, a step load disturbance of $\Delta PL = 0.05$ pu is applied at $t = 0$ s. By the assumption that the output power of wind generations and solar PV generation are constant with steady wind speed and sun condition for a short period, i.e. $\Delta PW = 0$ pu and $\Delta PPV = 0$ pu. The performance of the ANFIS controller on load disturbance investigated. A clear comparison with the conventional PID controller, Interval type-1 and Interval type-2 fuzzy controller under the consideration of constraints and without constraints, different performance measures such as settling time, rise time, overshoots and undershoot are computed as shown in Table 4, 5 and 6. The total simulation time is 70 second.

5.1.1 Case1(A)-Without considering the constraints of MT, DG and EVs.

For this scenario, there are no output constraints of MT, DG, and EVs. The design of ANFIS neuro-fuzzy based controller is set as follows: as presented in chapter 4 section 4.2.3. Part (II) Procedural steps to design the ANFIS). Figure 19, shows the membership editor (FIS editor) of Sugeno-type fuzzy inference system with two inputs, i.e. error and the derivative of error and the control output. Each input has a four membership functions with 16 rules are framed and shown in figure 20, 21 and 23 respectively. In figure 22 the output membership function with sixteen output variables is showed. The rules are viewed by rule viewer as shown in figure 24.

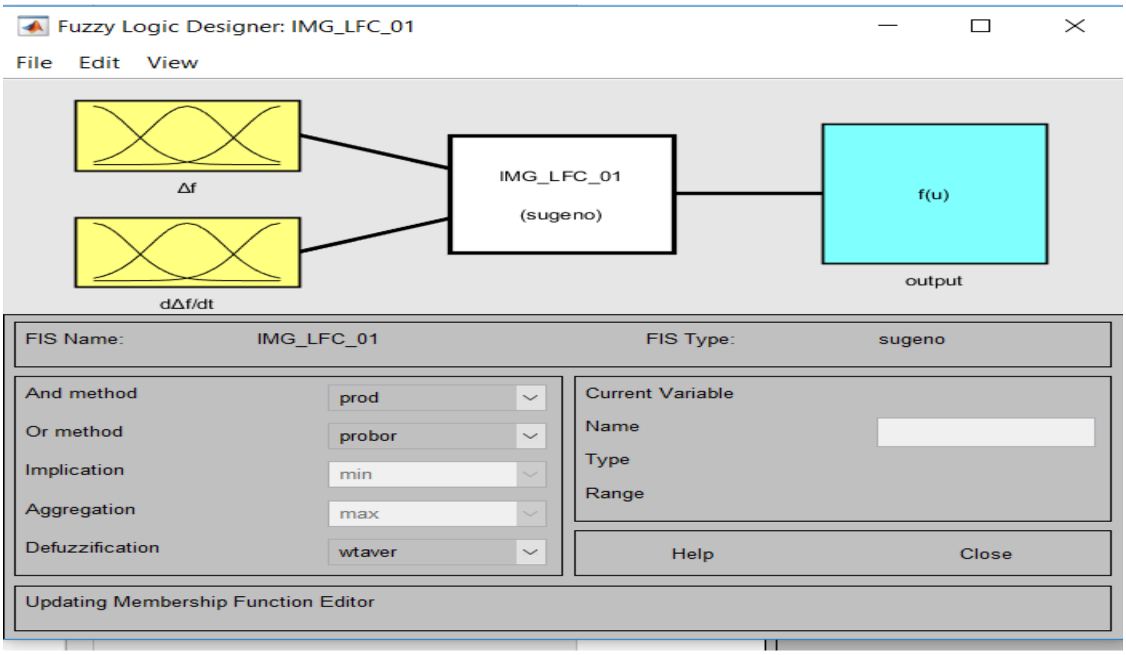

Figure 19 - FIS editor (Sugeno model) with two inputs and one output.

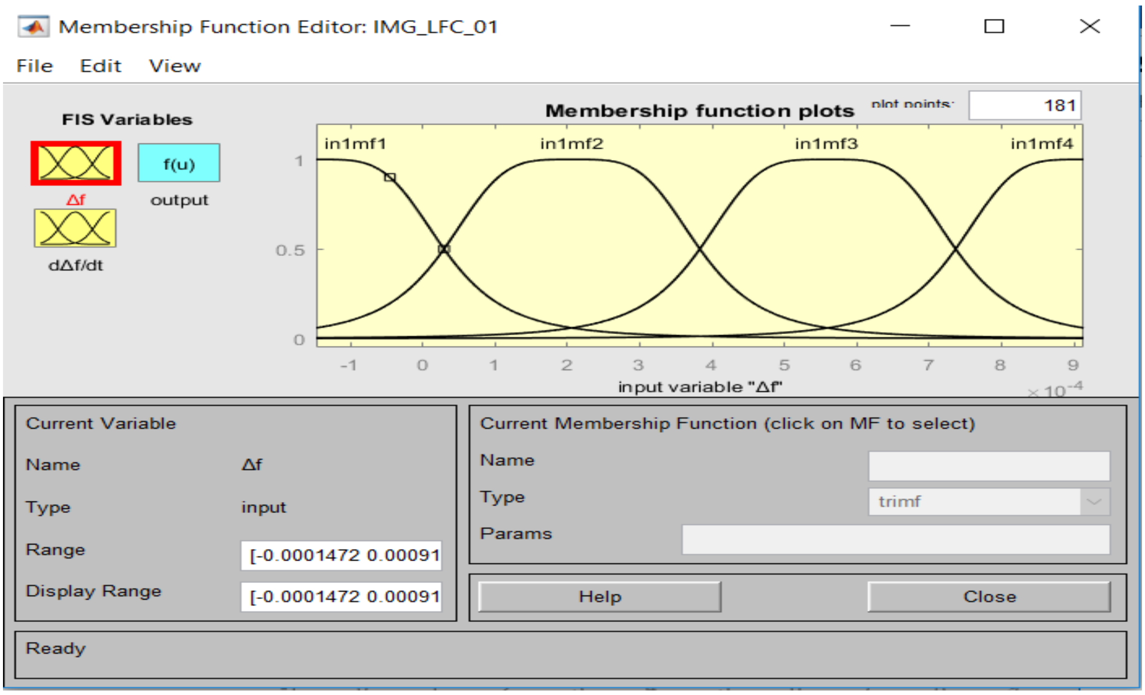

Figure 20 - The frequency deviation Input membership function after completion of training

.

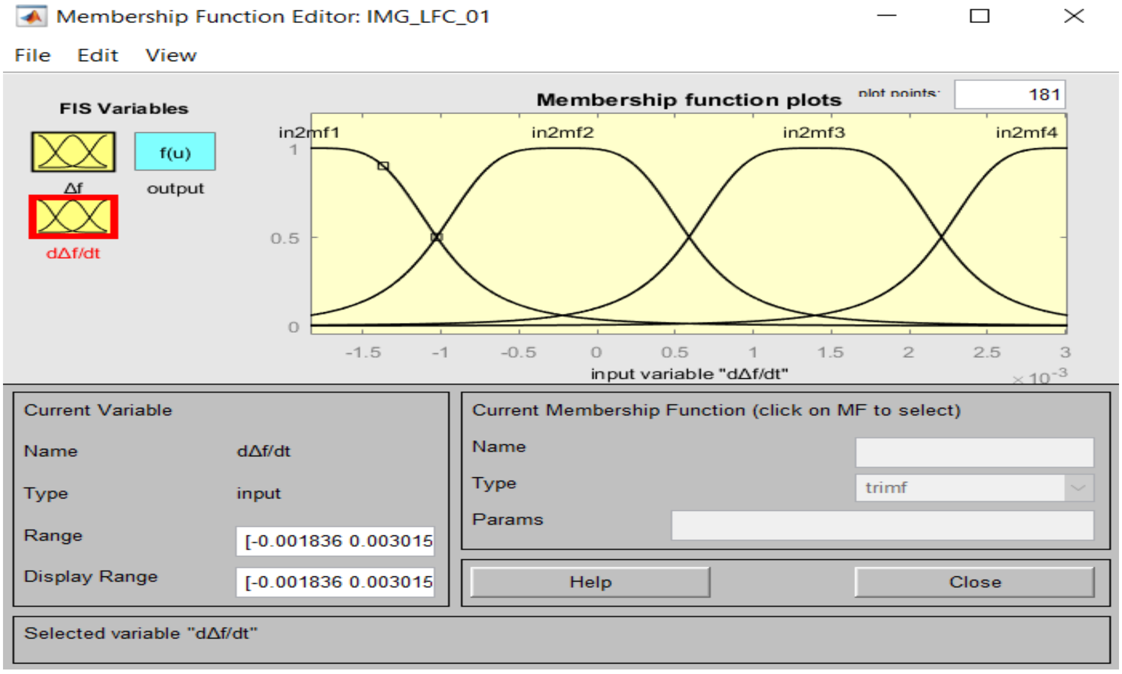

Figure 21 - Derivative of frequency deviation Input membership function after completion of training.

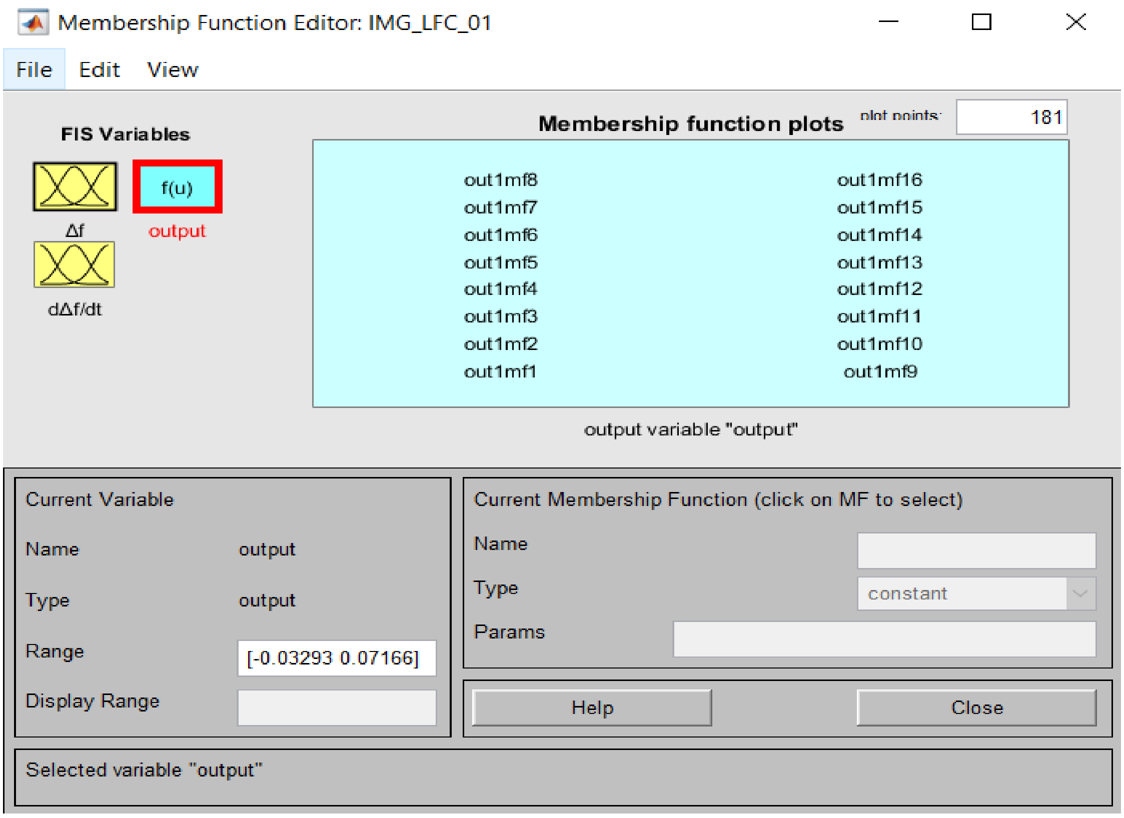

Figure 22 - Output membership function after completion of training.

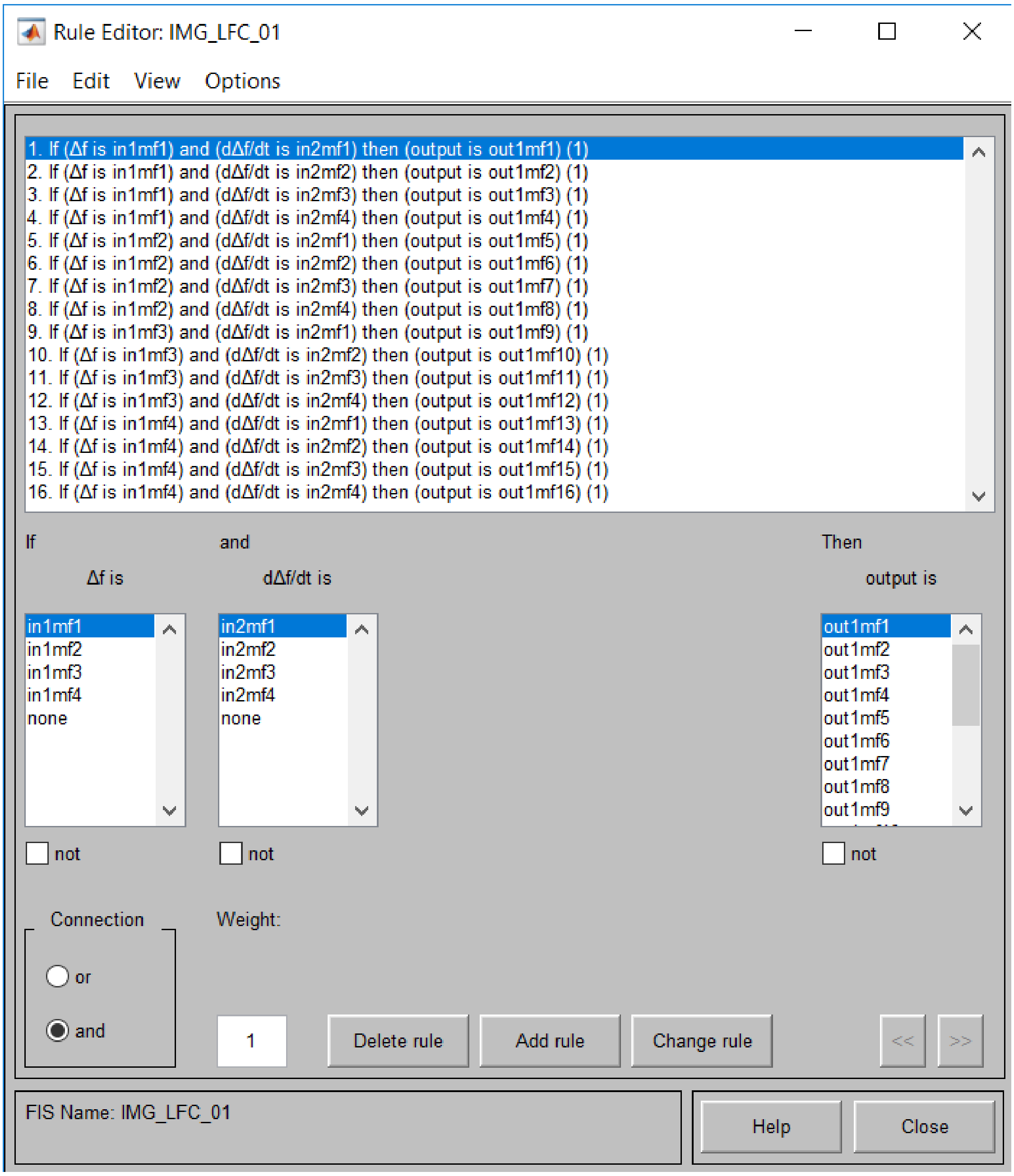

Figure 23 - ANFIS Rule Editor.

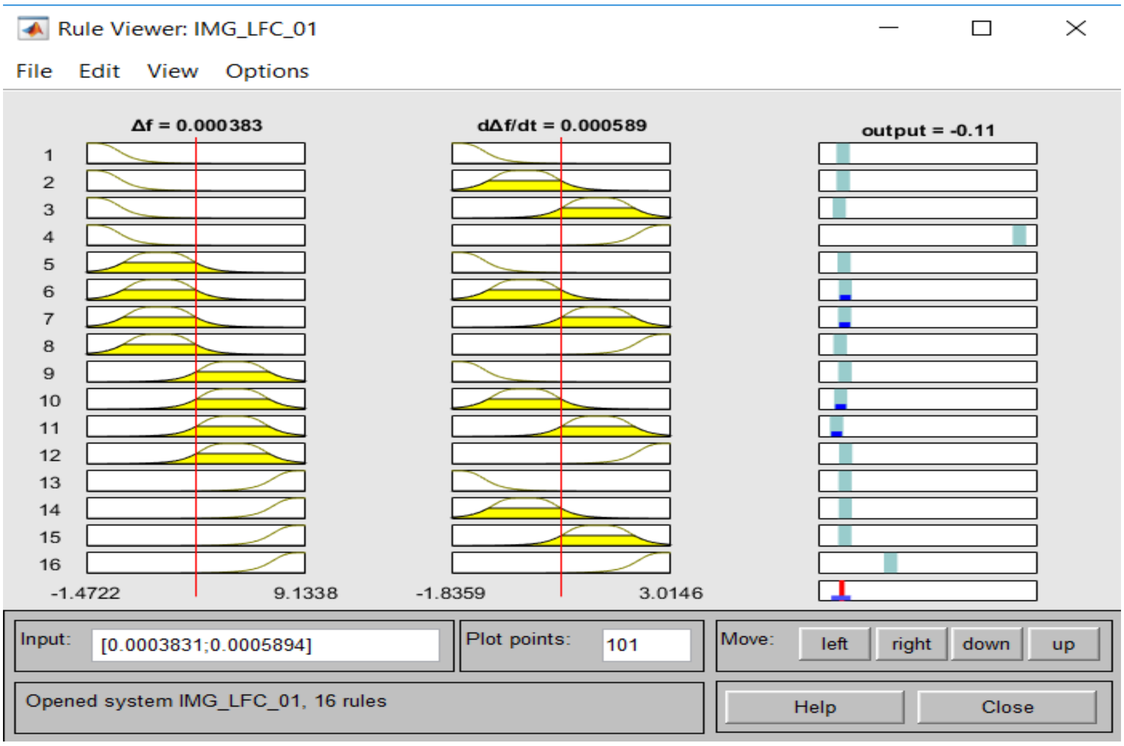

Figure 24 - ANFIS Rule Viewer.

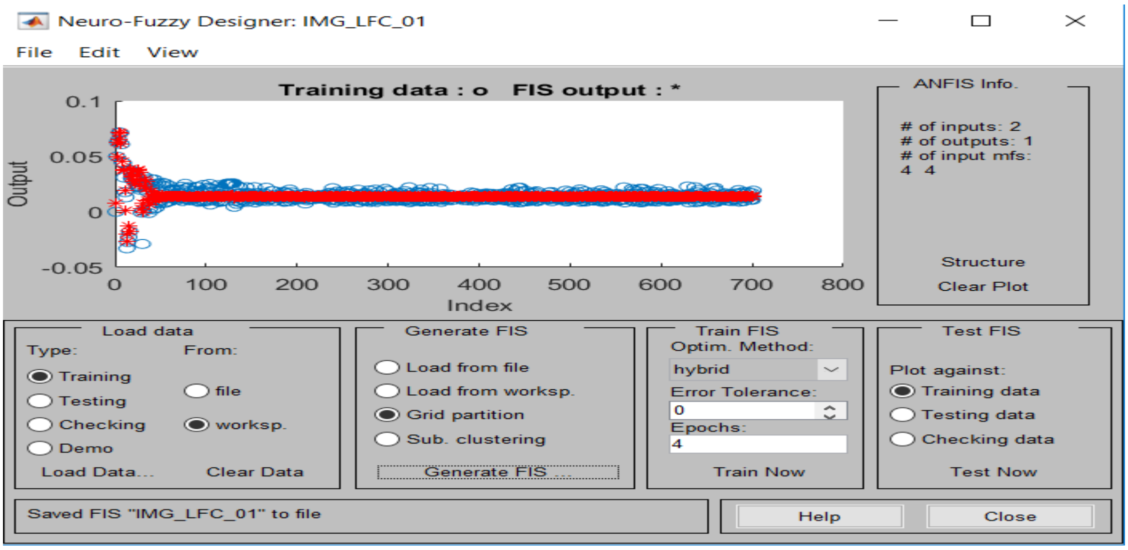

Figure 25 - ANFIS Designer, training data with hybrid optimization method.

Figure 25 shows the loading and training of data by using hybrid optimization method with epochs 4 and zero error tolerance. Grid partition technique generates the FIS. From MATLAB simulation, the ANFIS information is as follows:

ANFIS info:

Number of nodes: 53
Number of linear parameters: 48
Number of nonlinear parameters: 24
Total number of parameters: 72
Number of training data pairs: 701
Number of checking data pairs: 0
Number of fuzzy rules: 16

Start training ANFIS …

1 0.00404137
2 0.00428166

Designated epoch number reached --> ANFIS training completed at epoch 2.

The ANFIS structure is showed on Figure 17. The variation of the controlled output (output) with the changes of the frequency deviation (Δf) and the derivative of the changing frequency deviation (dΔf/dt) is shown in Figure 26.

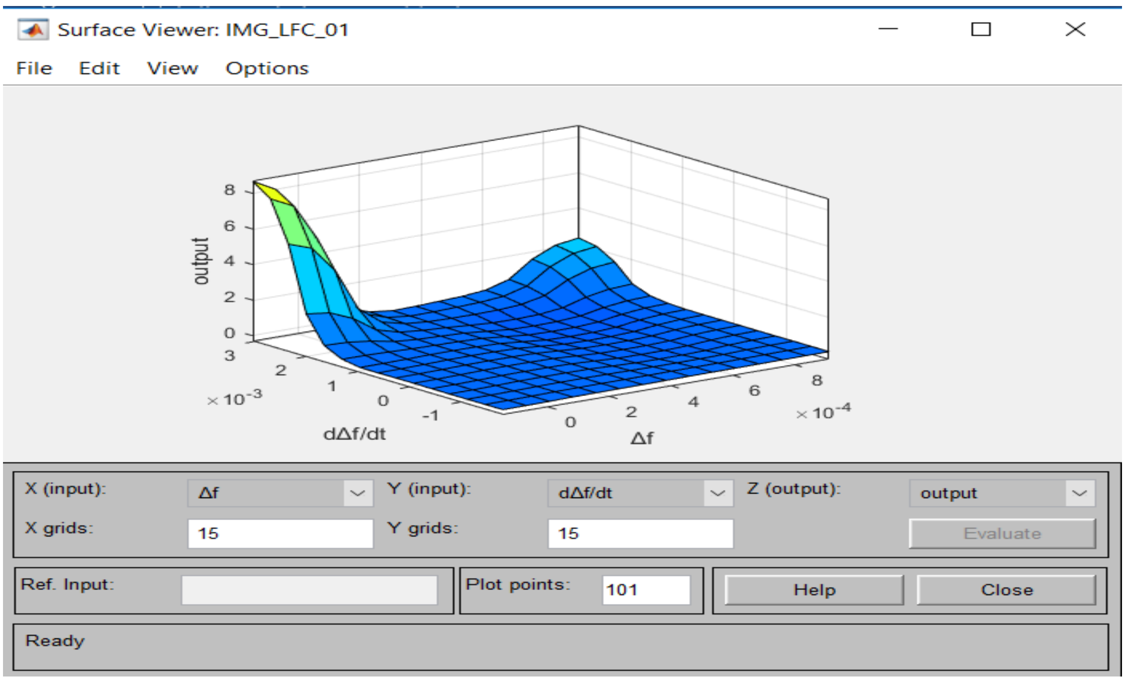

Figure 26 - Surface view created by ANFIS.

The frequency deviation in isolated MG using PID control, IT1 Fuzzy control, IT2 Fuzzy control and ANFIS control are shown in Figure 27.

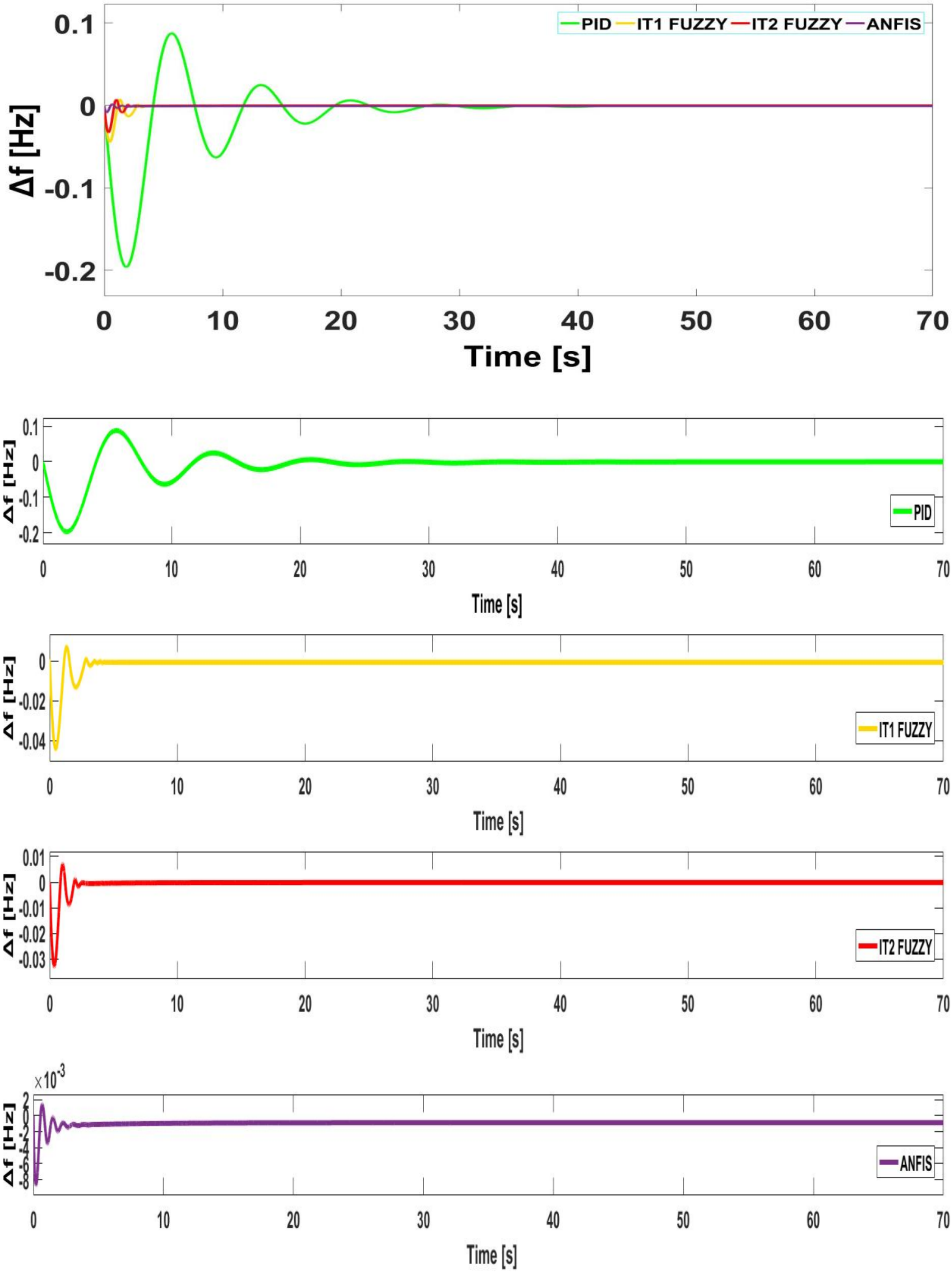

Figure 27 - Frequency deviation of the isolated micro-grid without constraints in case 1(A).

Table 4 - Comparison between conventional PID controller, type-1 and type-2 fuzzy controller and ANFIS controller.

Without considering the constraints of MT, DG and EVs				
Controllers	Rise time	Over shoot (Hz)	Under shoot (Hz)	Settling time (s)
PID	972.136 ms	8.746×10^{-2}	-1.962×10^{-1}	36.469
FUZZY (IT1)	445.119 ms	6.868×10^{-3}	-4.432×10^{-2}	3.594
IT2 FUZZY	298.757 ms	6.370×10^{-3}	-3.299×10^{-2}	2.784
ANFIS	174.568 ms	1.422×10^{-3}	-9.134×10^{-3}	2.061

According to the comparison of Table 4 and Figure 27. The overshoot and undershoot in the first swing has significantly reduced, and the proposed ANFIS controller has quickly damped the system frequency oscillation, the settling time and the rise time is also much shorter, better than in comparison with PID, IT1, and IT2 controllers. We can see that from figure 28 that ANFIS controller achieve stables output power of MT, DG, and EVs in a shorter time and less adjustment frequency, this illustrates that the equipment life of EVs batteries, DG and MT.

(I)

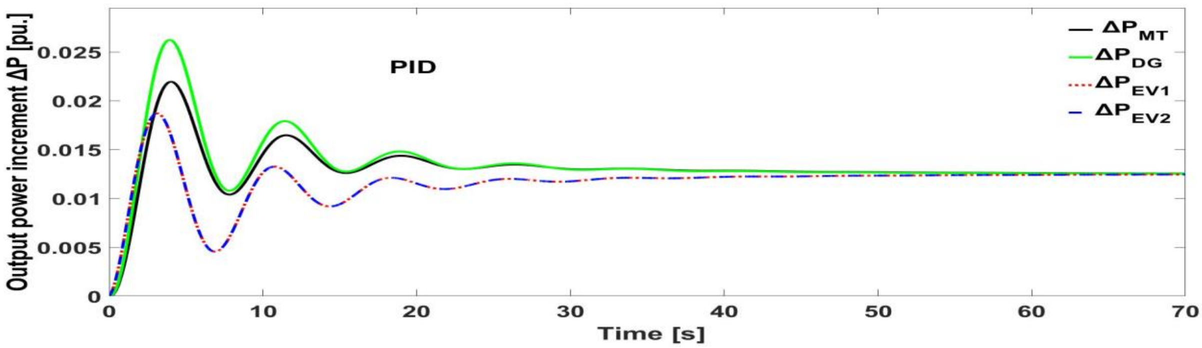

(II)

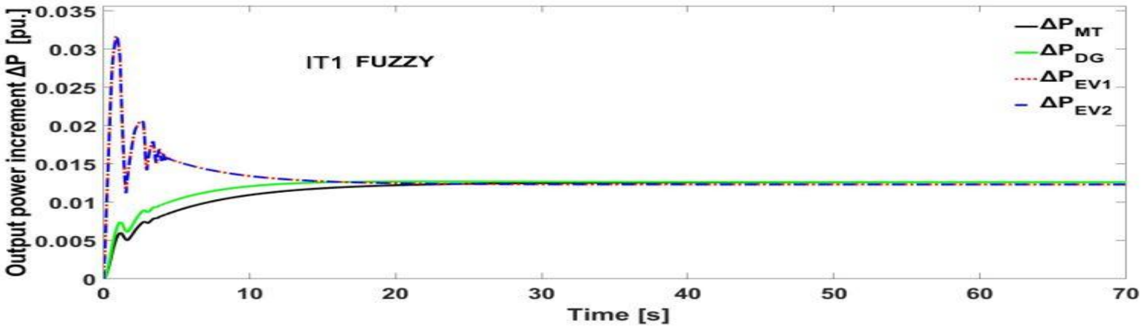

(III)

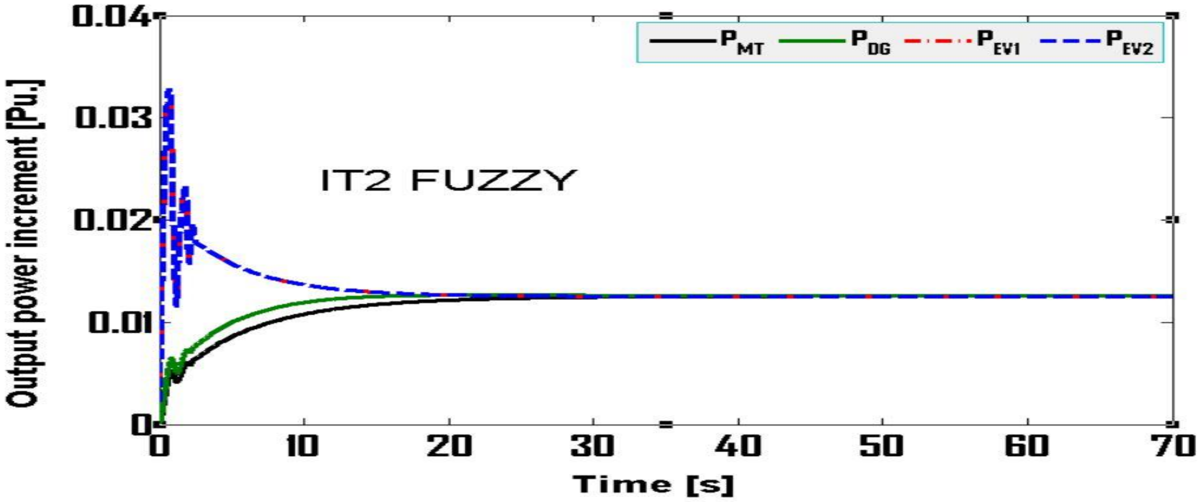

(IV)

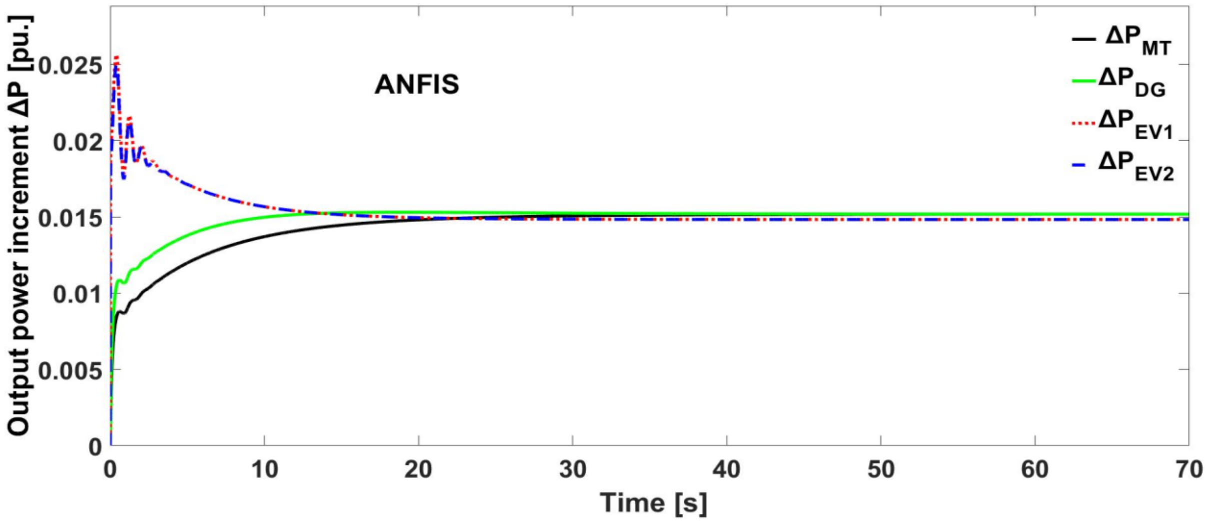

Figure 28 - The output power increment of MT, DG, EV1, and EV2 without considering constraints in case 1(A); (I) using PID controller, (II) using IT1 Fuzzy controller, (III) using IT2 Fuzzy controller and (IV) using ANFIS controller.

5.1.2 Case 1(B)-With considering the constraints of MT, DG and EVs

The frequency deviation of the isolated MG system using PID controller, IT1 controller, and ANFIS controller is shown in figure 29 under consideration of the constraints. Figure 30 shows the outputs of MT, DG and EVs under PID controller, IT1 controller and ANFIS controller.

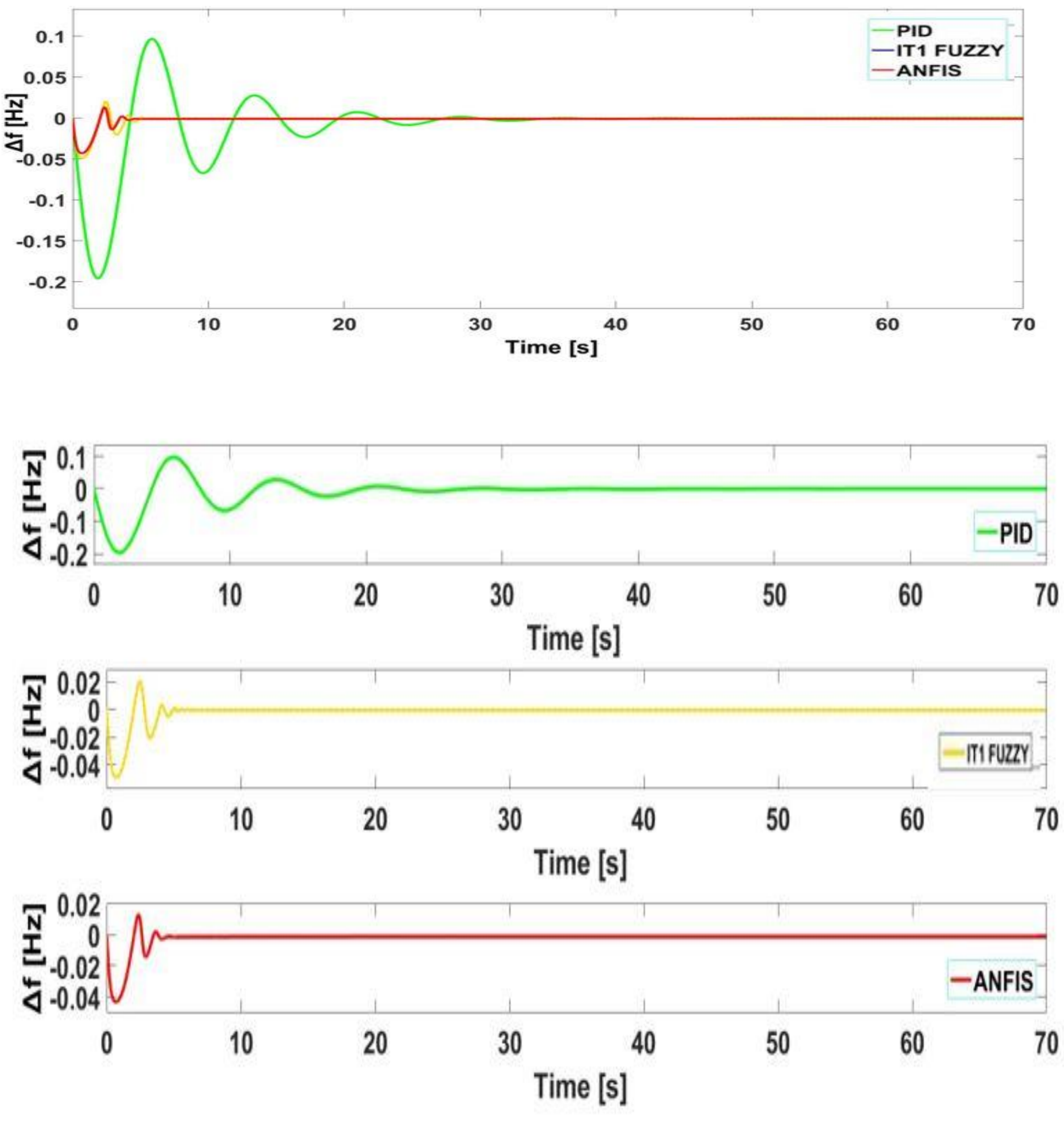

Figure 29 - Frequency deviation of the isolated micro-grid with constraints in case 1(B).

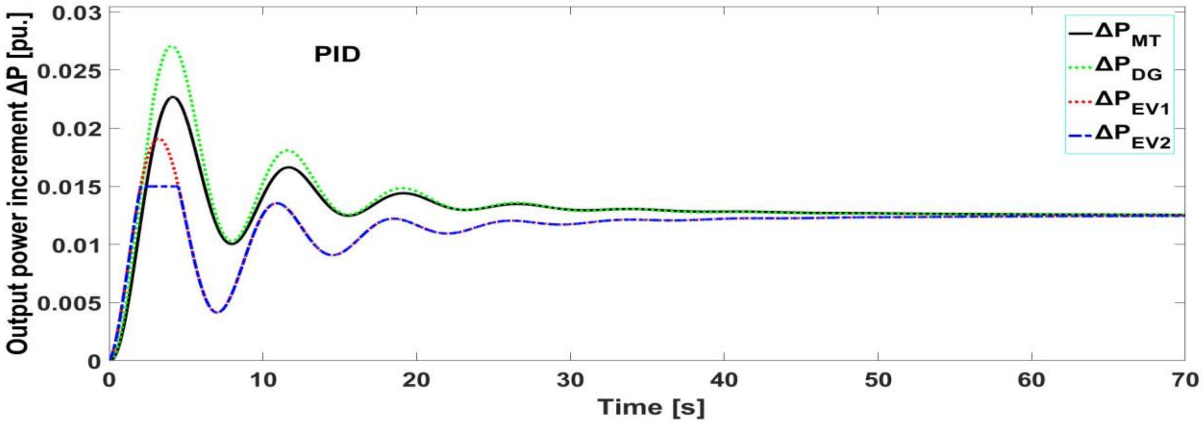

(I)

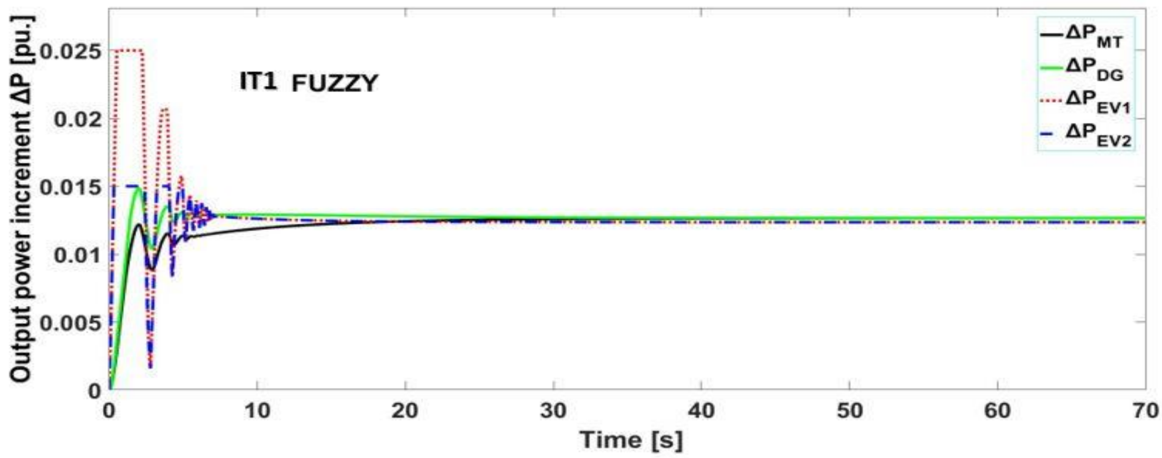

(II)

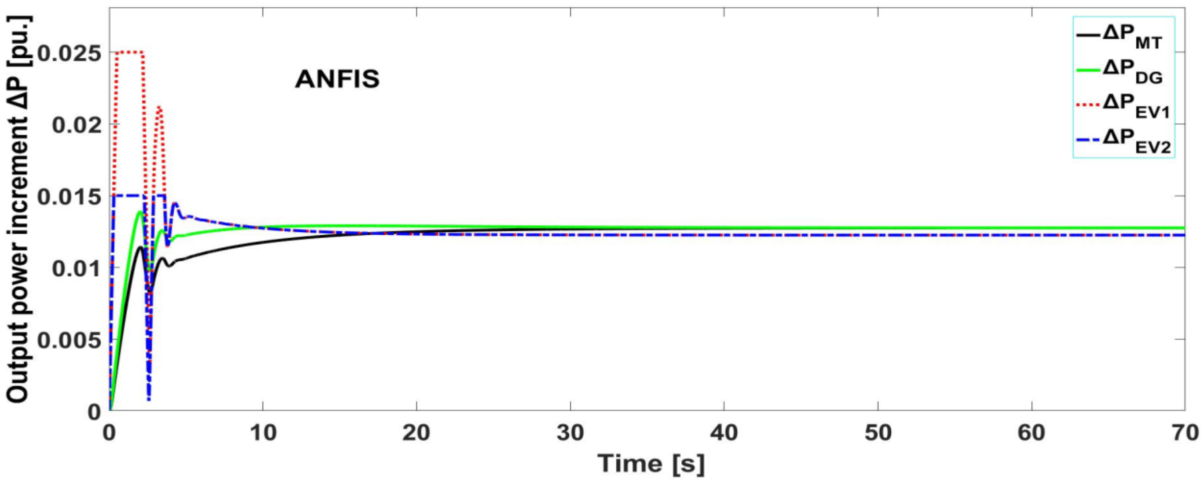

(III)

Figure 30 - The output power increment of MT, DG, EV1, and EV2 with considering constraints in case 1(B); (I) using PID controller, (II) using IT1 Fuzzy controller and (III) using ANFIS controller.

As a result suggest, in figure 29, the system can diminish the frequency oscillation under the load disturbance, the ANFIS controller still provides a better diminishing performance over the

PID controller and IT1 controller. On the other hand, in figure 30, the output power increment of the two EVs are various from each other because of their different inverter capacity limit. Using a well-tuned PID and FUZZY, i.e. IT1 fuzzy controller, the output power increment of both EV1 and EV2 reaches the upper capacity limit of their respective inverter and remain saturated for a long time. The stability of the output power of EVs much better in the ANFIS controller than PID controller and IT1 fuzzy controller as shown in figure 30.

5.1.3. Comparative study (Without and with considering the constraints of MT, DG and EVs)

Because of the EVs have been considered in this thesis as an equivalent power source, the different structures of electric vehicles have no impact on the controller. So, the impact of different electric vehicle capacity on the LFC is determined by the constraints of inverter capacity limit of equivalent EVs. Figure 31 shows, the comparison of PID controller, FUZZU (IT1 Fuzzy) controller and ANFIS controller with and without considering the constraints. In table 5 and 6 presents the comparison of the performance of ANFIS with PID and IT1 Fuzzy without and with the considering of constraints, respectively.

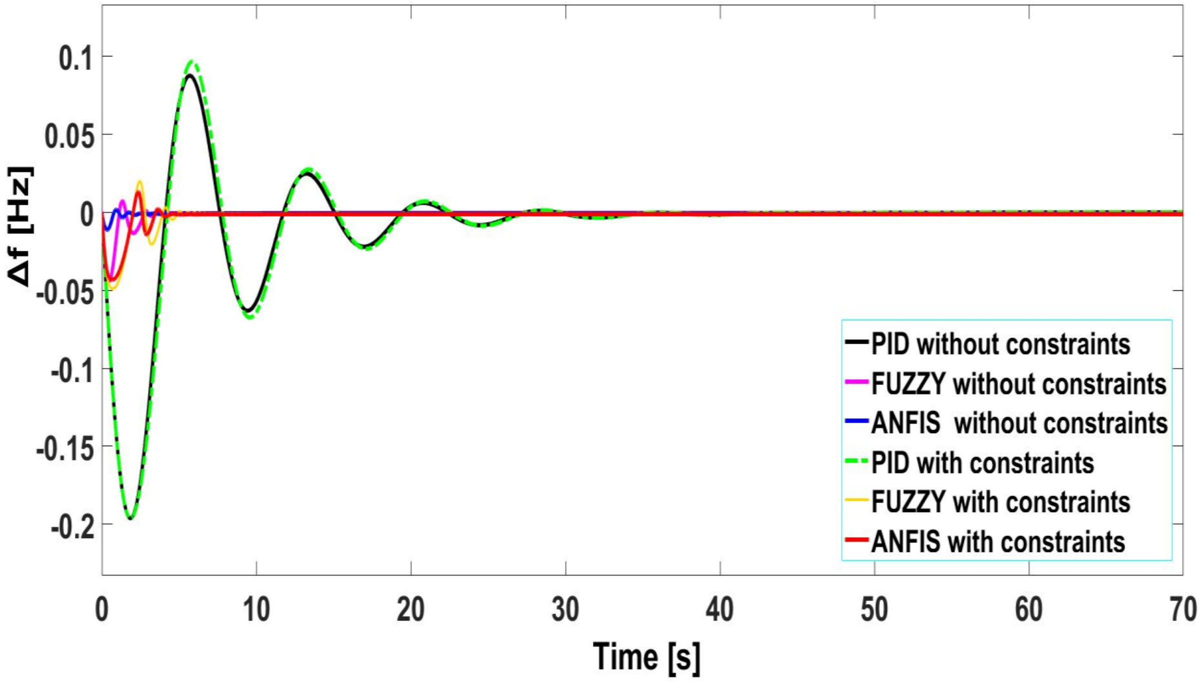

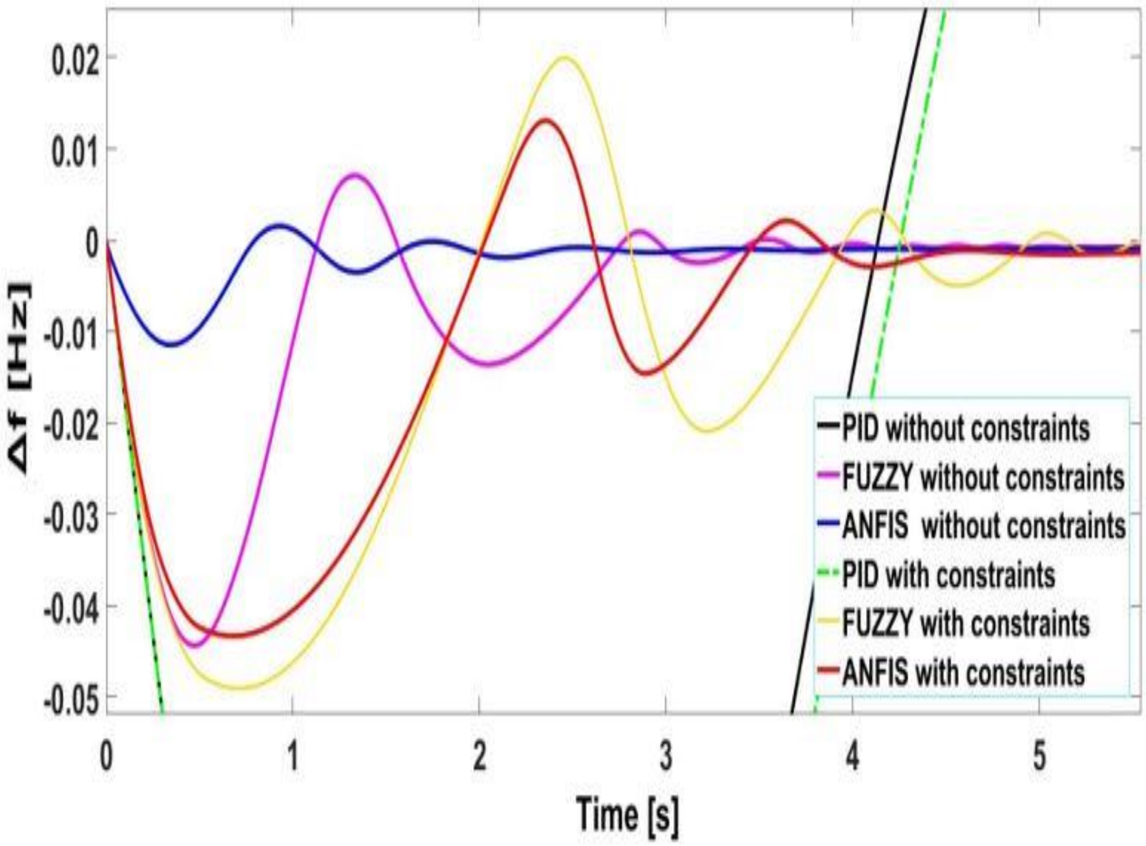

Figure 31 - The comparison of the system frequency deviation with and without constraints.

Table 5 - Comparison of the performance of ANFIS with PID and IT1 Fuzzy without the considering of constraints (Fig. 27 and Fig. 31)

Without the considering of constraints of MT, DG and EVs				
Controllers	Rise time	Over-shoot (Hz)	Under shoot (Hz)	Settling time (s)
PID	972.136 ms	8.746×10^{-2}	-1.962×10^{-1}	36.469
FUZZY(IT1)	445.119 ms	6.868×10^{-3}	-4.432×10^{-2}	3.594
ANFIS	174.568 ms	1.422×10^{-3}	-9.134×10^{-3}	2.061

Table 6 - Comparison of the performance of ANFIS with PID and IT1 Fuzzy with the consideration constraints (Fig. 29 and Fig. 31)

With the considering of constraints of MT, DG and EVs				
Controllers	Rise time	Over-shoot (Hz)	Under shoot (Hz)	Settling time (s)
PID	1.565 s	9.642×10^{-2}	-1.963×10^{-1}	39.839
FUZZY(IT1)	300.669 ms	1.995×10^{-2}	-4.906×10^{-2}	5.241
ANFIS	293.672 ms	1.31×10^{-2}	-4.332×10^{-2}	4.465

The dynamic responses obtained from the first case simulation tabulated in Tables 4, 5, and 6, regarding rising time, overshoot, undershoot and settling time of the frequency deviation. This result reveals that ANFFIS based neuro-fuzzy controller rise time, overshoot, undershoot and settling time-frequency deviation (oscillations) due to 0.05 pu step load disturbance in comparison to conventional PID controller, interval IT1 controller, and IT2 fuzzy controller. Therefore, the intelligent control techniques approach using Neuro-Fuzzy concept is more accurate and faster than the PID controller and better performance than Interval Type-1 Fuzzy controller and Interval Type-2 Fuzzy controller scheme.

5.2 Case 2: Load disturbance and one of the EVs removed from the LFC system after 60 second.

In this scenario, at the beginning of the simulation, the isolated grid is in steady state. The performance of the proposed controller on load disturbance is illustrated. As in case 1 here is also, by assumption that the output power of wind generations and solar PV generation are constant with stable wind speed and sun condition for a short period, i.e. $\Delta P_W = 0$ pu and $\Delta P_{PV} = 0$ pu.

In case 2(A) and case 2(B), without and with considering constraints a load disturbance $\Delta P_L = 0.05$ pu is applied at t = 15 s, and EV2 will be removed from the load frequency control system as soon as its energy is smaller than E_{min} at t = 60 s. The total simulation time is 100 s, for this case.

5.2.1. Case 2(A)-Without considering the constraints of MT, DG and EVs

Frequency deviation of the isolated micro-grid while using PID, IT1, IT2 and ANFIS controllers without constraints are shown in figure 32. The output power increment of MT, DG, and EVs is presented in figure 33 without consideration of constraints, under control PID, IT1, IT2 and ANFIS controllers.

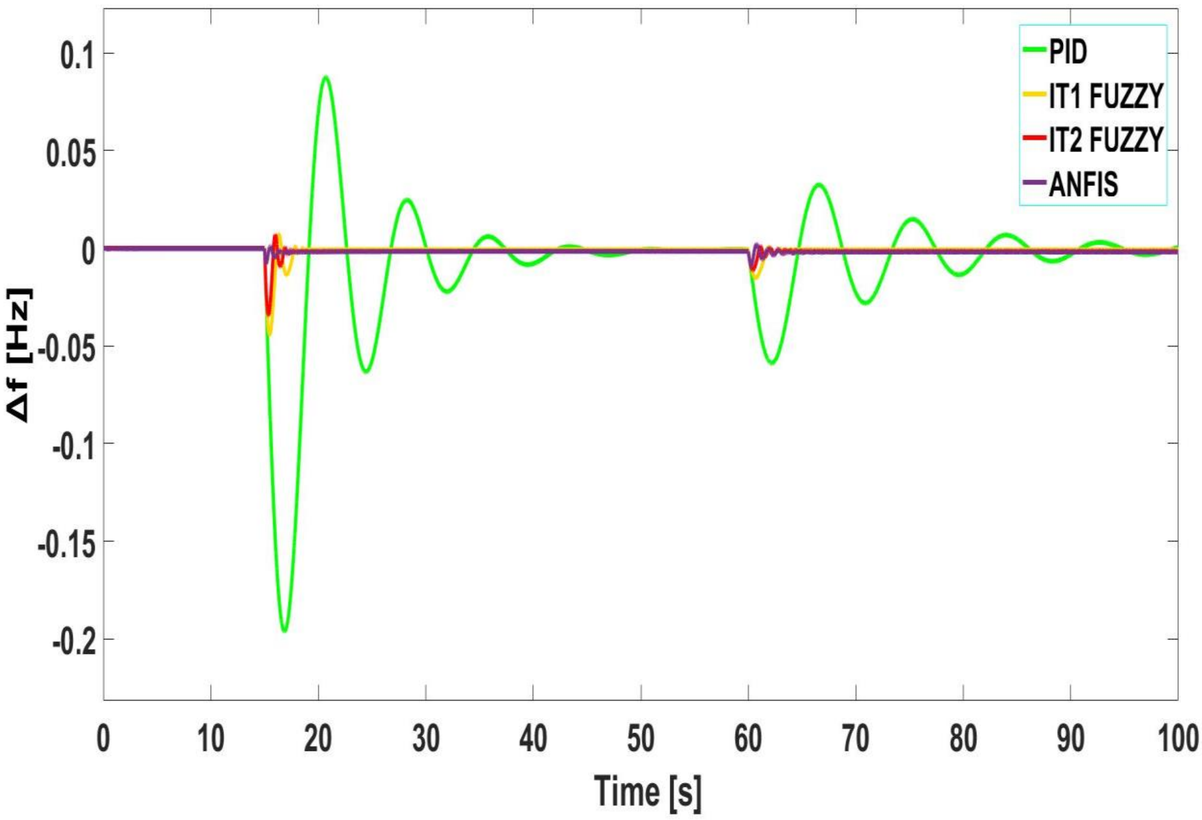

Figure 32 - The frequency deviation of the isolated micro-grid without constraints in case-2(A).

(I)

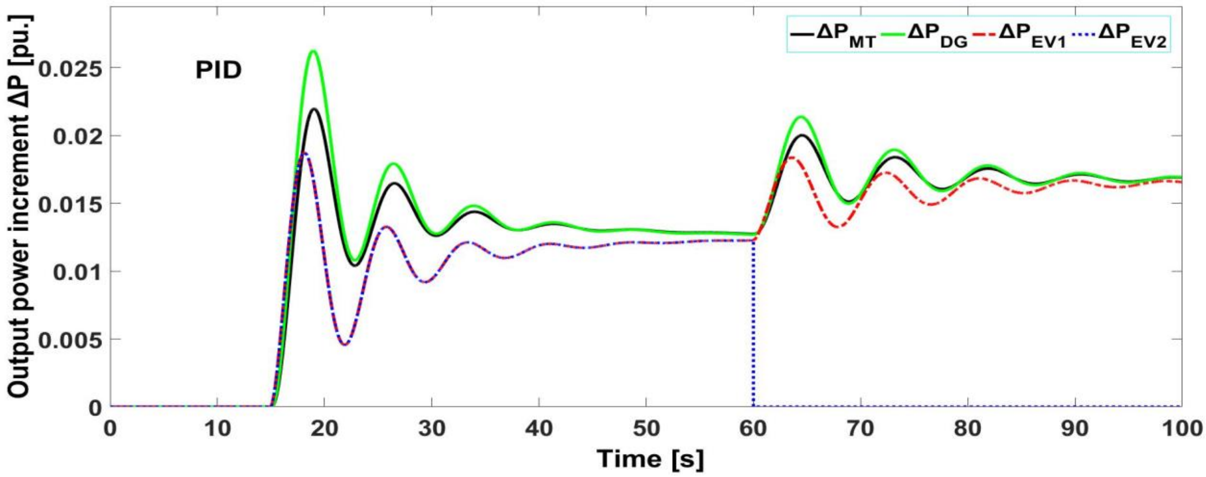
PID
ΔP_MT ΔP_DG ΔP_EV1 ΔP_EV2
Output power increment ΔP [pu.]
0 0.005 0.01 0.015 0.02 0.025
0 10 20 30 40 50 60 70 80 90 100
Time [s]

(II)

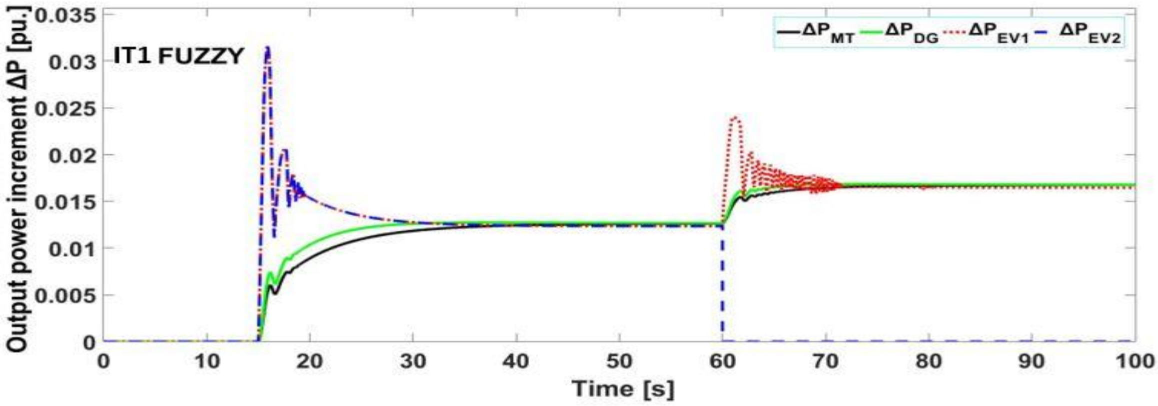
IT1 FUZZY
ΔP_MT ΔP_DG ΔP_EV1 ΔP_EV2
Output power increment ΔP [pu.]
0 0.005 0.01 0.015 0.02 0.025 0.03 0.035
0 10 20 30 40 50 60 70 80 90 100
Time [s]

(III)

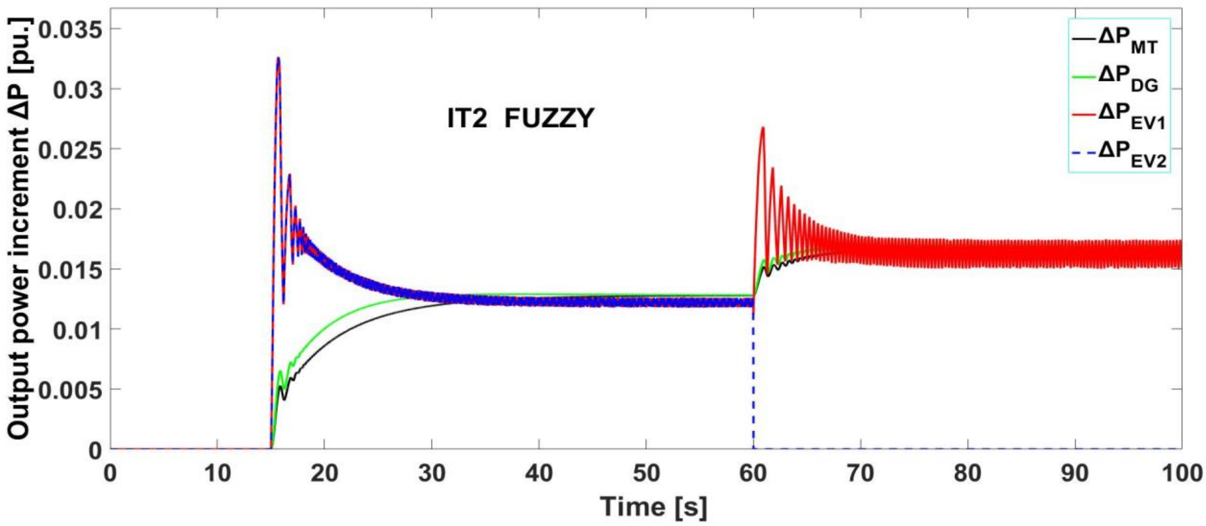
IT2 FUZZY
ΔP_MT
ΔP_DG
ΔP_EV1
ΔP_EV2
Output power increment ΔP [pu.]
0 0.005 0.01 0.015 0.02 0.025 0.03 0.035
0 10 20 30 40 50 60 70 80 90 100
Time [s]

(IV)

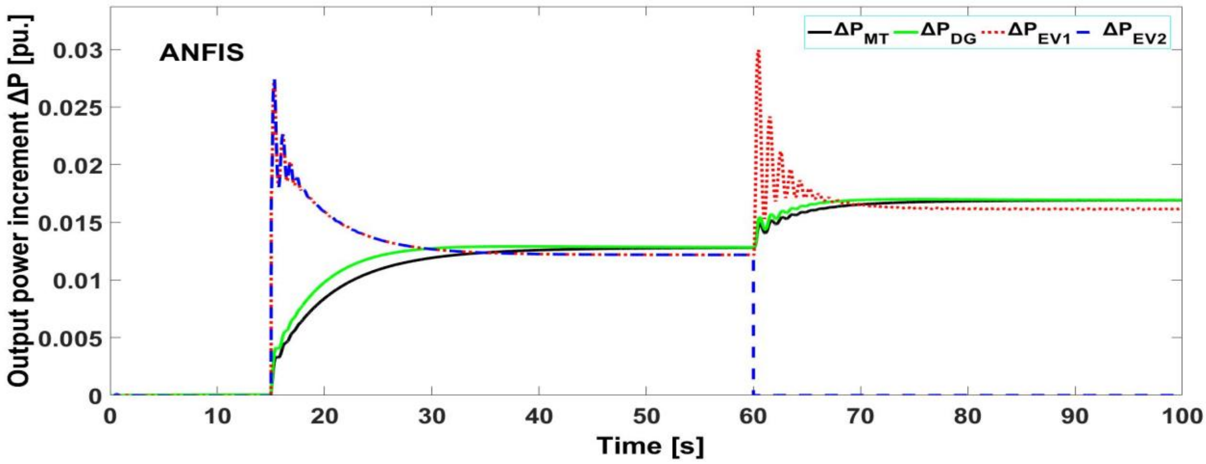

Figure 33 - The output power increment of MT, DG, EV1, EV2 without considering constraints in case 2(A); (I) using PID controller, (II) using IT1 Fuzzy controller, (III) using IT2 Fuzzy controller and (IV) using ANFIS controller.

As we seen from figure 32, the response speed of LFC system slows down, because of the total energy of EV2 reached Emin at t = 60 s, but the ANFIS based controller still damps the frequency oscillation well with the remain controllable units, i.e. MT, DG and EV1.

5.2.2. Case 2(B)-With considering the constraints of MT, DG and EVs

In this case, the constraints of inverter capacity limit of MT, DG, and EVs are considered, the output power increment of EVs is determined by constraints as shown in figure 35. So, EVs require a longer time to damp the frequency oscillation under the same disturbance, i.e. in case 2(A), because of constraints.

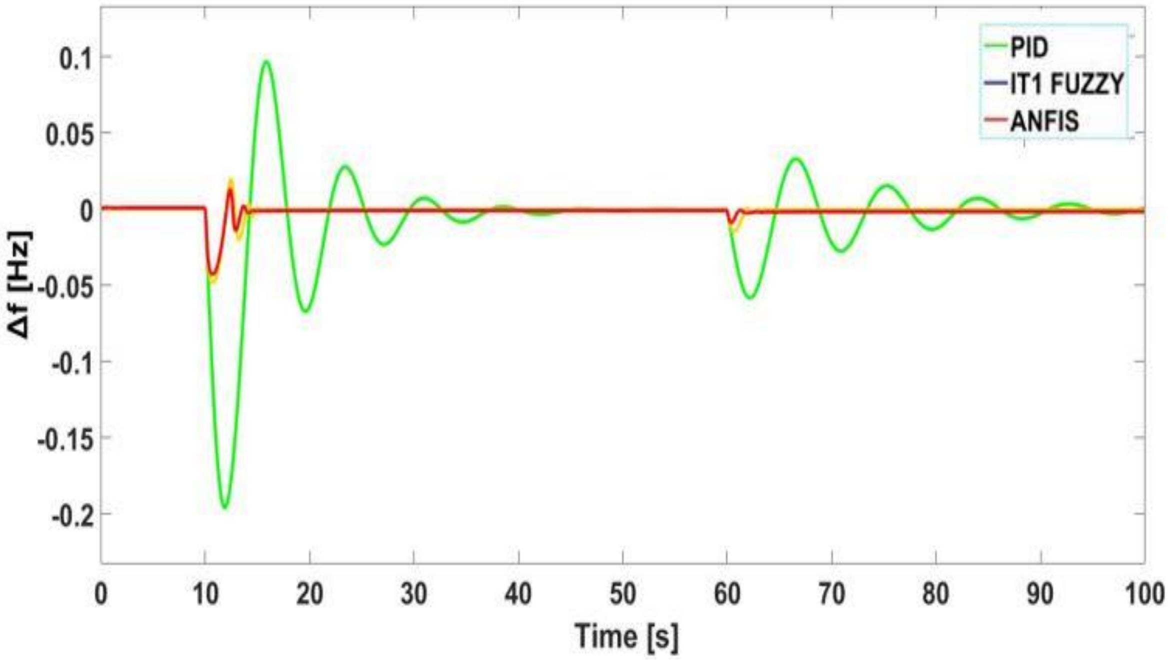

Figure 34 - The frequency deviation of the isolated micro-grid with constraints in case 2(B).

(I)

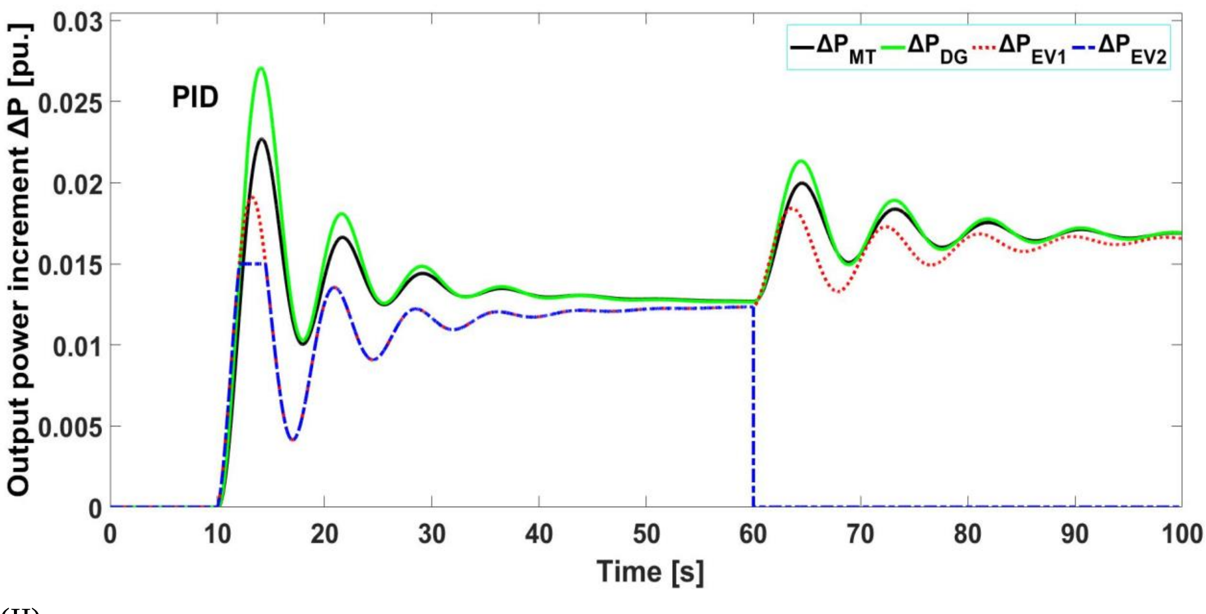

(II)

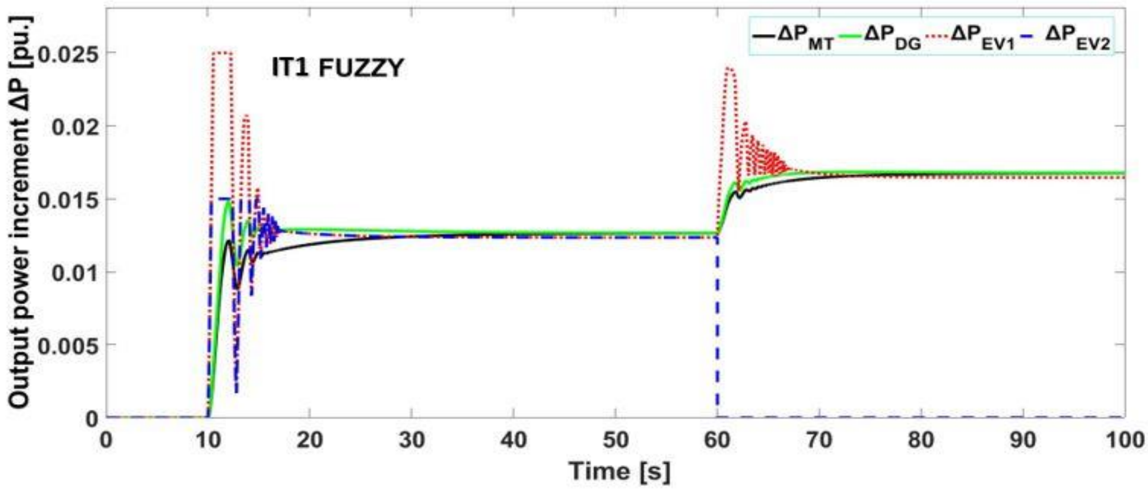

(III)

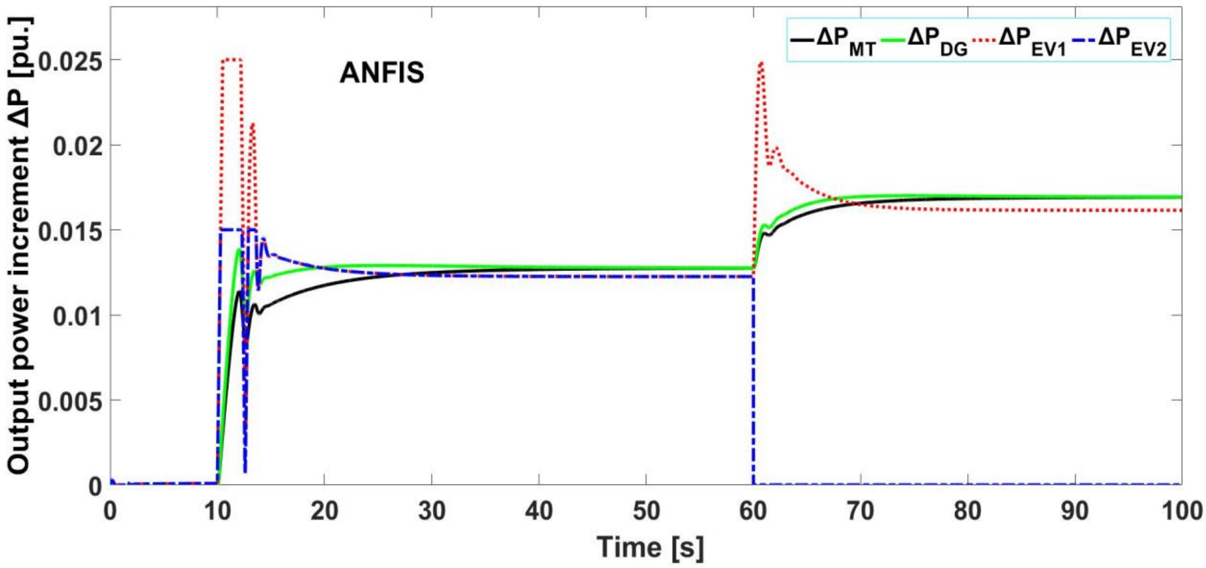

Figure 35 - The output power increment of MT, DG, EV1, and EV2 with constraints in case 2(B); (I) using PID controller, (II) using IT1 Fuzzy controller and (III) using ANFIS controller.

As shown in figure 35, due to different EVs constraints their output power increments are different, the output power increment of the two EVs hit the upper capacity limit their respective inverter, therefore becomes saturated for relatively long time. As can be seen from the results, MT, DG and the two EVs participate in damping frequency oscillation under various controls considering constraints. As we seen from figure 33 and figure 35, how the output power increment of EVs are determined on constraints, consequently, EVs require alonger time to damp the frequency oscillation under the same disturbance in the previous case, i.e. without constraints.

5.3 Case 3: Active power disturbances from PVs

In this scenario, the load demand and the wind power generation is assumed to be constant, i.e. $\Delta P_W = 0$ and $\Delta P_L = 0$. Eight sequential active power disturbances from PVs are applied to the isolated MG system as shown in figure 36. Specifically, at t = 0 s a -0.035 pu. step disturbance is applied, at t = 35 s a 0.001 pu. step disturbance is applied, at t = 70 s a -0.025 pu. step disturbance is applied, at t = 105 s a -0.05 pu. step disturbance is applied, at t = 140 s a 0.01 pu. step disturbance is applied, at t = 175 s a -0.032 pu. step disturbance is applied, at t = 210 s a 0.009 pu. step disturbance is applied, and finally at t = 245 s a -0.025 pu. step disturbance is applied. The total simulation time is 280 second.

In case 3(A) and case 3(B), without and with considering the constraints of MT, DG and EVs, respectively active power disturbances is applied to the system.

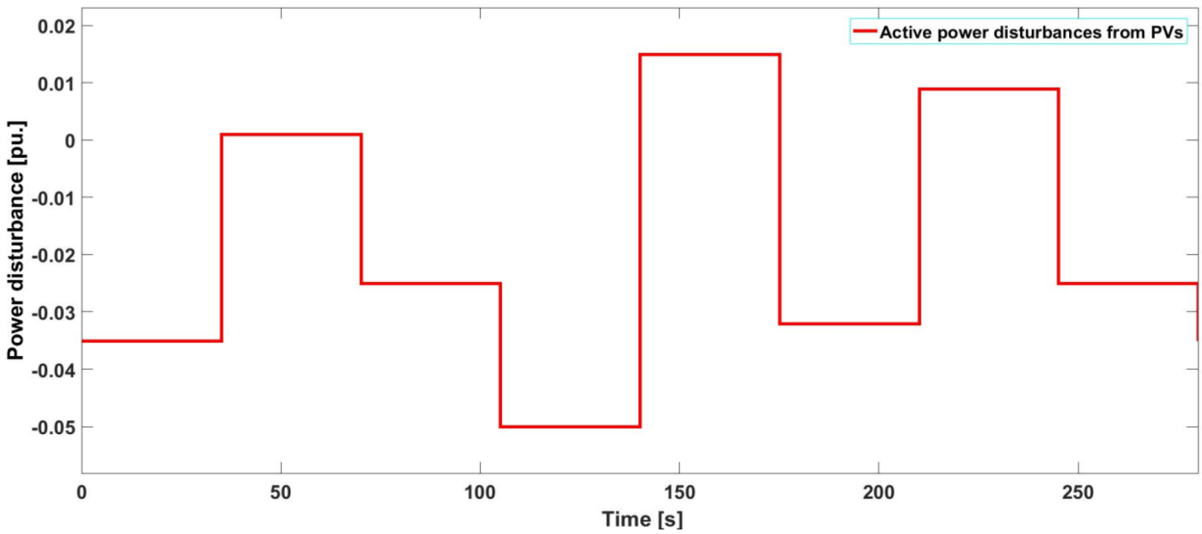

Figure 36 - The active power disturbance from Solar PVs.

5.3.1. Case 3(A)-Without considering the constraints of MT, DG and EVs.

The system frequency deviation using PID controller, IT1 fuzzy controller, IT2 fuzzy controller and ANFIS controller is shown in figure 37, According to this figure the proposed ANFIS controller efficiently handle the frequency fluctuation caused by solar PVs, and illustrate the superior diminishing performance over PID, IT1, and IT2 controllers.

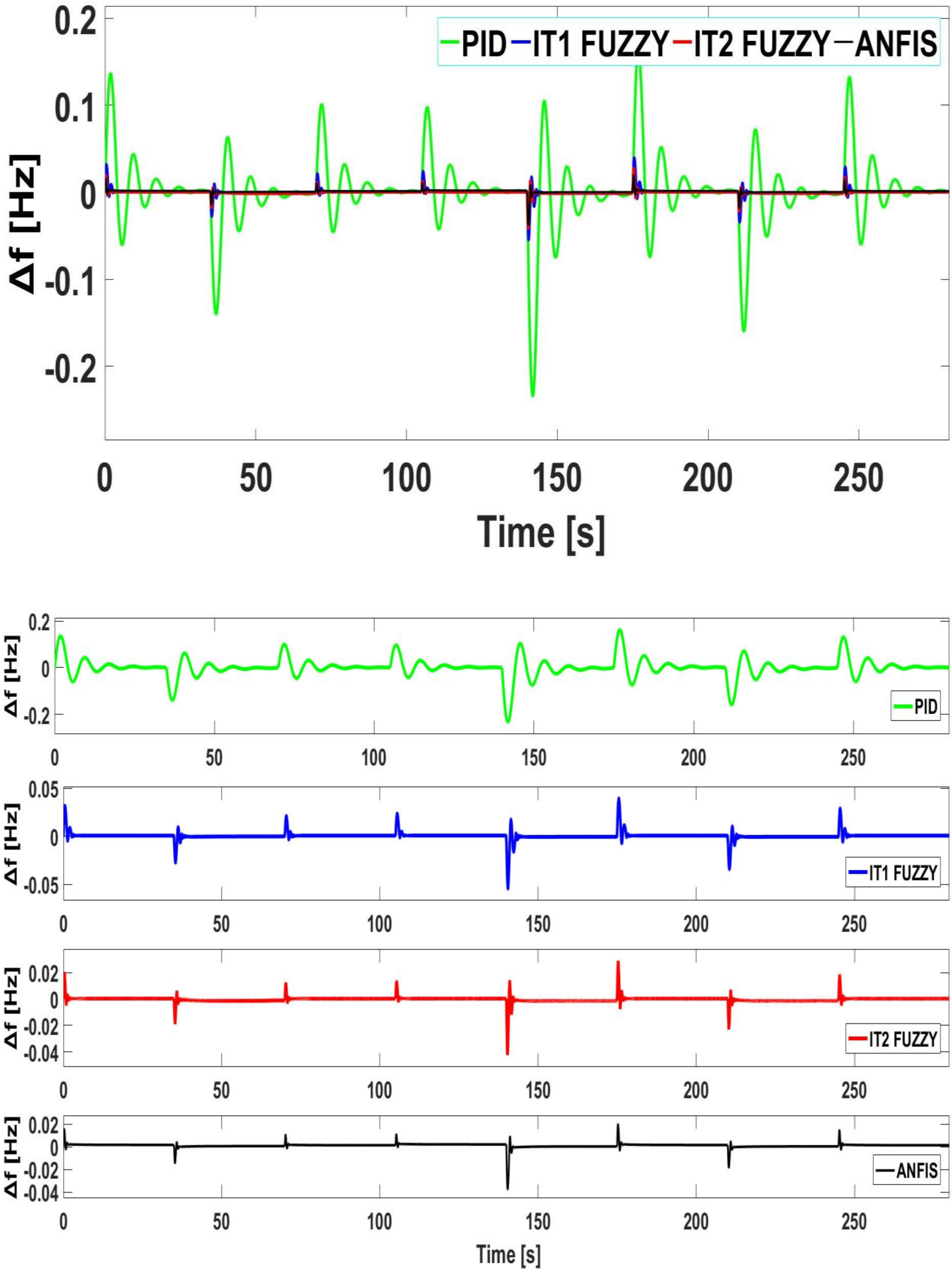

Figure 37 - The frequency deviation of the isolated micro-grid without constraints in case 3(A).

(I)

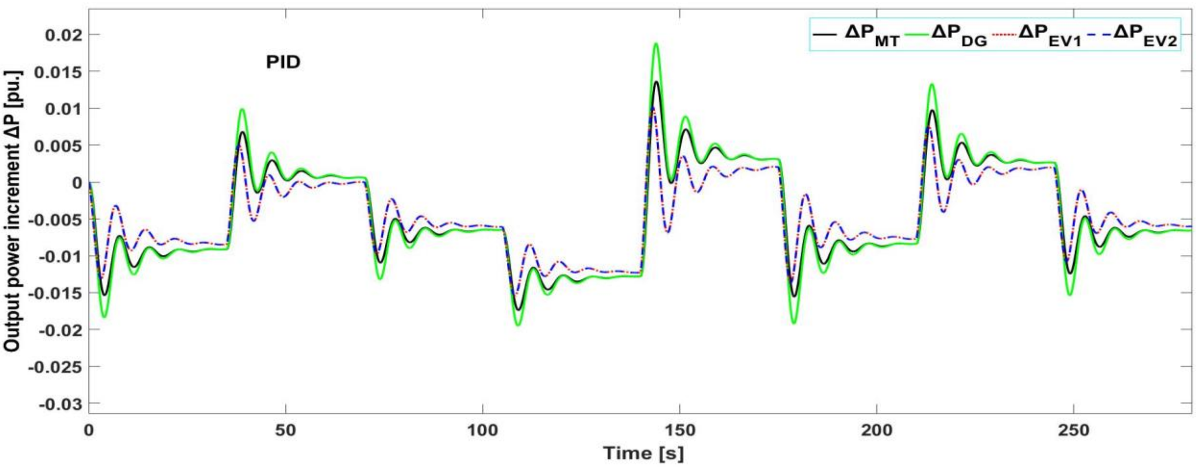
PID
ΔP_MT
ΔP_DG
ΔP_EV1
ΔP_EV2
Output power increment ΔP [pu.]
Time [s]

(II)

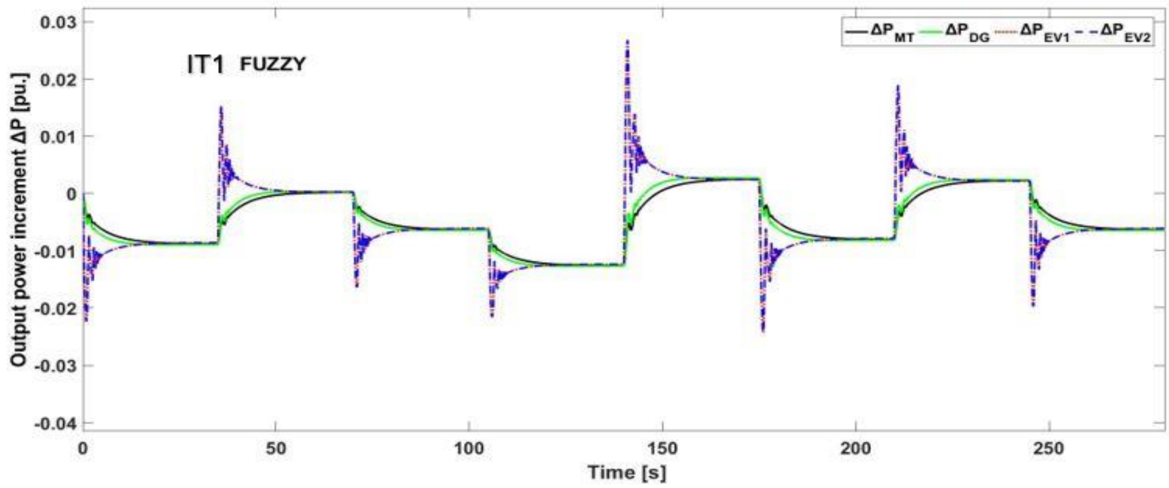
IT1 FUZZY
ΔP_MT
ΔP_DG
ΔP_EV1
ΔP_EV2
Output power increment ΔP [pu.]
Time [s]

(III)

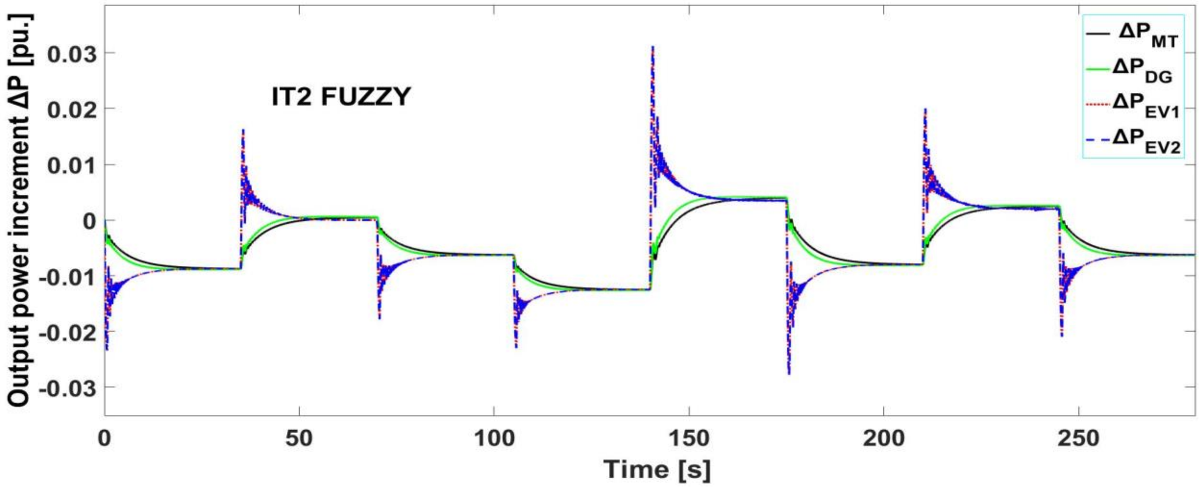
IT2 FUZZY
ΔP_MT
ΔP_DG
ΔP_EV1
ΔP_EV2
Output power increment ΔP [pu.]
Time [s]

(IV)

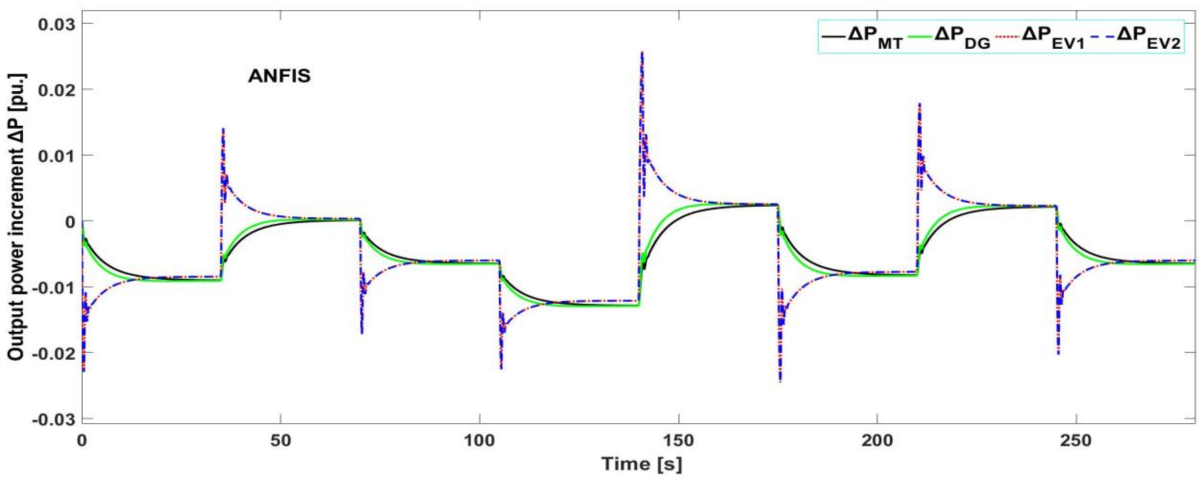

Figure 38 - The output power increment of MT, DG, EV1, and EV2 without considering constraints in case 3(A); (I) using PID controller, (II) using IT1 Fuzzy controller, (III) using IT2 Fuzzy controller and (IV) using ANFIS controller.

As it can be seen from figure 38 above, the output power increment curve of MT and DG are smoother than that of EVs, because of the inertia constant. The inertia constants of MT and DG are much larger than that of EVs. In the next subcase (case 3(B)), with the consideration of constraints in the isolated MG system, MT, DG, EVs have less output power fluctuation by using the proposed ANFIS control.

5.3.2. Case 3(B) With considering the constraints of MT, DG and EVs.

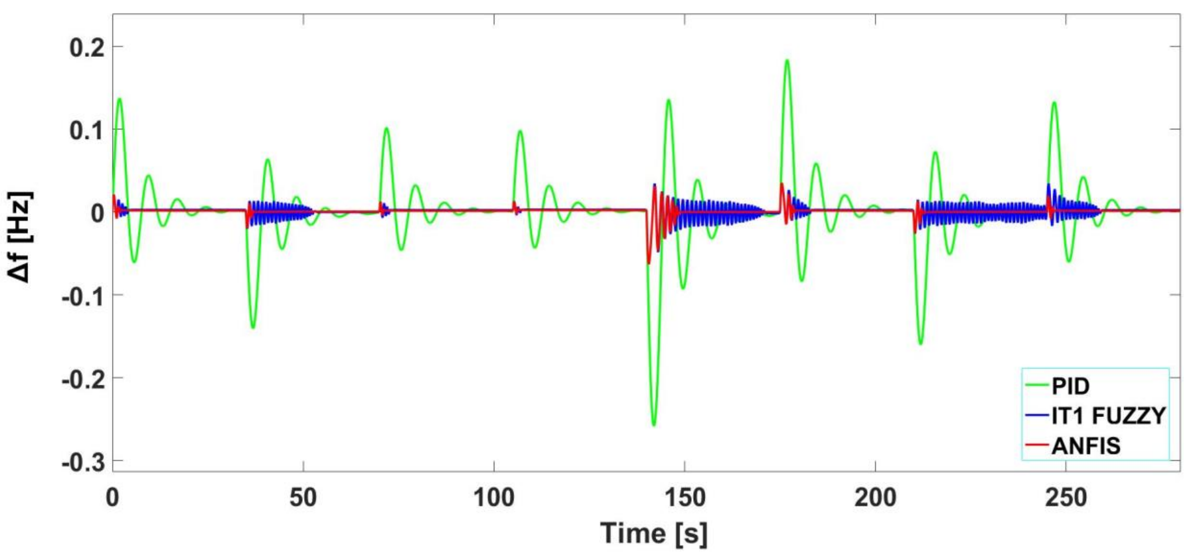

Figure 39 - The frequency deviation of the isolated micro-grid with constraints in case 3(B).

(I)

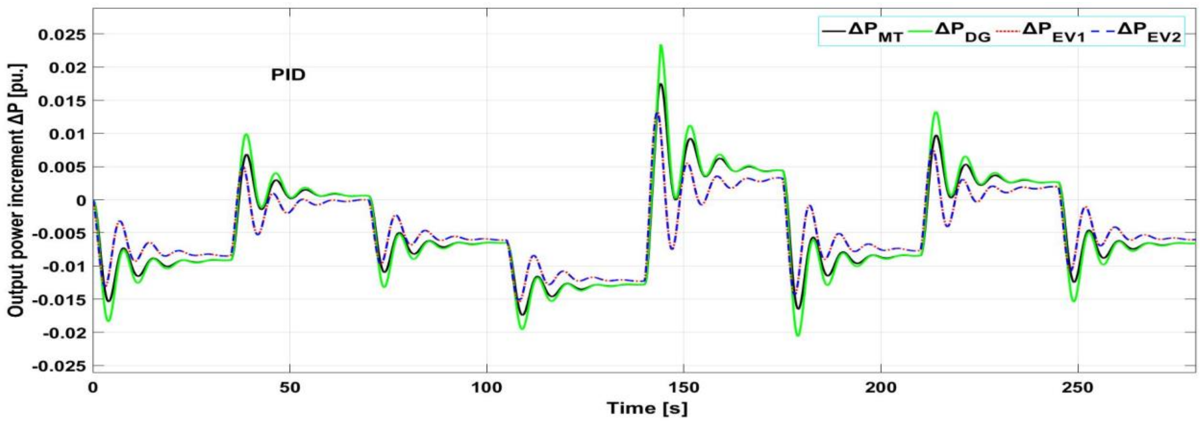

(II)

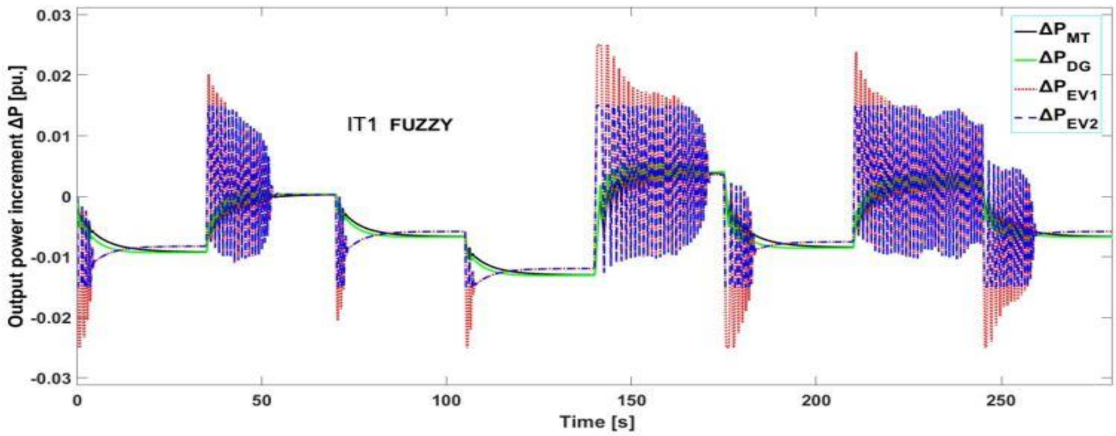

(III)

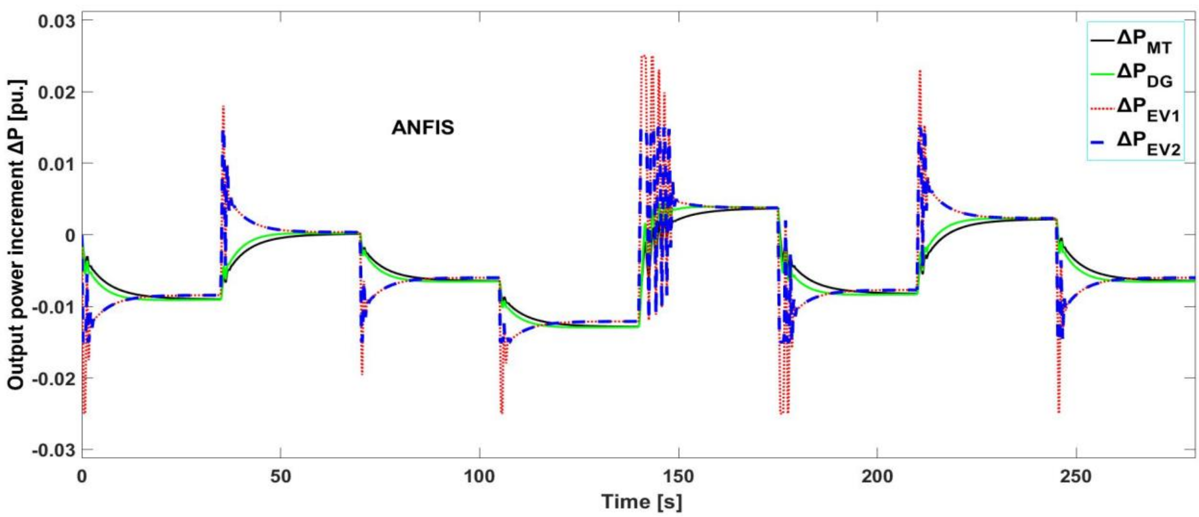

Figure 40 - The output power increment of MT, DG, EV1, and EV2 with considering

constraints in case 3(B); (I) using PID controller, (II) using IT1 Fuzzy controller and (III) using ANFIS controller.

5.4 Case 4: Active power fluctuation of wind power generation.

In case 4, the load demand and the solar power generation in the isolated grid are assumed to be constant, i.e. $\Delta P_L = 0$ and $\Delta P_{PV} = 0$. On the other hand, the output power of wind generation will fluctuate according to the change of weather condition particularly wind speed. Real wind generation fluctuations, as shown in figure 41, on a large wind turbine, site=NM92, Denmark [52]. $\Delta P_W = 0$ denotes a situation in which wind generation is equal to the average wind power during the period. The total simulation time is 70 second, and the simulation result without and with constraint are presented in case 4(A) and case 4(B), respectively.

Figure 42 and figure 44, show that the proposed ANFIS based Neuro-Fuzzy Controller effectively can highly improve the performance of the LFC system, and it has a superior damping performance over PID controller, IT1 fuzzy controller, and IT2 fuzzy controller. As we seen in figure 43 and figure 45, the output power increment curve of MT and DG are smoother than that of EVs, because of the inertia constant.

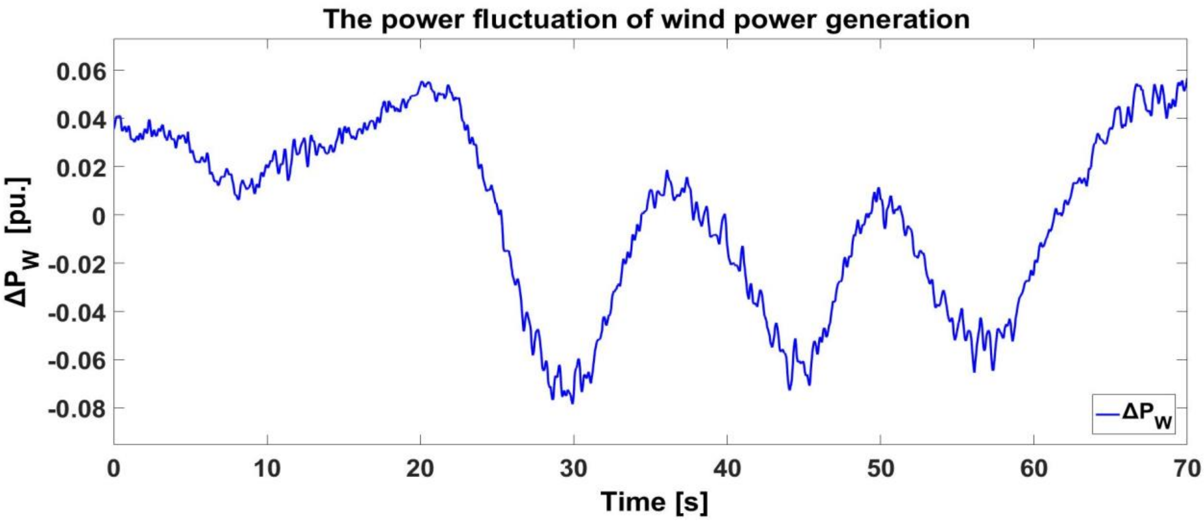

Figure 41 - The power fluctuation of wind power generation.

5.4.1. Case 4(A)-Without considering the constraints of MT, DG and EVs

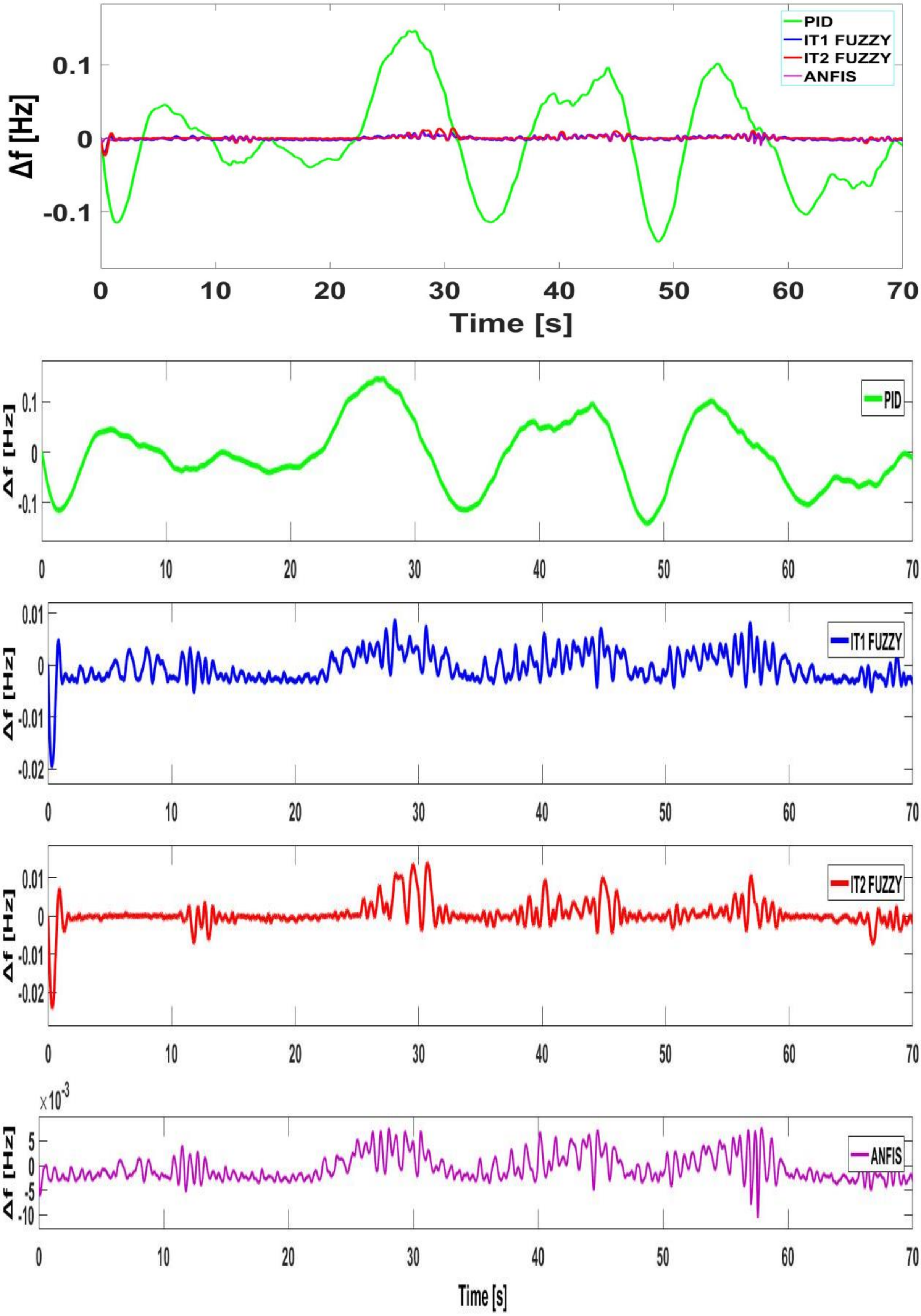

Figure 42 - The frequency deviation of the isolated micro-grid without constraints in case 4(A).

(I)

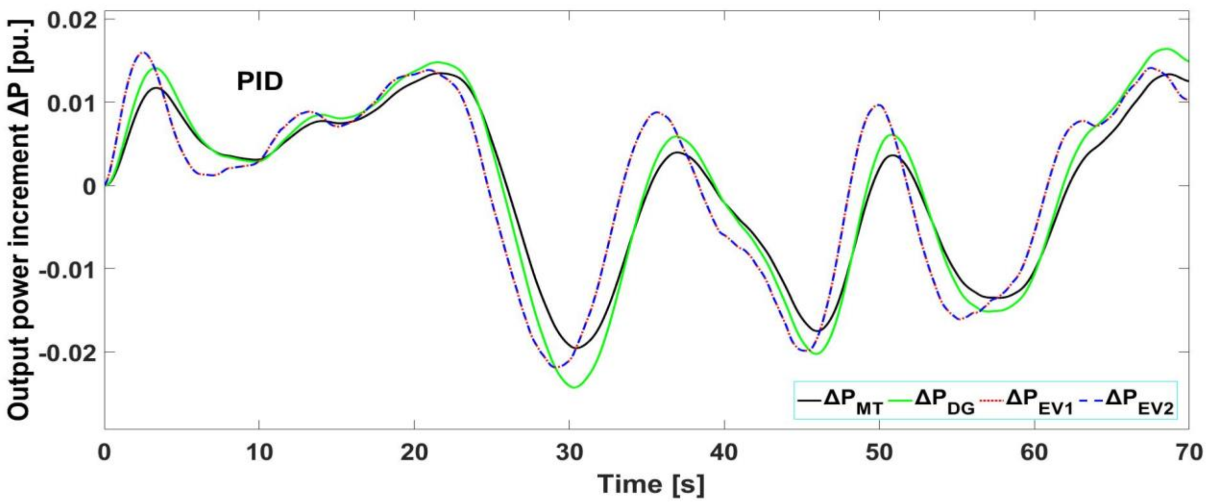

PID
Output power increment ΔP [pu.]
Time [s]
ΔP_{MT} ΔP_{DG} ΔP_{EV1} ΔP_{EV2}

(II)

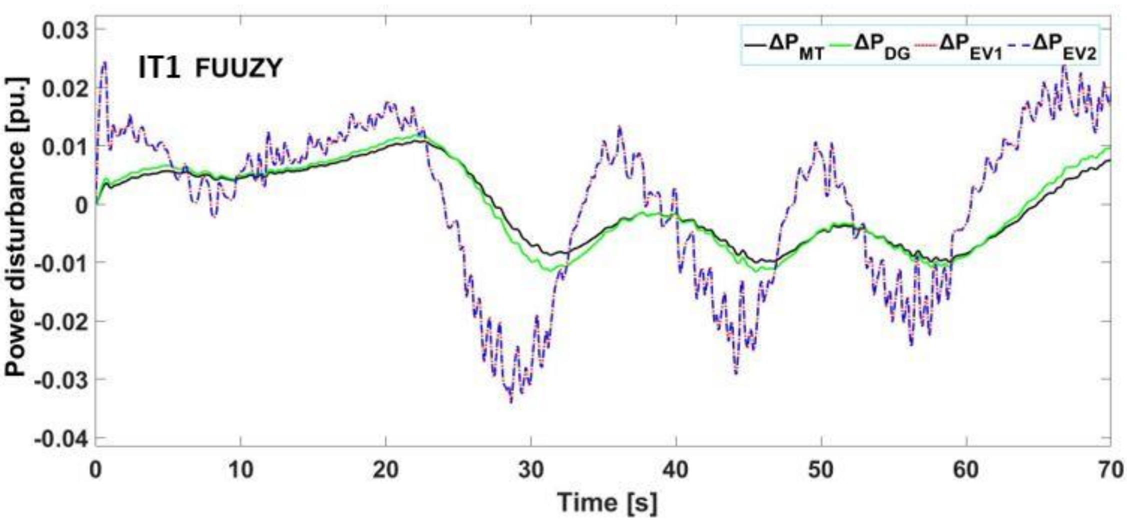

IT1 FUUZY
Power disturbance [pu.]
Time [s]
ΔP_{MT} ΔP_{DG} ΔP_{EV1} ΔP_{EV2}

(III)

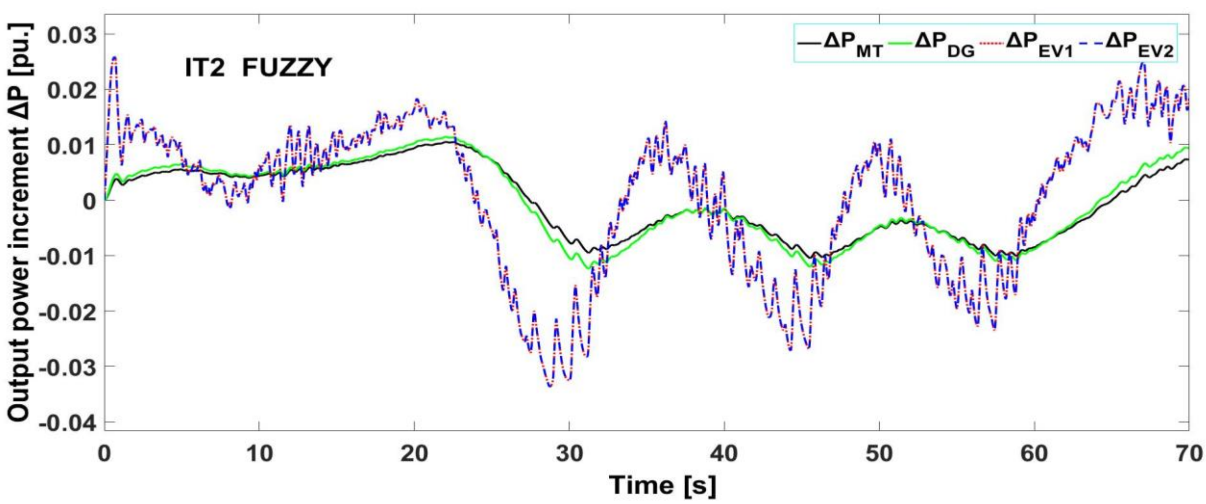

IT2 FUZZY
Output power increment ΔP [pu.]
Time [s]
ΔP_{MT} ΔP_{DG} ΔP_{EV1} ΔP_{EV2}

(IV)

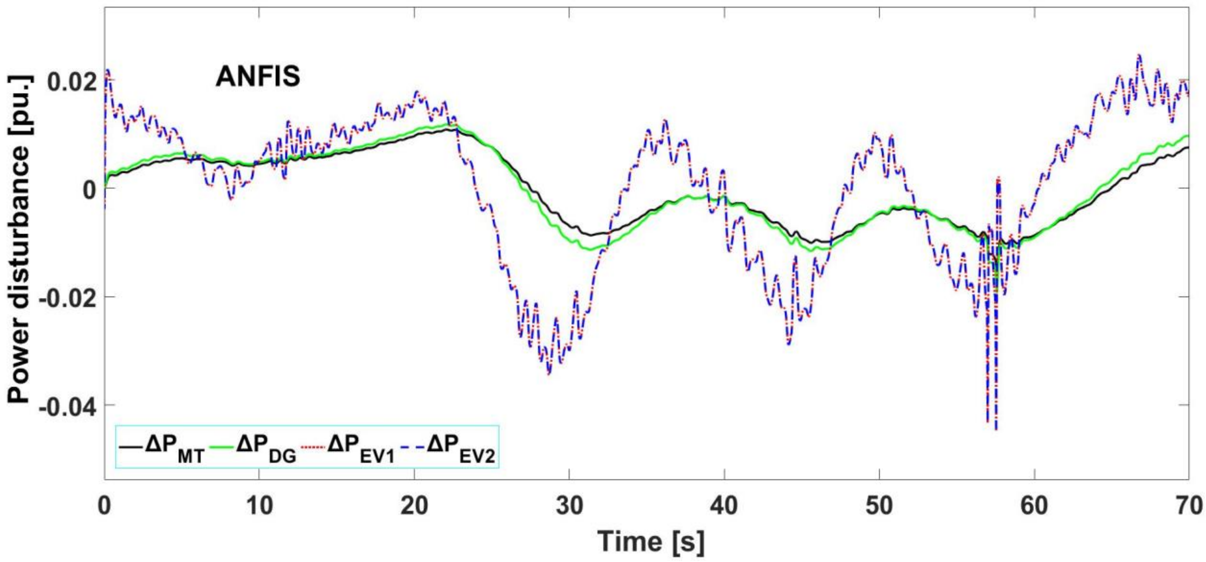

Figure 43 - The output power increment of MT, DG, EV1, and EV2 without considering constraints in case 4(A); (I) using PID controller, (II) using IT1 Fuzzy controller, (III) using IT2 Fuzzy controller and (IV) using ANFIS controller.

5.4.2. Case 4(B)-With considering the constraints of MT, DG and EVs

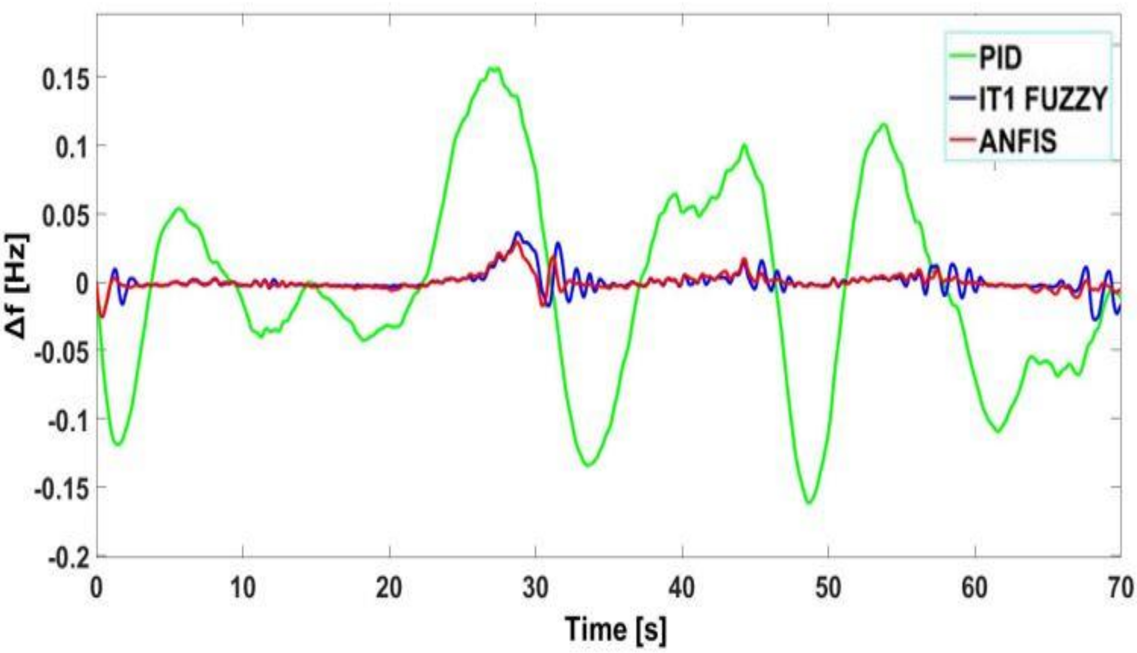

Figure 44 - The frequency deviation of the isolated micro-grid with constraints in case 4(B).

(I)

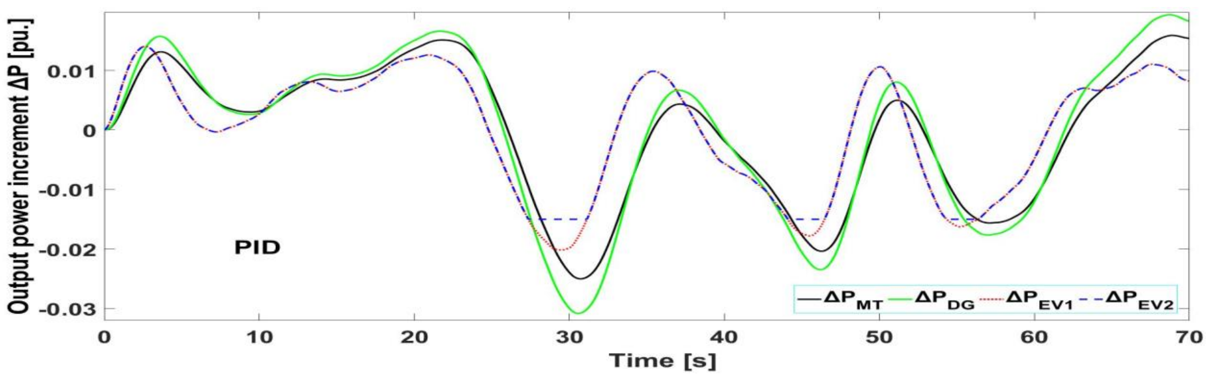

(II)

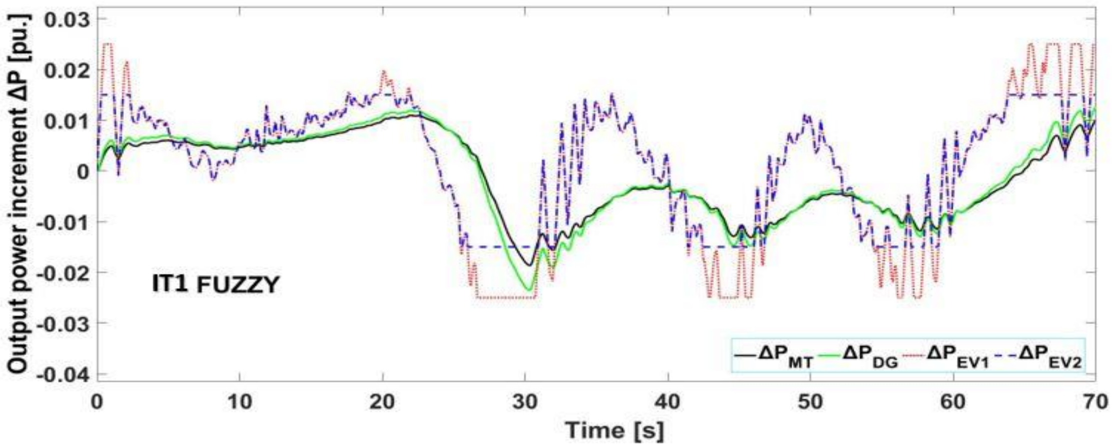

(III)

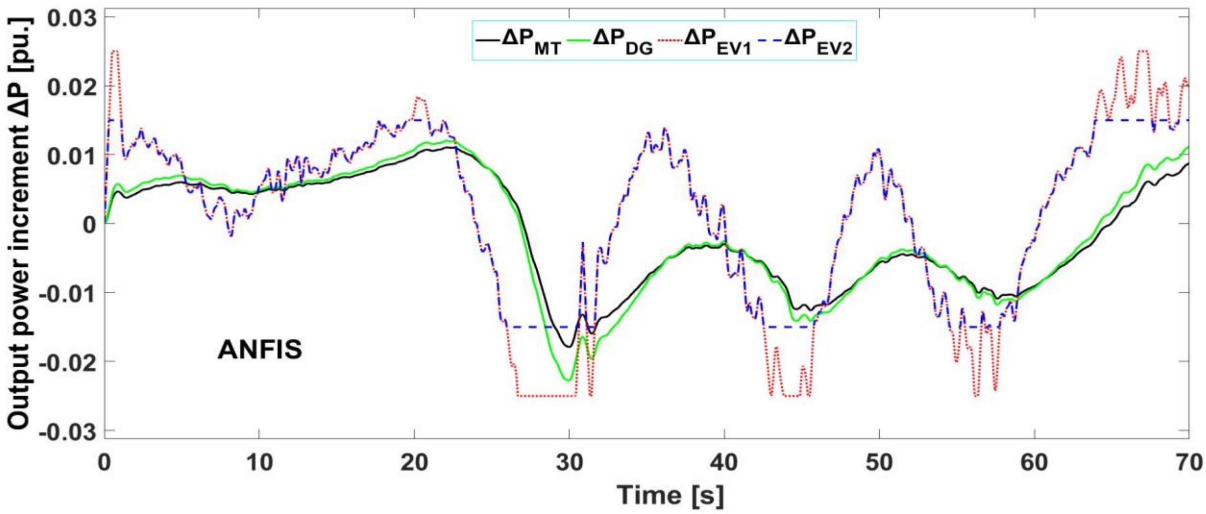

Figure 45 - The output power increment of MT, DG, EV1, and EV2 with considering constraints in case 4(B); (I) using PID controller, (II) using IT1 Fuzzy controller and (III) using ANFIS controller.

5.5 Case 5: Power fluctuation of wind power generation, load and solar PVs.

In this case, both wind power fluctuation, load disturbance and active power fluctuation from solar PVs power generation to the MG system. The same wind power fluctuation (ΔP_W) in case 4 is also applied in this case, The Solar PVs fluctuation (ΔP_{PV}) is as follows: Specifically, at t = 0 s a -0.035 pu. step disturbance is applied, at t = 20 s a 0.001 pu. step disturbance applied, at t = 40 s a -0.025 pu. step disturbance applied, at t = 60 s a -0.05 pu. step load disturbance ΔP_L = 0.05 pu. applied and at t = 40 seconds, see figure 46.

Figure 49 and figure 51, show that the proposed ANFIS based Neuro-Fuzzy Controller effectively can highly improve the performance of the LFC system, and it has a superior damping performance over PID controller, IT1 fuzzy controller and IT2 fuzzy controller. As we seen in figure 50 and figure 52, the output power increment curve of MT and DG are smoother than that of EVs, because the inertia constant of MT and DG is much larger than that of EVs. MT, DG and EVs have less output power fluctuation by using the ANFIS controller under the consideration of constraints in the system.

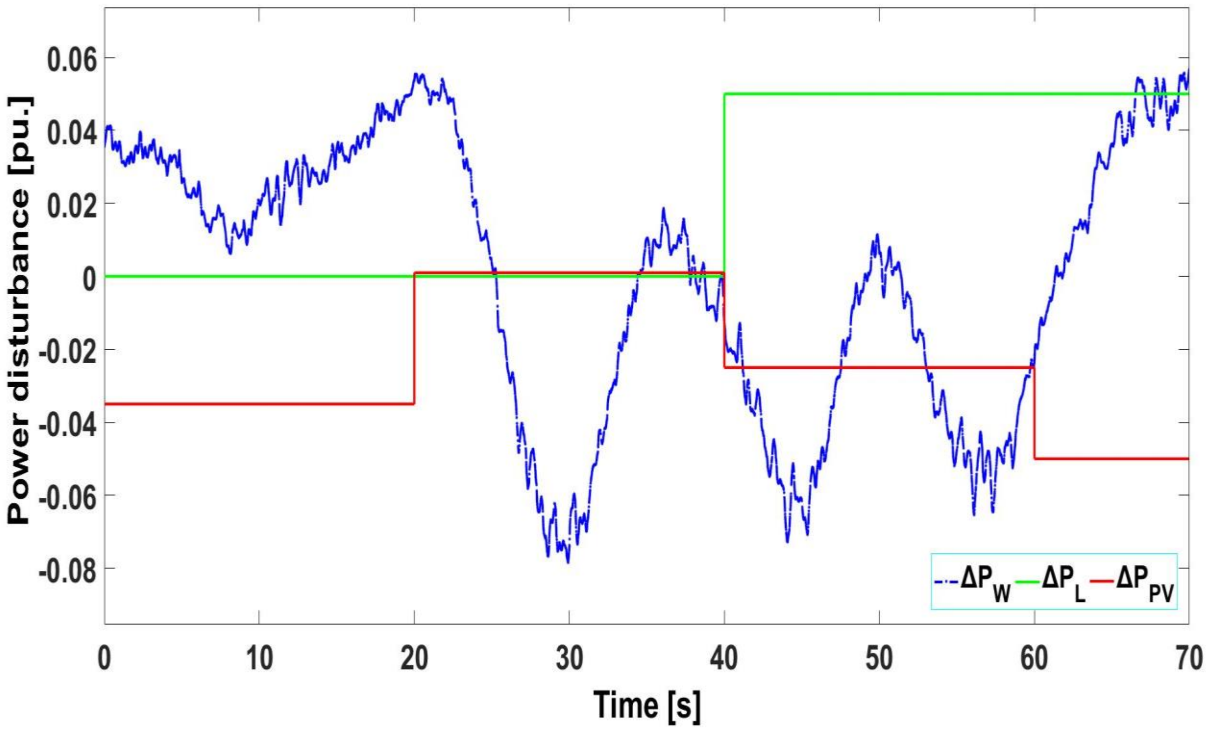

Figure 46 - The power disturbances applied in this case (case 5).

5.5.1. Case 5(A)-Without considering the constraints of MT, DG and EVs

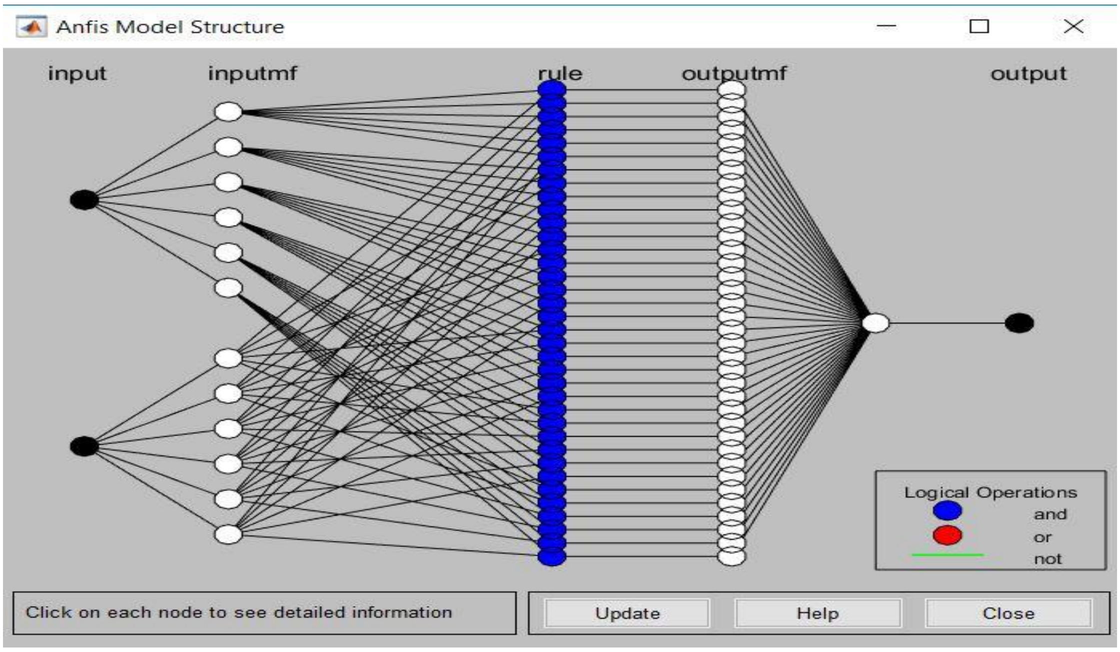

Figure 47 - MATLAB ANFIS model of rule base for this case.

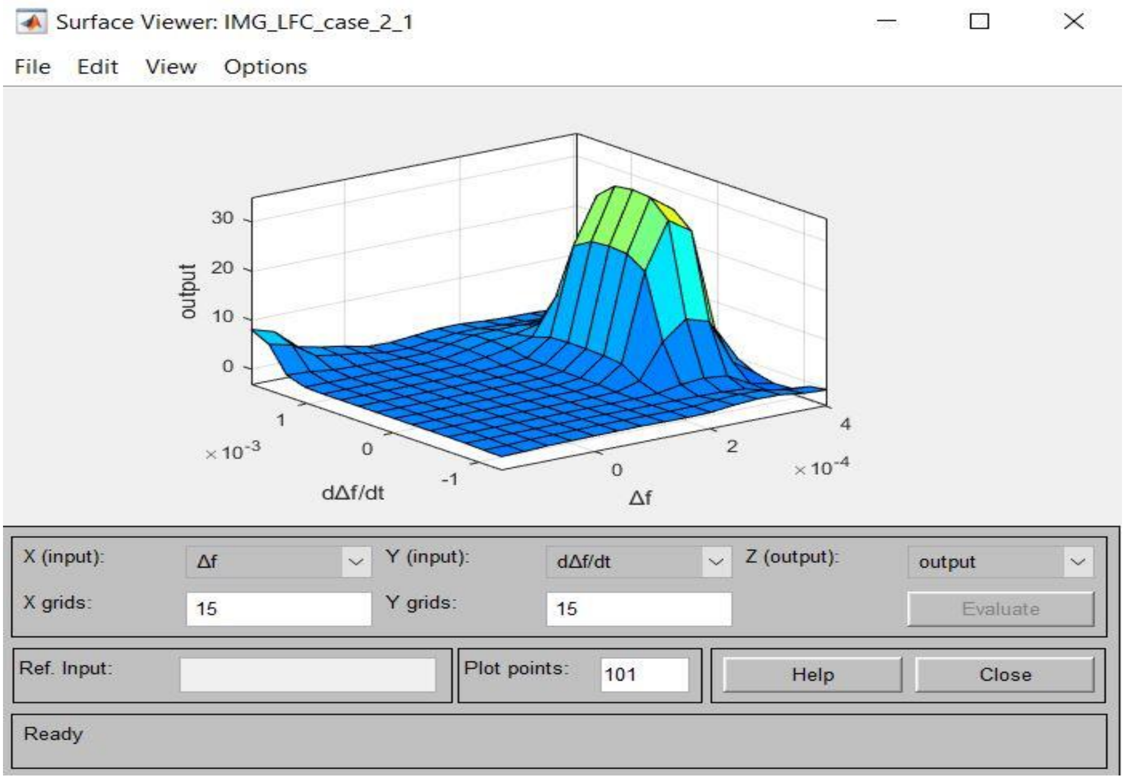

Figure 48 - Surface view created by ANFIS for in this case (case 5(A)).

ANFIS info:

Number of nodes: 101
Number of linear parameters: 108
Number of nonlinear parameters: 36
Total number of parameters: 144
Number of training data pairs: 701
Number of checking data pairs: 0
Number of fuzzy rules: 36

Start training ANFIS...

1 0.00903368
2 0.00931277

Designated epoch number reached --> ANFIS training completed at epoch 2.

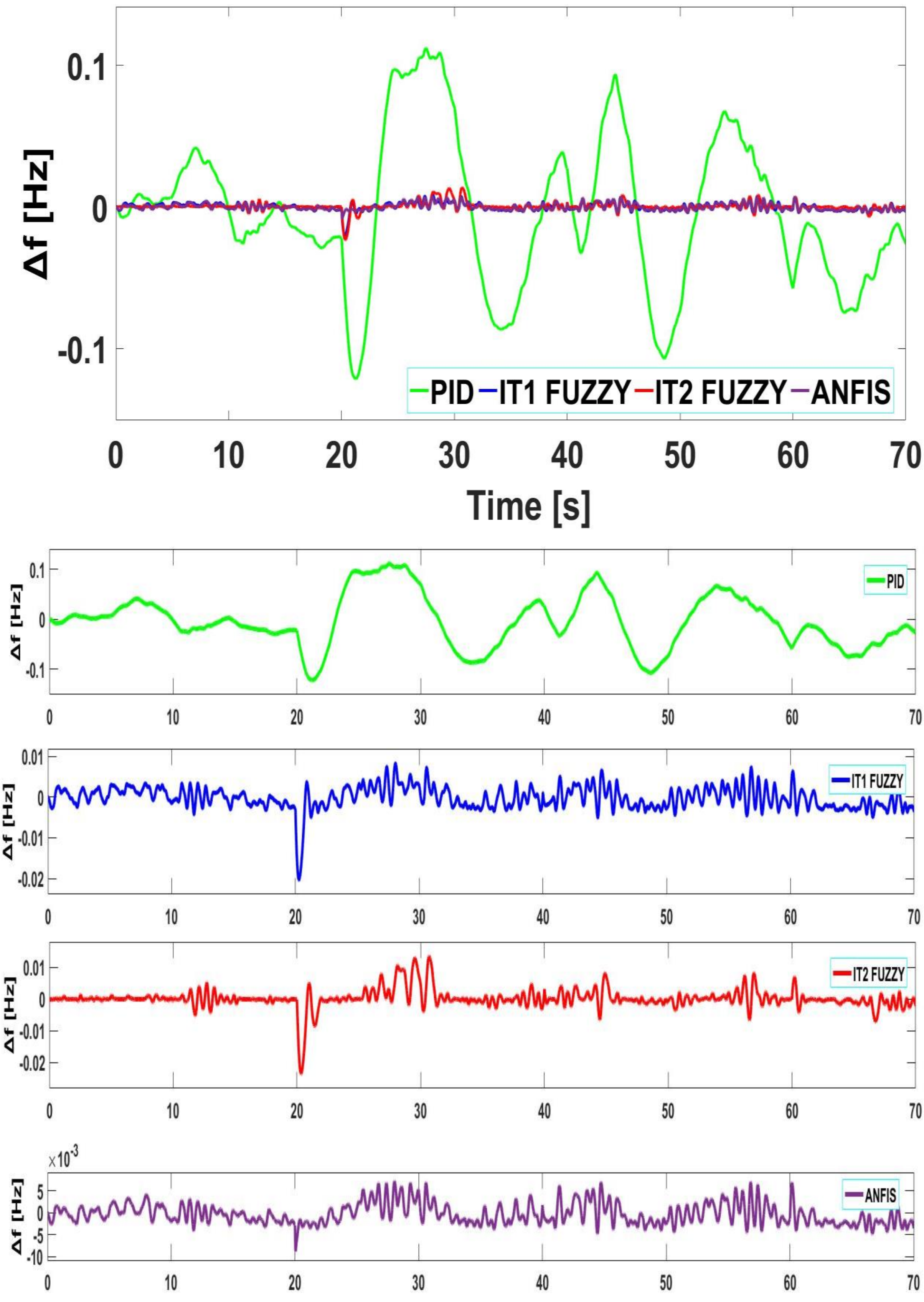

Figure 49 - The frequency deviation of the isolated micro-grid without constraints in case 5(A).

(I)

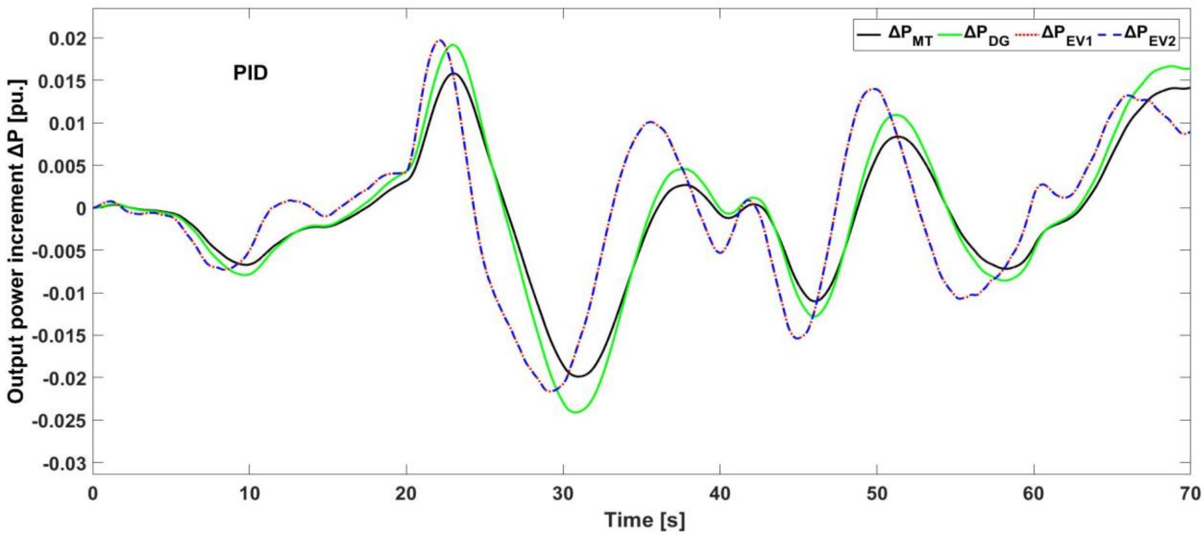
PID
ΔP_MT ΔP_DG ΔP_EV1 ΔP_EV2
Output power increment ΔP [pu.]
Time [s]
0.02
0.015
0.01
0.005
0
-0.005
-0.01
-0.015
-0.02
-0.025
-0.03
0
10
20
30
40
50
60
70

(II)

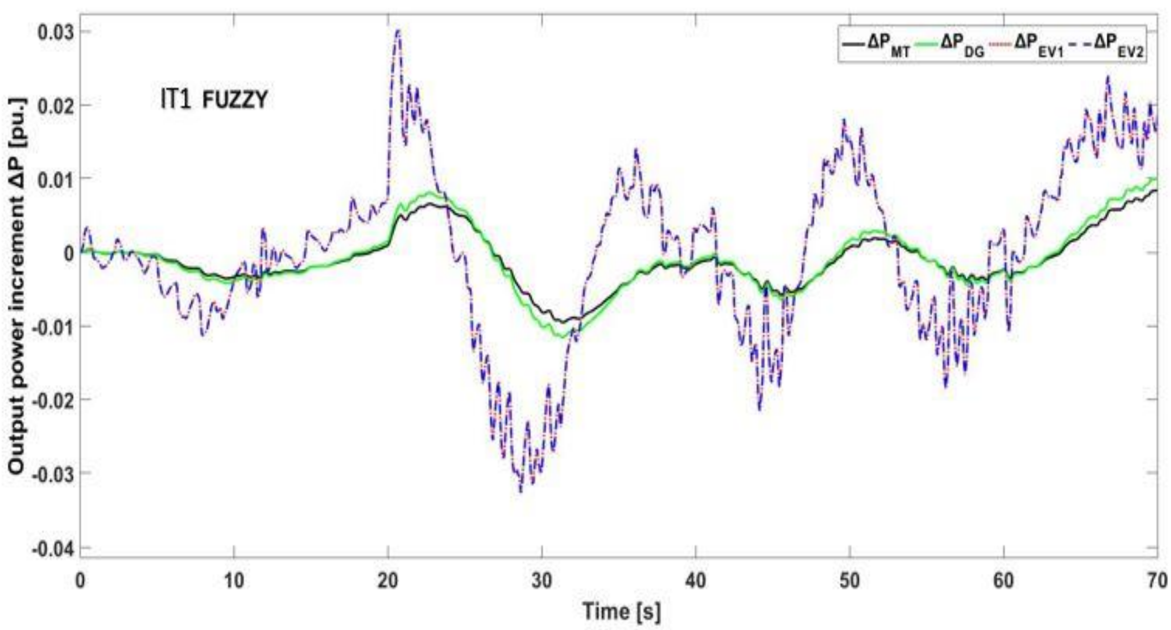
IT1 FUZZY
ΔP_MT ΔP_DG ΔP_EV1 ΔP_EV2
Output power increment ΔP [pu.]
Time [s]
0.03
0.02
0.01
0
-0.01
-0.02
-0.03
-0.04
0
10
20
30
40
50
60
70

(III)

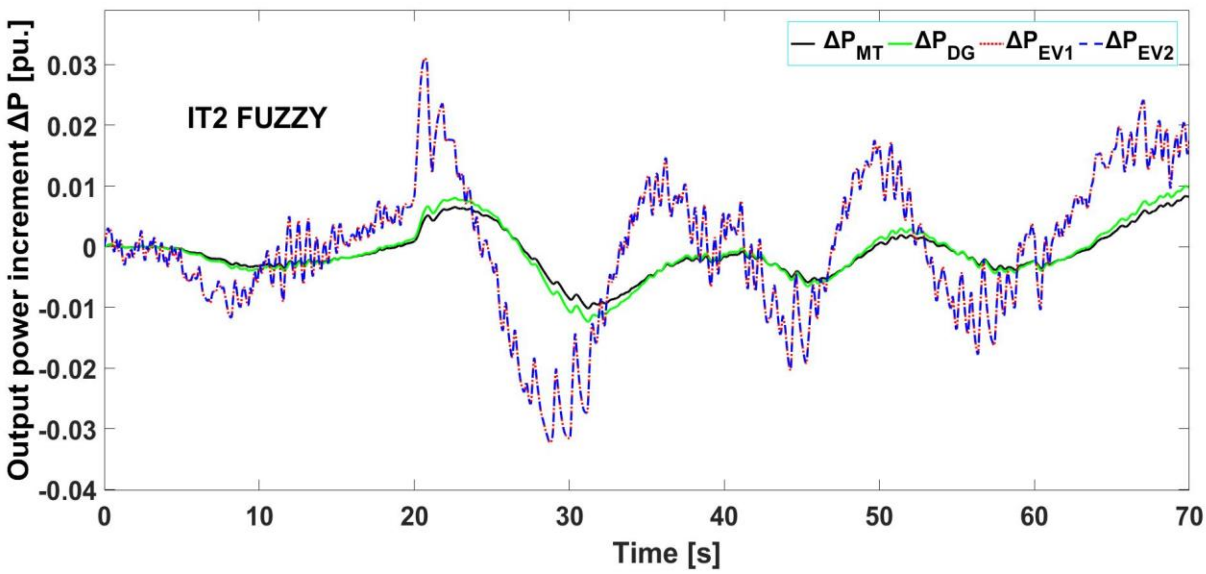

(IV)

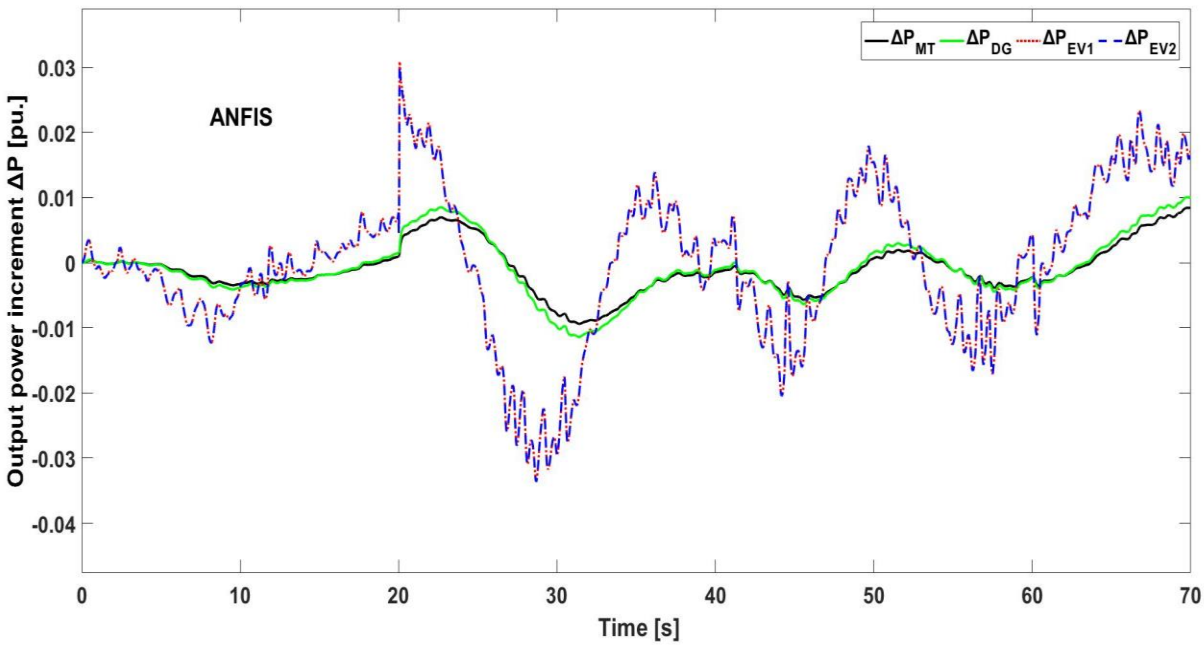

Figure 50 - The output power increment of MT, DG, EV1, and EV2 without considering constraints in case 5(A); (I) using PID controller, (II) using IT1 Fuzzy controller, (III) using IT2 Fuzzy controller and (IV) using ANFIS controller.

Figure 49, shows that ANFIS has a superior performance on the frequency deviation caused by all disturbances without constraints. Additionally, as shown in the above figure 50, the output power increment curve of EVs is less smooth than that of MT and DG because of smaller inertia constant. The ANFIS can more stable output power of MT, DG, and EVs, compared with PID, IT1 fuzzy and IT2 fuzzy.

5.5.2. Case 5(B)-With considering the constraints of MT, DG and EVs

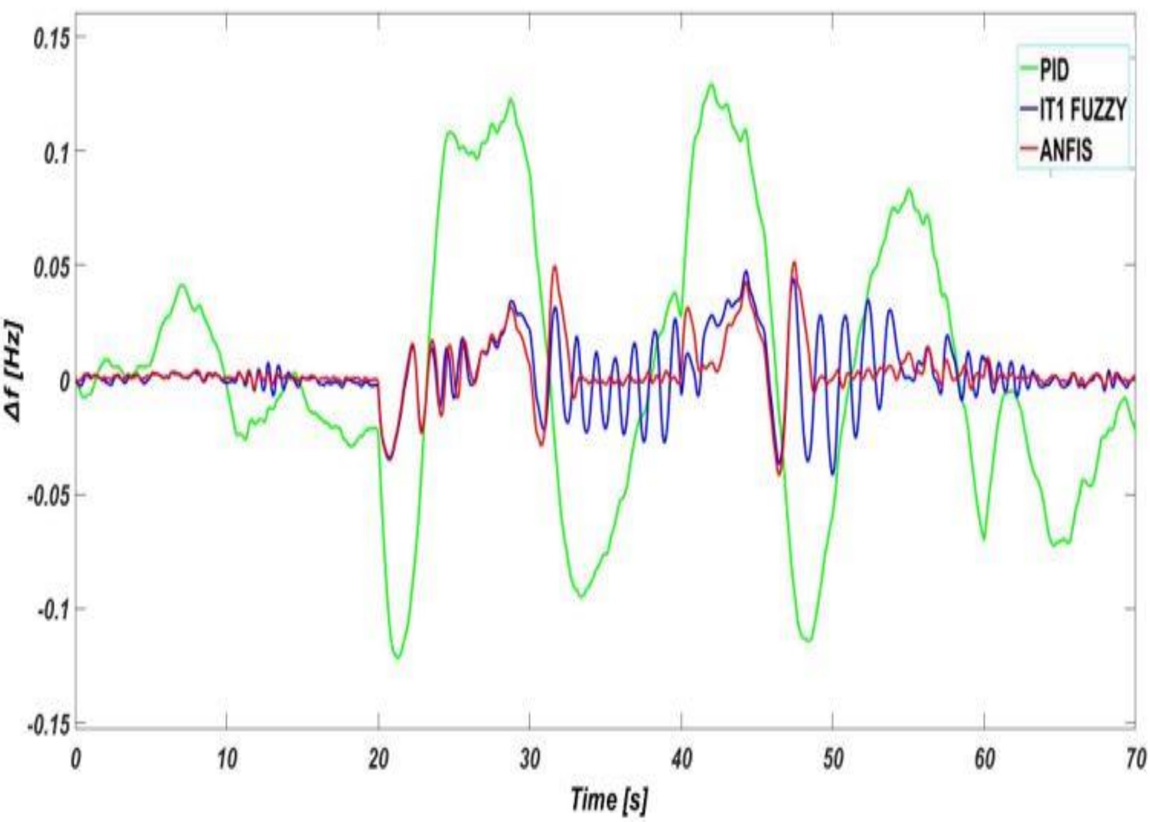

Figure 51 - The frequency deviation of the isolated micro-grid with constraints in case 5(B).

(I)

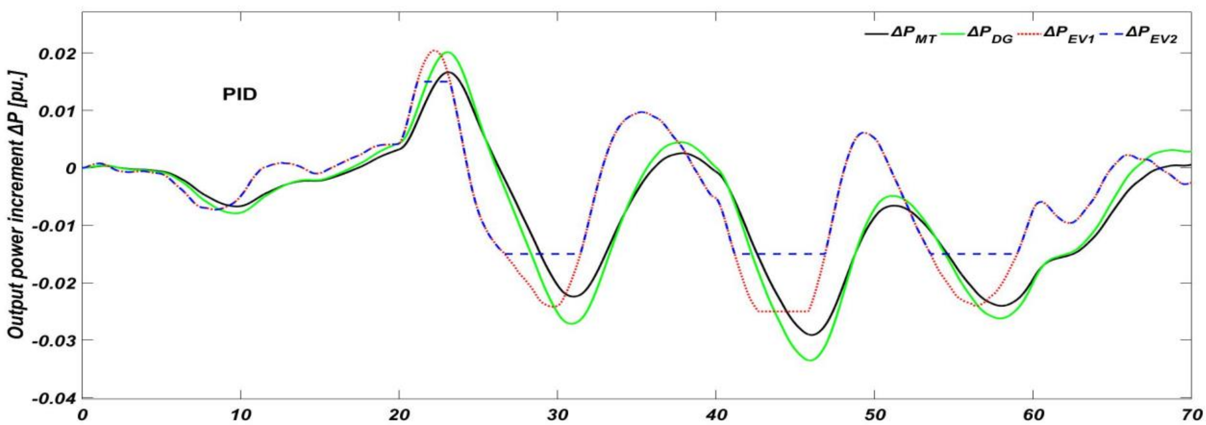

(II)

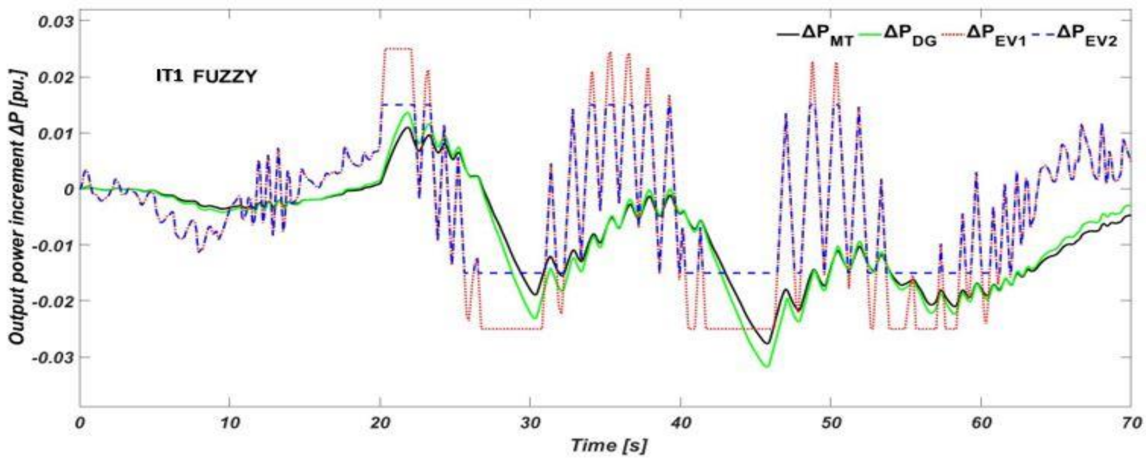

(III)

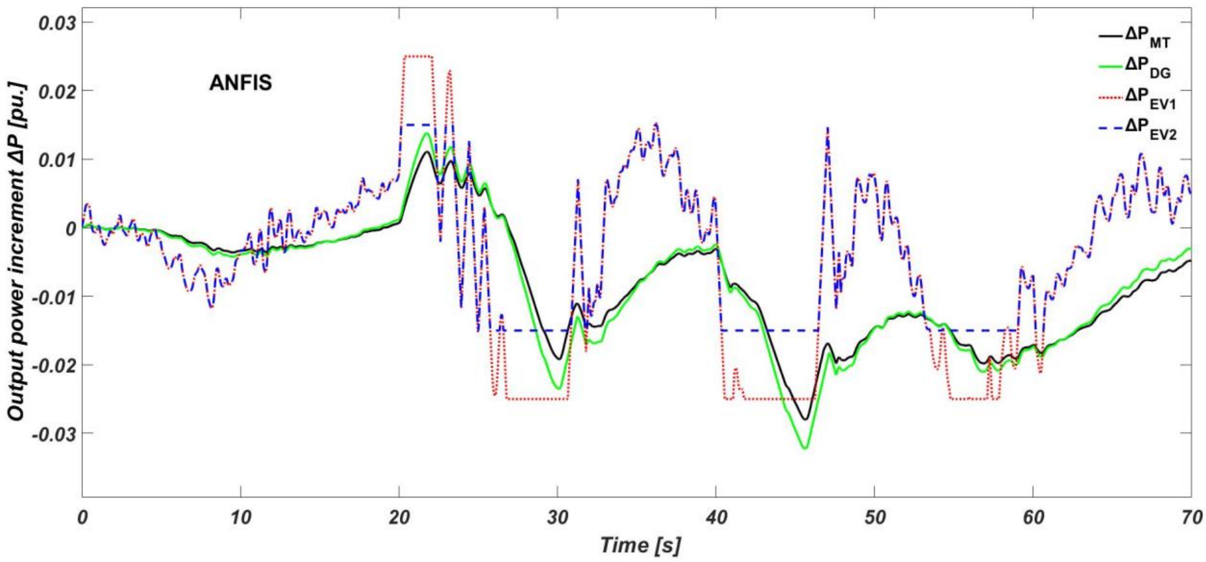

Figure 52 - The output power increment of MT, DG, EV1, and EV2 with considering constraints in case 5(b); (I) using PID controller, (II) using IT1 Fuzzy controller and (III) using ANFIS controller.

To evaluate the proposed LFC method in a more and challenging situation with constraints is presented here, as we seen from Figure 51, the ANFIS still quickly damps the frequency deviation. Figure 52 shows that the output power increment of MT, DG, EV1, and EV2 with the consideration of constraints, the ANFIS based Neuro-Fuzzy controller can still obtain a more stable output power of MT, DG, and EVs.

5.6. Case 6: power fluctuations of wind power generation, load, solar and with a sudden fault.

Finally, in this scenario, all disturbances that are used in case 5 (the sum of wind power generation fluctuation, active power fluctuation from solar PVs and ΔPL = 0.05 pu. at t = 40 second) is applied, and with an additional load disturbance for in this case ΔP_L^* is also considered, as shown in figure 53. At t = 24.5 s, a fault takes place at the connected grid, the circuit "Breaker" in figure 1 moves disconnect the MG from the utility, and the MG enters to isolated mode from grid-connected mode at 25 s. The power provided by utility to the MG is 0.03 pu, by assumption. So, MG experience a power shortage of 0.03 pu. at 25 second and at 55 s a load disturbance of -0.03 pu. is applied. Figure 53 shows all the power disturbances applied in this case. Without and with consideration of constraints presented in case 6(A) and case 6(B), respectively.

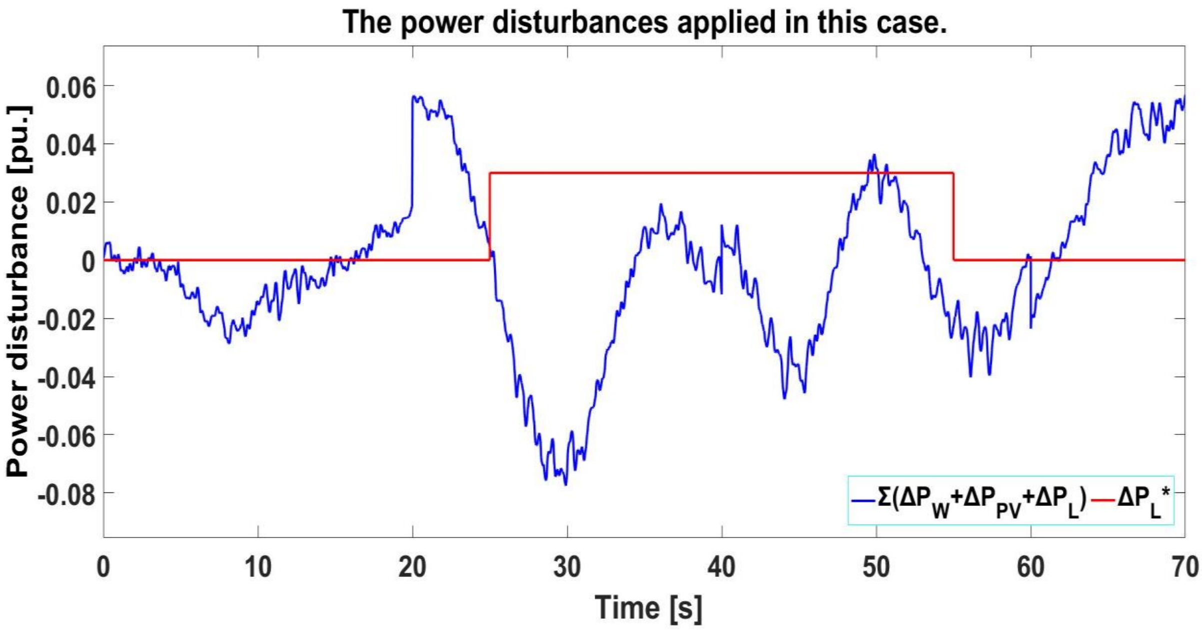

Figure 53 - The power disturbance applied in case 6.

5.6.1. Case 6(A) Without considering the constraints of MT, DG and EVs

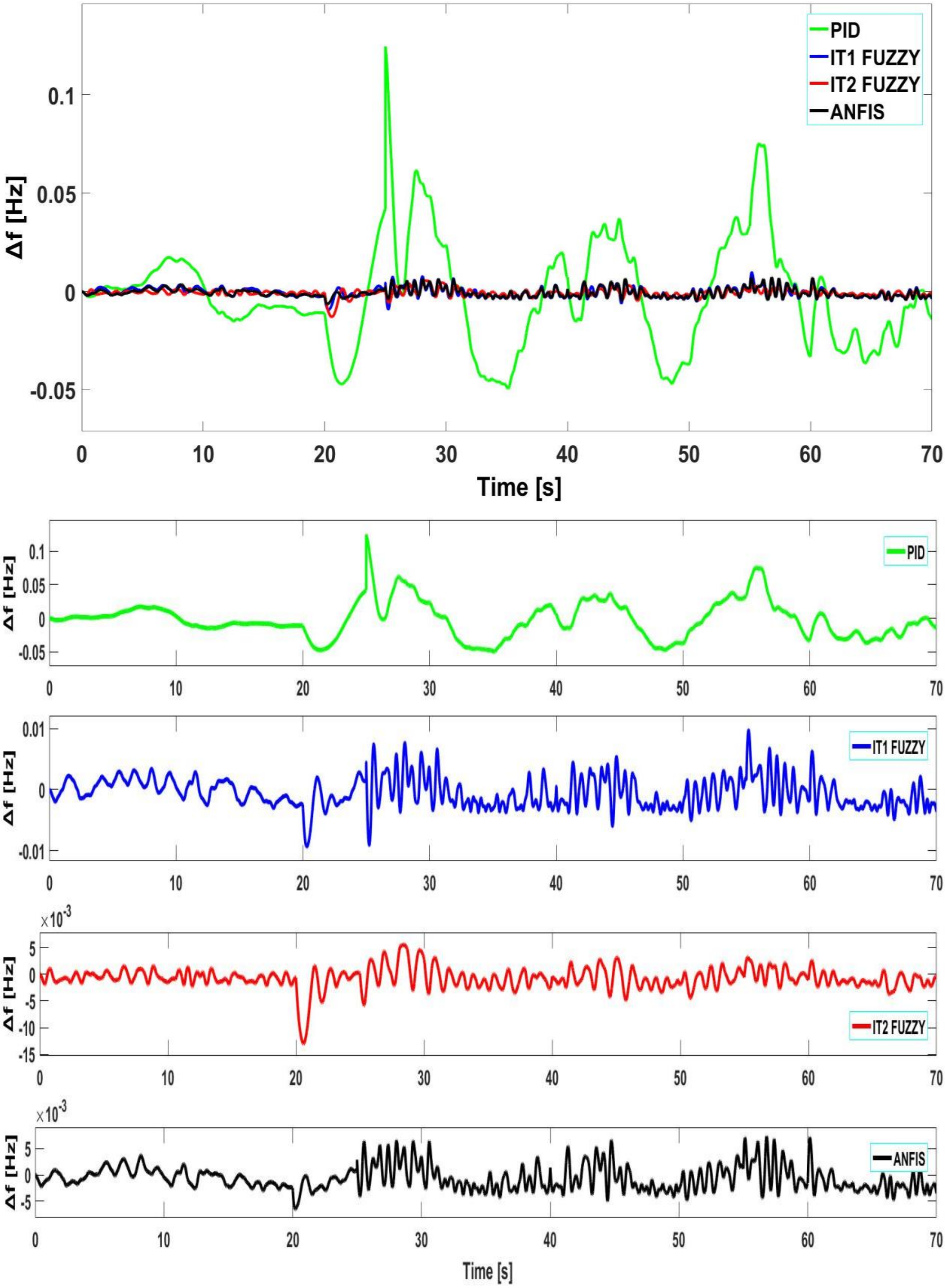

Figure 54 - The frequency deviation of the isolated micro-grid without constraints in case 6(A).

(I)

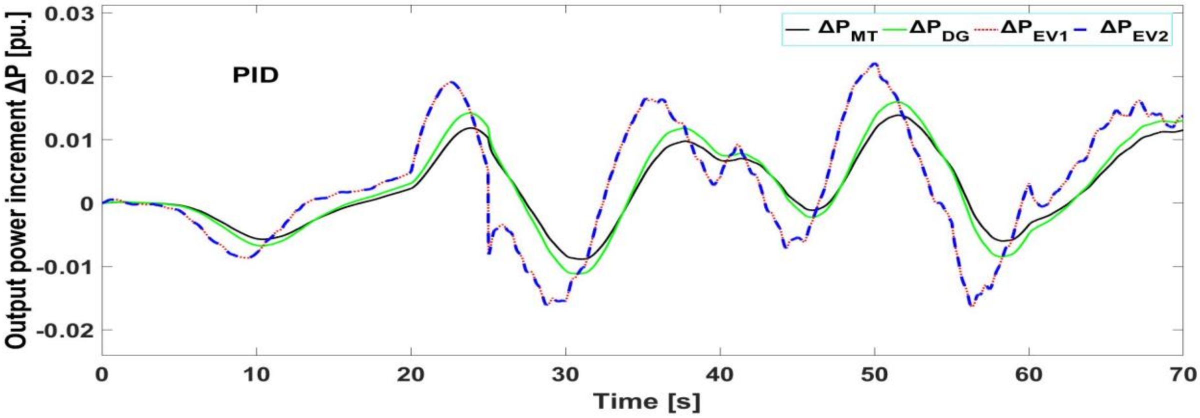
PID
ΔP_MT ΔP_DG ΔP_EV1 ΔP_EV2
Output power increment ΔP [pu.]
0.03
0.02
0.01
0
-0.01
-0.02
0 10 20 30 40 50 60 70
Time [s]

(II)

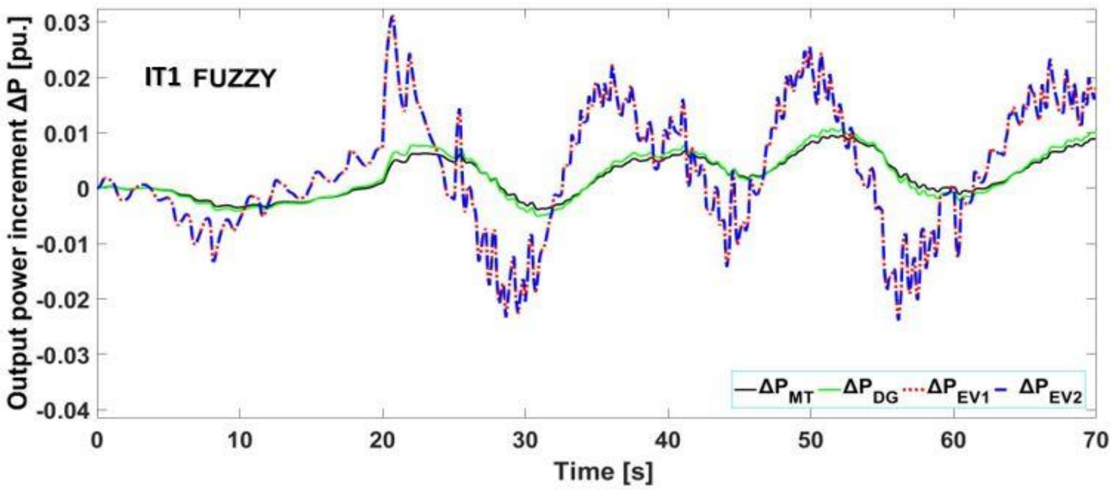
IT1 FUZZY
ΔP_MT ΔP_DG ΔP_EV1 ΔP_EV2
Output power increment ΔP [pu.]
0.03
0.02
0.01
0
-0.01
-0.02
-0.03
-0.04
0 10 20 30 40 50 60 70
Time [s]

(III)

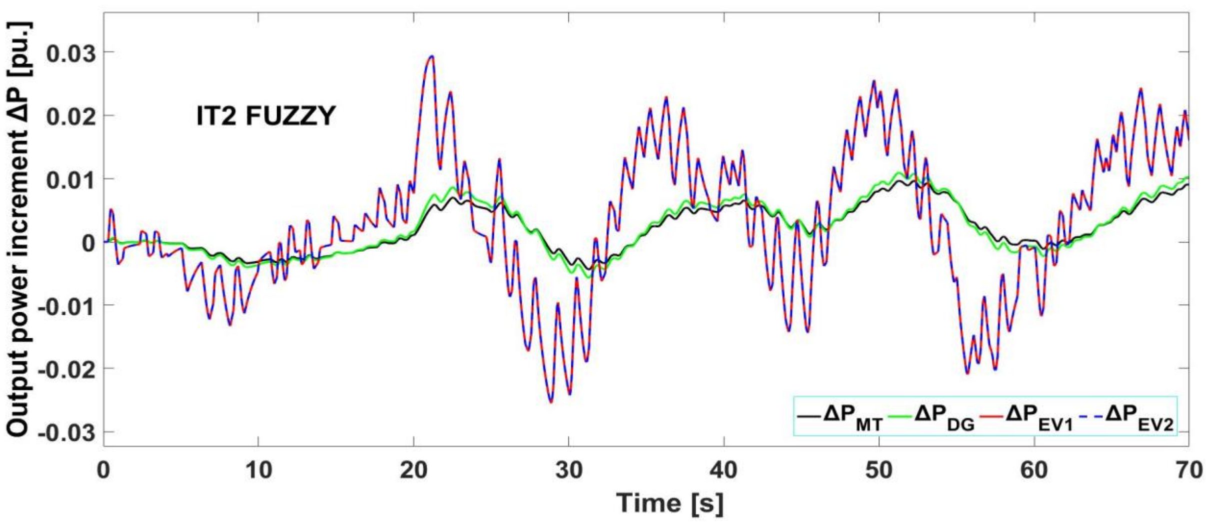
IT2 FUZZY
ΔP_MT ΔP_DG ΔP_EV1 ΔP_EV2
Output power increment ΔP [pu.]
0.03
0.02
0.01
0
-0.01
-0.02
-0.03
0 10 20 30 40 50 60 70
Time [s]

(IV)

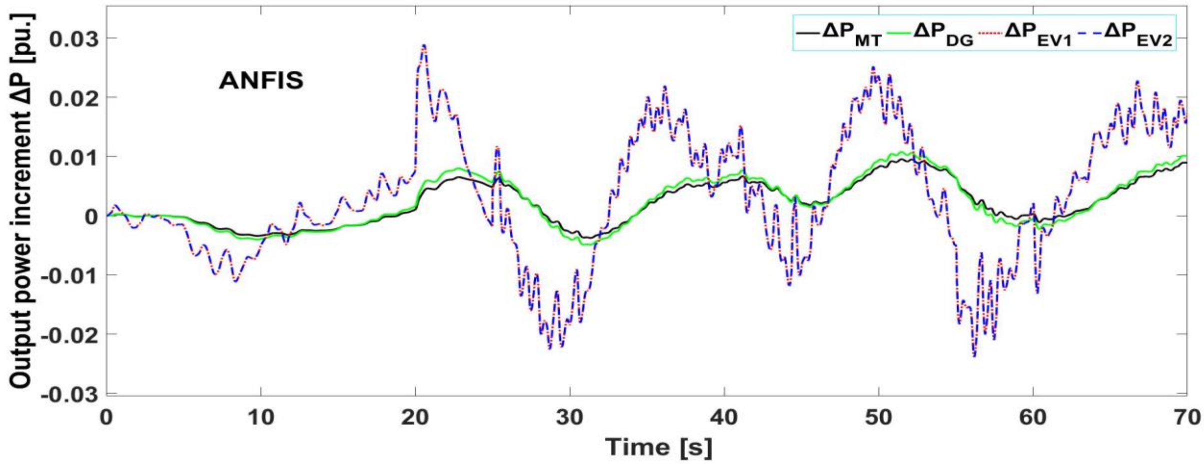

Figure 55 - The output power increment of MT, DG, EV1, and EV2 without considering constraints in case 6(A); (I) using PID controller, (II) using IT1 Fuzzy controller, (III) using IT2 Fuzzy controller and (IV) using ANFIS controller.

Figure 54, shows that ANFIS has a superior performance on the frequency deviation caused by all disturbances without constraints. Additionally, as shown in the above figure 55, the output power increment curve of EVs is less smooth than that of MT and DG because of smaller inertia constant. The ANFIS can more stable output power of MT, DG, and EVs, compared with PID, IT1 fuzzy and IT2 fuzzy.

5.6.2. Case 6(B) With considering the constraints of MT, DG and EVs

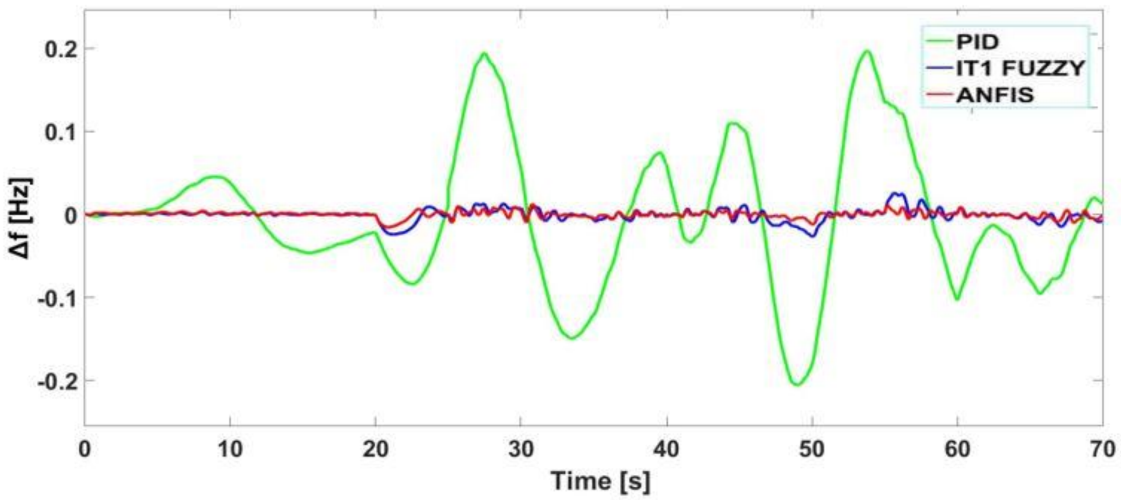

Figure 56 - The frequency deviation of the isolated micro-grid with constraints in case 6(B).

(I)

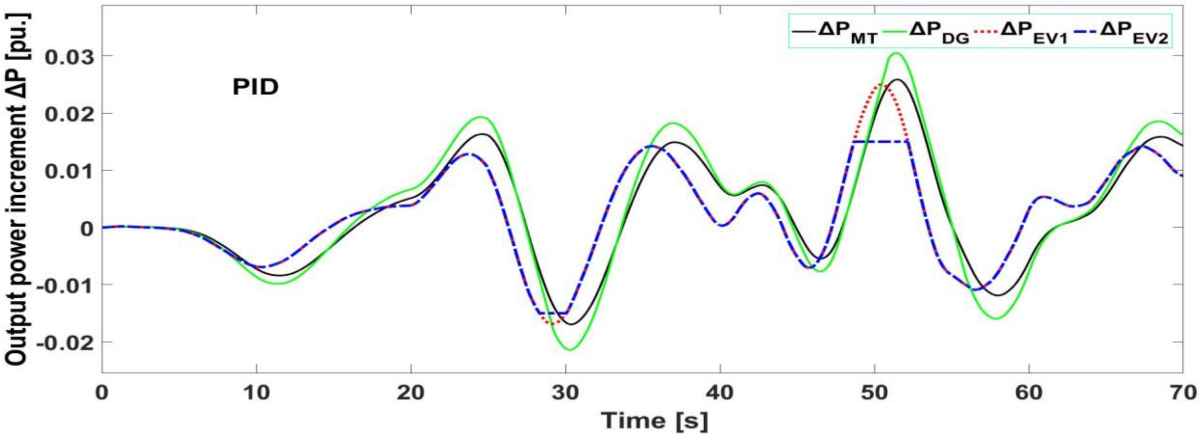

(II)

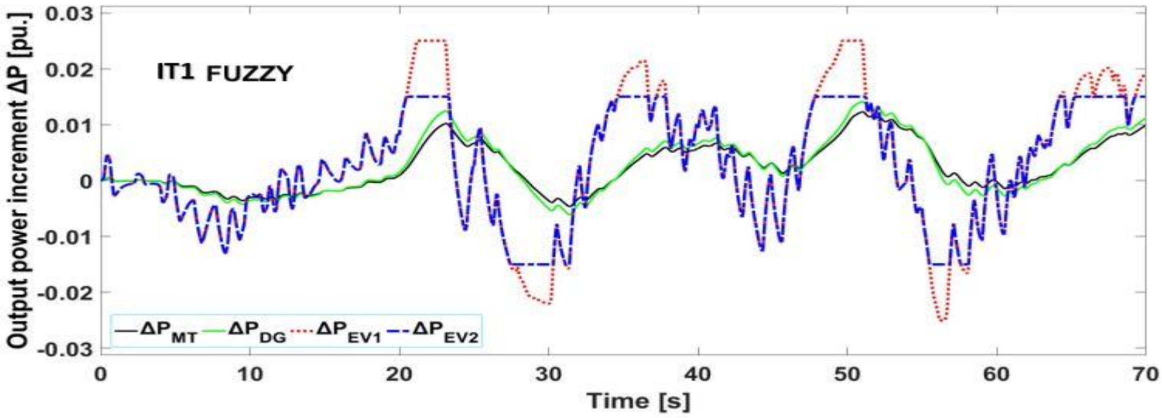

(III)

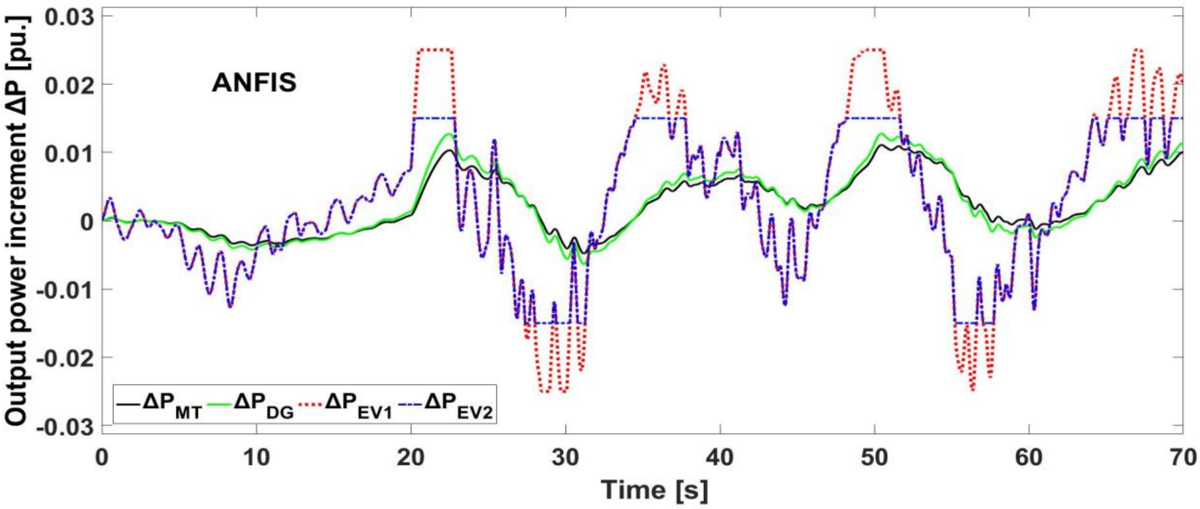

Figure 57 - The output power increment of MT, DG, EV1, and EV2 with considering constraints in case 6(B); (I) using PID controller, (II) using IT1 Fuzzy controller and (III) using ANFIS controller.

To evaluate the proposed LFC method in a more and challenging situation with constraints is presented here. As we seen from Figure 56, the ANFIS still quickly damps the frequency deviation. Figure 57 shows that the output power increment of MT, DG, EV1, and EV2 with the consideration of constraints, the ANFIS based Neuro-Fuzzy controller can still obtain more stable output power of MT, DG and EVs.

CHAPTER 6
Conclusions and Future Scopes

6.1 Summary of contributions and conclusion

The consistent increase in the penetration of renewable energy sources and continuous load disturbances in a power system, especially in isolated MG, the virtual inertia system might not stable and cannot maintain and stabilize the frequency deviation within the acceptable frequency performance, leading to instability and system collapse. In this, an intelligent control technique which is based on Adaptive Neuro-Fuzzy Inference System architecture for LFC in an isolated MG system using V2G integration has been proposed under different conditions with fluctuating renewable energy generation and load disturbance. The performance of the proposed intelligent controller has compared with conventional proportional-integral-derivative (PID) controller, Interval type-1 (IT1) Fuzzy controller and Interval type-2 (IT2) Fuzzy controller design methods.

The research performed in this thesis work includes the followings: -

I) A deep literature study of V2G technology, the role of V2G technology in a power system, load frequency control, LFC in micro-grid, LFC in MG with V2G, an intelligent technique for LFC in micro-grids and an intelligent technique for LFC in MG with V2G (Chapter 2).

II) State space modeling of the isolated micro-grid using V2G integration for LFC, which included MG modelling, model of MT, model of electric vehicles, model of DG, wind turbine and solar PV model, and the general scheme of the isolated micro-grid using V2G integrations (Chapter 3).

III) An intelligent coordination control techniques for LFC between micro-turbine, diesel generator and EVs to achieve a satisfied performance on load frequency. Artificial intelligent controllers for LFC, (a) Interval Type-1 Fuzzy Logic controller design for LFC (Chapter 4) 4.2.1), (b) Interval Type-2 Fuzzy Logic controller design for LFC (Chapter 4), 4.2.2), and (c) Adaptive Neuro-Fuzzy controller (ANFIS) design for LFC (Chapter 4), 4.2.3).

IV) Demonstrated the performance of ANFIS with system stability performances, the considered isolated micro-grid with MT, DG, EVs, solar PV, and wind farm is modelled in MATLAB/SIMULINK environment (Chapter 5).

- The state space modelling for LFC of the isolated Wind-Solar PV-Micro Turbine-Diesel Based Micro-Grid using V2G Integration has been developed with conventional controller, i.e. PID controller. The performance of the system with PID controller has been used for comparison with the proposed intelligent controllers designed in the thesis has been proposed under different conditions with fluctuating renewable energy generation and load disturbance.

- Interval Type-1 Fuzzy logic controller (Mamdani model) has been designed and investigated with the basic structure for isolated micro-grid load frequency control under the consideration constraints and without constraints of MT, DG, and EVs. The IT1 Fuzzy logic controller (Mamdani model) showed better performance than the conventional PID controller.

- Interval Type-2 Fuzzy logic controller (Mamdani model) has been designed and investigated. The result show that using IT2 fuzzy controller (Mamdani model) in real-world application might be a good option since this type of system is a better suitable system than PID and IT1 Fuzzy logic controllers to manage high levels of uncertainty, as shown in the results in Table 4.

- A novel Adaptive Neuro-Fuzzy Inference System architecture for an isolated wind-Solar PV-Micro Turbine-Diesel based micro-grid system using (V2G) integration has been designed to improve system frequency stability. The performance improvement of the proposed controller is to compare with conventional PID, IT1 Fuzzy controller and IT2 fuzzy controller regarding of rise time, over-shoot, under-shoot and settling time of the frequency deviation, (Chapter 5), Case 1)).

It is concluded that the proposed intelligent controller, ANFIS based Neuro-Fuzzy controller, it significantly improved the stability, reliability, economical and dynamic performance of the device and the whole isolated micro-grid. It has been shown that the ANFIs based Neuro-Fuzzy controller is effective and provides significant improvement in system performance by combine the benefits of the parallel and learning abilities of neural networks with human like knowledge representation and explanation abilities of fuzzy system. According the general scheme of the MG with LFC controller (Chapter 3) 3.6) model, both load disturbance and the output power of renewable energy sources are considered as ΔP. Therefore, the proposed controller can be used in different configurations of MG, including different loads, renewable energy sources and grid topologies. This has shown the credibility to implement the proposed method in real the power system.

6.2 Future Scopes

The following investigations are recommended for future research based on the results presented in this thesis work: -

- This thesis presented and proposed for only active power controls of MT, DG, and EVs for LFC. But in the real time when there is a power interruption both the voltage and frequency fluctuation occur, so the use of reactive power to stabilize the system has to be done in the future by using intelligent control techniques.
- In this thesis, the isolated micro-grid is based on two renewable energy, i.e. wind energy source and Solar PV energy source. In the power industry, many another type of renewable energies, for example, Tide power is also receiving increasing interest, so in the future may be to integrate more renewable energy sources and design the corresponding solution.
- The communication delay may have an influence on the performance of the controller since the optimal decisions of the stated coordinated controller depend on real-time information from micro-grid distribution system.
- Further study can be made using optimisation methods such as Particle Swarm Optimization, Genetic Algorithm, etc. to tune the controller's parameters.

References

1. Manoj Singh Bish, Sathans “Fuzzy based intelligent frequency control strategy in standalone hybrid AC microgrid” IEEE Control Applications (CCA), 11 December 2014. Date Added to IEEE Xplore: 11 December 2014 IEEE Conference on Control Applications (CCA).

2. Machowski, Jan, Janusz Bialek, and Jim Bumby. “Power system dynamics: stability and control”. John Wiley & Sons, 2011.

3. Jun Yang, Zhili Zeng, Yufei Tang, Jun Yan, Haibo He, Yunliang Wu, " Load frequency control in an isolated micro grid system with electric vehicles based on MGPT" Energies 2015, Vol. 8, pp. 2145-2164.

4. Ma, Y., Zhang, B., Zhou, X., Gao, Z., Wu, Y., Yin, J., & Xu, X. (2016, May). “An overview on V2G strategies to impacts from EV integration into power system.” In Control and Decision Conference (CCDC), 2016 Chinese (pp. 2895-2900). IEEE.

5. Singh, Mukesh, Praveen Kumar, and Indrani Kar. "Implementation of vehicle to grid infrastructure using fuzzy logic controller." IEEE Transactions on Smart Grid 3.1 (2012): 565-577.

6. Shumei, C., Xiaofei, L., Dewen, T., Qianfan, Z., & Liwei, S. (2011, August). “Theconstruction and simulation of V2G system in micro-grid”. In Electrical Machines and Systems (ICEMS), 2011 International Conference on (pp. 1-4). IEEE.

7. Monteiro, V., Pinto, J. G., Exposto, B., Gonçalves, H., Ferreira, J. C., Couto, C., & Afonso, J. L. (2012, October). “Assessment of a battery charger for electric vehicles with reactive power control”. In IECON 2012-38th Annual Conference on IEEE Industrial Electronics Society (pp. 5142-5147). IEEE.

8. Han, Sekyung, Soohee Han, and Kaoru Sezaki. "Development of an optimal vehicle-to-grid aggregator for frequency regulation." IEEE Transactions on smart grid 1.1 (2010): 65-72.

9. Pillai, Jayakrishnan Radhakrishna, and Birgitte Bak-Jensen. "Integration of vehicle-to-grid in the western Danish power system." IEEE Transactions on Sustainable Energy 2.1 (2011): 12-19.

10. Madawala, Udaya K., and Duleepa J. Thrimawithana. "A bidirectional inductive power interface for electric vehicles in V2G systems." IEEE Transactions on Industrial Electronics 58.10 (2011): 4789-4796.

11. Wang, Zhenpo, and Shuo Wang. "Grid power peak shaving and valley filling using vehicle-to-grid systems." IEEE Transactions on Power delivery 28.3 (2013): 1822-1829.

12. Bevrani, Hassan, et al. "Intelligent LFC concerning high penetration of wind power: synthesis and real-time application." IEEE Transactions on Sustainable Energy 5.2 (2014): 655-662.

13. Bevrani, Hassan. “Robust power system frequency control”. Vol. 85. New York: Springer, 2009. (Book)

14. Ashmole, P. H., D. R. Battlebury, and R. K. Bowdler. "Power-system model for large frequency disturbances." Electrical Engineers, Proceedings of the Institution of 121.7 (1974): 601-608.

15. Jiang, L., et al. "Delay-dependent stability for load frequency control with constant and time-varying delays." IEEE Transactions on Power systems 27.2 (2012): 932-941.

16. Foord, T. R. "Step response of a governed hydrogenerator." Electrical Engineers, Proceedings of the IEEE, 125.11

17. Doolla, Suryanarayana, and T. S. Bhatti. "Load frequency control of an isolated small-hydro power plant with reduced dump load." IEEE Transactions on Power Systems 21.4 (2006): 1912-1919.

18. Schlueter, R. A., et al. "Modification of power system operation for significant wind generation penetration." IEEE Transactions on Power Apparatus and Systems 1 (1983): 153-161.

19. Fosha, Charles, and Olle Elgerd. "The megawatt-frequency control problem: a new approach via optimal control theory." IEEE Transactions on Power Apparatus and Systems 4.PAS-89 (1970): 563-577.

20. Vachirasricirikul, Sitthidet, and Issarachai Ngamroo. "Robust controller design of microturbine and electrolyzer for frequency stabilization in a microgrid system with plug-in hybrid electric vehicles." International Journal of Electrical Power & Energy Systems 43.1 (2012): 804-811.

21. Li, Xiangjun, Yu-Jin Song, and Soo-Bin Han. "Frequency control in micro-grid power system combined with electrolyzer system and fuzzy PI controller." Journal of Power Sources 180.1 (2008): 468-475.

22. Han, Sekyung, Soohee Han, and Kaoru Sezaki. "Development of an optimal vehicle-to-grid aggregator for frequency regulation." IEEE Transactions on smart grid 1.1 (2010): 65-72.

23. Shimizu, Koichiro, et al. "Load frequency control in power system using vehicle-to-grid system considering the customer convenience of electric vehicles." Power System Technology (POWERCON), 2010 International Conference on. IEEE, 2010.

24. Pillai, Jayakrishnan Radhakrishna, and Birgitte Bak-Jensen. "Integration of vehicle-to-grid in the western Danish power system." IEEE Transactions on Sustainable Energy 2.1 (2011): 12-19.

25. Clement-Nyns, Kristien, Edwin Haesen, and Johan Driesen. "The impact of charging plug-in hybrid electric vehicles on a residential distribution grid." IEEE Transactions on Power Systems 25.1 (2010): 371-380.

26. Singh, Mukesh, Indrani Kar, and Praveen Kumar. "Influence of EV on grid power quality and optimizing the charging schedule to mitigate voltage imbalance and reduce power loss." Power Electronics and Motion Control Conference (EPE/PEMC), 2010 14th International. IEEE, 2010.

27. Umrao, Rahul, et al. "Load frequency control methodologies for power system." Power, Control and Embedded Systems (ICPCES), 2012 2nd International Conference on. IEEE, 2012.

28. Mallesham, G., S. Mishra, and A. N. Jha. "Automatic generation control of microgrid using artificial intelligence techniques." 2012 IEEE Power and Energy Society General Meeting. IEEE, 2012.

29. Fozdar, Manoj, C. M. Arora, and V. R. Gottipati. "Recent trends in intelligent techniques to power systems." Universities Power Engineering Conference, 2007. UPEC 2007. 42nd International. IEEE, 2007.

30. Tang, Yufei, et al. "Frequency control using on-line learning method for island smart grid with EVs and PVs." 2014 International Joint Conference on Neural Networks (IJCNN). IEEE, 2014.

31. Khooban, Mohammad-Hassan, et al. "A robust adaptive load frequency control for micro-grids."ISA transactions 65 (2016): 220-229.

32. Awad, Bieshoy, Janaka Ekanayake, and Nick Jenkins. "Intelligent load control for frequency regulation in MicroGrids." Intelligent Automation & Soft Computing 16.2 (2010): 303-318.

33. Bevrani, Hassan, Mohammad Ramin Feizi, and Sirwan Ataee. "Robust Frequency Control in an Islanded Microgrid: $H\infty$ and μ-Synthesis Approaches." IEEE Transactions on Smart Grid 7.2 (2016): 706-717.

34. Izumi, Yuya, Tomonobu Senjyu, and Atsushi Yona. "Load frequency control by using demand response with $\mathscr{H}\infty$ in isolated power systems." *Harmonics and Quality of Power (ICHQP), 2012 IEEE 15th International Conference on*. IEEE, 2012.

35. Senjyu, Tomonobu, et al. "A hybrid power system using alternative energy facilities in isolated island." IEEE Transactions on energy conversion 20.2 (2005): 406-414.

36. Toge, Masato, Yu Kurita, and Shinichi Iwamoto. "Supplementary load frequency control with storage battery operation considering SOC under large-scale wind power penetration." Power and Energy Society General Meeting (PES), 2013 IEEE. IEEE, 2013.

37. Al-Barazanchi, Sardar Adil Mohammed, and Ahmet Mete Vural. "Modeling and intelligent control of a stand-alone PV-Wind-Diesel-Battery hybrid system." Control, Instrumentation, Communication and Computational Technologies (ICCICCT), 2015 International Conference on. IEEE, 2015.

38. S. Prakash and S. K. Sinha "Four area Load Frequency Control of interconnected hydro-thermal power system by Intelligent PID control technique" 2012 Students Conference on Engineering and Systems, March 2012, pp.1-6

39. Eberhart, Russell C. "Overview of computational intelligence [and biomedical engineering applications]." *Engineering in Medicine and Biology Society, 1998. Proceedings of the 20th Annual International Conference of the IEEE*. Vol. 3. IEEE, 1998.

40. Chai, Yuanyuan, Limin Jia, and Zundong Zhang. "Mamdani model based adaptive neural fuzzy inference system and its application in traffic level of service evaluation." Fuzzy Systems and Knowledge Discovery, 2009. FSKD'09. Sixth International Conference on. Vol. 4. IEEE, 2009.

41. Bevrani, Hassan, and Pourya Ranjbar Daneshmand. "Fuzzy logic-based load-frequency control concerning high penetration of wind turbines." *IEEE systems journal* 6.1 (2012): 173-180.

42. Bevrani, Hassan, et al. "Intelligent frequency control in an AC microgrid: Online PSO-based fuzzy tuning approach." IEEE Transactions on Smart Grid 3.4 (2012): 1935-1944.

43. Jang, J-SR. "ANFIS: adaptive-network-based fuzzy inference system." IEEE transactions on systems, man, and cybernetics 23.3 (1993): 665-685.

44. Nath, Vivek, and D. K. Sambariya. "Design and performance analysis of adaptive neuro fuzzy controller for load frequency control of multi-power system." Intelligent Systems and Control (ISCO), 2016 10th International Conference on. IEEE, 2016.

45. Dhanalakshmi, R., and S. Palaniswami. "ANFIS based Neuro-Fuzzy Controller in LFC of Wind-Micro Hydro-Diesel Hybrid Power System." International Journal of computer applications 42.6 (2012): 28-35.

46. Menghal, P. M., and A. Jaya Laxmi. "Scalar control of an induction motor using artificial intelligent controller." Power, Automation and Communication (INPAC), 2014 International Conference on. IEEE, 2014.

47. Zubieta, Luis Eduardo. "Are microgrids the future of energy? Dc microgrids from concept to demonstration to deployment." *IEEE Electrification Magazine* 4.2 (2016): 37-44.

48. Khodaei, Amin. "Provisional microgrid planning." *IEEE Transactions on Smart Grid* (2015).

49. Surya Prakash, A.K. Bhardwaj and S.K. Shinha "Neuro fuzzy hybrid intelligent approach for four -area load frequency control of interconnected power system" 2012 2nd International Conference on Power, Control and Embedded Systems, Dec. 2012, pp.1-7. IEEE, 29 April 2013.

50. J. M. Mendel "Uncertain Rule-Based Fuzzy Logic Systems: Introduction and New Directions" Prentice Hall, 2001.

51. Souran, Davood M., et al. "A performance comparison of classical PID, Type-1 and Type-2 fuzzy controller in a three-tank level control system." Robotics and Manufacturing Automation (ROMA), 2014 IEEE International Symposium on. IEEE, 2014.

52. Database of Wind Characteristics. Available online: http://www.winddata.com/ (accessed on 3. March 2017 12:19 AM).

53. World Energy Council https://www.worldenergy.org/